



**Aalto University
School of Chemical
Engineering**

Jenna Lehtola

LEACHING OF METALS FROM WASTE GAS PURIFICATION DUST

Master's Programme in Chemical, Biochemical and Materials
Engineering
Major in Sustainable Metals Processing

Master's thesis for the degree of Master of Science in Technology
submitted for inspection, Espoo, 24 March, 2017.

Supervisor

Professor Mari Lundström

Instructors

M. Sc. Heini Elomaa & M. Sc. Sipi Seisko

Author Jenna Lehtola		
Title of thesis Leaching of metals from waste gas purification dust		
Department Department of Chemical and Metallurgical Engineering		
Professorship Hydrometallurgy and corrosion	Code of professorship MT-85	
Thesis supervisor Professor Mari Lundström		
Thesis advisor(s) / Thesis examiner(s) M. Sc. Heini Elomaa & M. Sc. Sipi Seisko		
Date 24 March 2017	Number of pages 61 + 48	Language English

Abstract

The production of waste is increasing, and the portion of waste that is incinerated is growing as well. This results in an increasing amount of incineration ashes that need to be treated properly. Besides from being a waste management challenge, these ashes contain metals of value, and can be considered as secondary raw materials.

In this thesis, the leaching of metals from fly ash/waste gas purification dust (WGPD) from an incinerator in Finland was investigated. The focus lays on leaching of copper, iron, nickel, lead and zinc. Acetic acid ($C_2H_4O_2$), citric acid ($C_6H_8O_7$), ethaline, hydrochloric acid (HCl), oxalic acid ($C_2H_2O_4$), and sulfuric acid (H_2SO_4) were tested in solution mapping test in order to find the most effective lixiviant for waste gas purification dust. Hydrochloric acid and citric acid were found to be the most efficient inorganic and organic lixiviant, respectively. These acids were then further researched by batch leaching test series. From batch leaching results, metal extraction models were built using Modde 8.0 software.

Another objective of this thesis was to reduce the total metal concentration in the leach residue of WGPD below 1000 ppm. A further interest was the selectivity of metal dissolution towards iron (Fe), with the goal of finding a solvent that would extract the metals of interest, but leave iron in the WGPD. This selectivity was found in acetic acid.

It was further found that the content of iron, nickel and zinc in the leach residue increased in all batch leaching experiments. This increase of concentration is due fact that a major part (ca. 70 – 90%) of the WGPD mass was dissolved during the leaching decreasing the total solid mass remarkably. As a consequence, the metal content per mass unit of solids increased. This makes it challenging to reach the goal of decreasing the total metal content in the leach residue below 1000 ppm, even with good metal extraction into the leach solution.

The lead concentration was shown to be reduced from the original concentration (ppm in WGPD) during leaching at 90 °C HCl (0.3 and 0.6 M) and at 50 and 70 °C in citric acid (0.6 M), despite of the mass reduction during the leaching. This suggests that citric acid can be an effective leaching agent for lead removal from WGPD.

Keywords fly ash, acid leaching, metal extraction, waste incineration

Författare Jenna Lehtola

Titel Lakning av metaller ur avgasreningsdamm

Institution Insitutionen för kemiteknik och metallurgi

Professur Hydrometallurgi och korrosion**Kod för professuren** MT-85

Övervakare Professor Mari Lundström

Handledare / Granskare DI Heini Elomaa & DI Sipi Seisko

Datum 24.03.2017**Sidantal** 61 + 48**Språk** Engelska

Sammandrag

Avfallsproduktionen ökar konstant, och andelen avfall som går till förbränning ökar samtidigt. Detta leder till en ökad mängd aska, som måste behandlas adekvat. Denna aska är, förutom en utmaning ur avfallshanteringsperspektiv, även en möjlig sekundär råvara tack vare sitt innehåll av potentiellt värdefulla metaller.

I denna avhandling undersöktes lakning av metaller ur flygaska från ett avfallsförbränningsverk i Finland. Fokus låg på lakning av koppar, järn, nickel, bly och zink. Ättiksyra ($C_2H_4O_2$), citronsyra ($C_6H_8O_7$), etalin, saltsyra (HCl), oxalsyra ($C_2H_2O_4$) och svavelsyra (H_2SO_4) testades i lösningskartläggningsprover för att hitta det mest effektiva lösningsmedlet för flygaska. Saltsyra och citronsyra fanns vara de mest effektiva oorganiska respektive organiska lösningsmedlen. Dessa syror undersöktes därför vidare i testserier med reaktorlakning. Från reaktorlakningens resultat byggdes lakningsmodeller med hjälp av programmet Modde 8.0.

Ett annat mål med detta arbete vara att minska den totala metallkoncentrationen i lakningsresten av flygaskan till under 1000 ppm. Förutom detta låg intresset på selektiv lakning mot järn, med målet att hitta ett lösningsmedel som lakar ut andra metaller ur flygaskan men lämnar järnet oberört. Denna selektivitet fanns till viss mån hos ättiksyran.

Vidare påvisades att halterna av järn, nickel och zink i lakningsresten ökade i alla reaktorlakningstester. Denna ökning berodde på att merparten (ca. 70 - 90%) av flygaskans massa löstes upp i lakningen, vilket markant minskade på den totala massan av fast ämne. Som en följd av detta ökade de relativa metallhalterna per massenhet. Detta leder till att det är utmanande att nå målet att minska på den totala metallhalten till under 1000 ppm, även om lakningen av metaller vore effektiv. I dessa försök var lakningen inte alltid på en optimal nivå.

Massminskningsproblemen till trots, visade sig blykoncentrationen ha minskat i flygaskans lakningsrest vid lakning i saltsyra vid 90 °C (0.3 och 0.6 M) och i citronsyra vid 50 och 70 °C (0.6 M). Detta indikerar att citronsyra har potential som ett effektivt lösningsmedel för att laka ut bly ur flygaska.

Nyckelord flygaska, lakning med syra, metallextaktion, avfallsförbränning

FOREWORD

This Master's thesis was carried out in the Department of Chemical and Metallurgical Engineering at Aalto University's School of Chemical Technology between September 2016 and March 2017. I want to thank Ekokem Oyj for funding this project. The support of projects CMeco (Circular Metal Ecosystem) funded by TEKES and Clic Innovation Oy as a part of the Material Value Chains (ARVI) project is acknowledged. "RawMatTERS Finland Infrastructure" (RAMI) supported by Academy of Finland is also greatly acknowledged.

I am grateful to professor Mari Lundström for taking me to work in the lab of Hydrometallurgy and Corrosion, and for her never ending energy, expertise and inspiration.

M.Sc. Heini Elomaa and M. Sc. Sipi Seisko have been an irreplaceable duo during this work. Beyond academic support and expertise, they offered me shoulders to cry on and ears to complain to, as well as the occasional beverage to keep up the good spirit.

In fact, all my colleagues in the awesome lab team, who are always very helpful and great team players, are to thank for their support and help. The coffee breaks have been an irreplaceable breathing space to weather the brain between turns.

My whole education career, starting in 1997, has led to this thesis, starting with the education system of Finland, which has provided me with world class basic education. As a part of this, the relatively unique system with state funded school lunch has been a great facilitator of studying.

The greatest of thanks go to my parents, who have always believed I was smart, even when I did not, and my whole big family who has supported me, not only during study life, but my whole life. Janni and Jere, thanks for all your various kinds of support. Mummo ja vaari, kiitos. Markus, my partner (and IT-support guy), thank you for your patience and love.

I would also like to thank my fellow students, without whom student life would have been so much poorer on experiences and happiest of memories. I am grateful also of all my other friends, especially some special ladies from Borgå. Thanks also to Teknologföreningen, Vuorimieskilta, and Otaniemi. The happiest time of my life, as I can remember, has been the N years in Teekkarikylä.

A special thanks goes to the coffee producers who produced all the cups of coffee I drank during the writing of this thesis.

Espoo, 22th of March 2017.

Jenna Lehtola

Contents

FOREWORD	IV
I THEORETICAL PART	1
1 Introduction	1
2 Waste incineration.....	3
3 Waste incineration ash	5
3.1 Typical components in waste incineration ash.....	5
3.2 Treatment of waste incineration ash.....	6
3.2.1 Separation methods	6
3.2.2 Residue thermal treatment.....	8
3.2.3 Residue solidification/stabilization (S/S) treatment.....	8
3.3 Fly ash properties	9
4 Leaching of fly ash.....	13
4.1.1 Effect of concentration	14
4.1.2 Effect of temperature.....	18
4.1.3 Effect of retention time	20
II EXPERIMENTAL PART	23
5 Experimental methods and materials	23
5.1 Waste gas purification dust	23
5.2 Studied leaching solutions.....	26
5.3 Equilibrium potentials	28
5.4 Experimental setup and leaching procedure.....	29
5.4.1 Preparations.....	29
5.4.2 Solution mapping tests	30
5.4.3 Batch leaching tests for WGPD	32
6 Results and Discussion.....	34
6.1 Mapping test results.....	34
6.1.1 Effect of temperature.....	42
6.1.2 Effect of concentration	43
6.2 Batch leaching test results	47
6.2.1 Effect of temperature.....	49
6.2.2 Effect of concentration	51
6.2.3 Effect of leaching time	53

6.2.4	SEM analysis of the leaching residue of WGPD after batch leaching.....	54
6.2.5	Batch leaching residue chemical analysis	55
6.2.6	Extraction modelling.....	58
7	Conclusions	60
8	References	62
	Appendix	66

I THEORETICAL PART

1 Introduction

Waste from municipalities or enterprises is conventionally managed through recycling, put in landfills or incinerated. Waste incineration is increasing in Finland, which leads to increasing production of ashes. In 2014, 2.6 million tons of municipal waste was produced in Finland, of which 1.3 million tons was delivered to energy recovery, 856 000 tons were recycled or recovered as material, and 460 000 tons were landfilled [1]. These ashes need to be treated using methods that ensure safety for the environment and human health. As it is increasingly difficult to find sites for landfills, and the material cycles are becoming more sustainable, an increasing part of the streams currently classified as waste is becoming a resource. Municipal solid waste incineration (MSWI) ash can be utilized in e.g. cement and concrete production, glasses and ceramics, stabilizing agents, adsorbents, zeolite production, road pavement and in agriculture [2], as long as the levels of toxic compounds are controlled and below allowed values. Moreover, the ashes from waste incineration contain significant amounts of metals and can be considered as a secondary raw material.

In this thesis, the leaching of metals from fly ash was investigated. The ash used in these experiments is waste gas purification dust (WGPD), and comes from a waste incineration plant in Finland. There was a need to investigate this particular WGPD, since the hydrometallurgical recovery of metals from this WGPD fraction was not investigated earlier. Also, as far as could be found in literature review, ethaline, or any other deep eutectic solvent, has not been investigated as a potential lixiviant for WGPD before this. First, six different solutions were tested in mapping tests in order to find the most effective lixiviant. The solutions investigated were acetic acid ($C_2H_4O_2$), citric acid ($C_6H_8O_7$), ethaline, hydrochloric acid (HCl), oxalic acid ($C_2H_2O_4$), and sulfuric acid (H_2SO_4). The metals of interest in this work were copper (Cu), iron (Fe), nickel (Ni), lead (Pb), and zinc (Zn). After mapping, the most efficient solution was further tested in batch leaching test series. In these tests, the leaching behavior was examined as a function of the temperature and acid concentration. The pH and redox potential were measured during both mapping and batch leaching experiments. Finally, mathematical models for metals dissolution into the chosen lixiviant were built.

Besides from investigating the leaching behavior of solvents, the objective was to reduce the WGPD leach residue metal concentrations of especially lead, zinc, and copper, but also nickel and arsenic, to less than 1000 ppm. Another interest was the selectivity of metal dissolution towards iron, with the goal of finding a solvent that would extract the metals of interest, but leave iron undissolved.

The thesis literature part focus was on waste incineration process. Also, the types of ash, their properties and their treatment methods, with special focus on ethaline, were considered. In the experimental part, the methods and materials of the performed leaching experiments are reviewed, and results are presented, discussed and compared to the results from literature. The aim of the work is to suggest the most promising leaching environment for Pb, but also for Zn, Cu and other metals present in the WGPD.

2 Waste incineration

According to the basic principle of recycling, everything that it is possible for, is recycled or reused, whereafter energy is recovered, and finally rest is landfilled. Waste incineration is one possible thermal treatment for waste, the others being pyrolysis and gasification [3]. In Europe, waste incineration is by far the most modern and dominant method used.

Incineration is an environmental friendly and economic way to treat waste streams that cannot be recycled or reused. The incineration takes place at waste incinerator plants, of which many nowadays are waste-to-energy plants. The mass and volume of the waste is reduced and hazardous components are made inert, while the plant is generating thermal energy that is transformed into electrical energy. At the same time, the emission of pollutants is minimized. [3]

The waste incineration process starts with adding the fuel, which is the waste, into the feed hopper by crane. From there the waste goes via the feed chute into the furnace. The heat of the furnace heats circulating water into steam, which goes into turbines that generate electrical energy. Air flow is secured to the furnace to make sure the combustion is as complete as possible. [4] The schematic figure of a waste incineration plant is depicted in Figure 1.

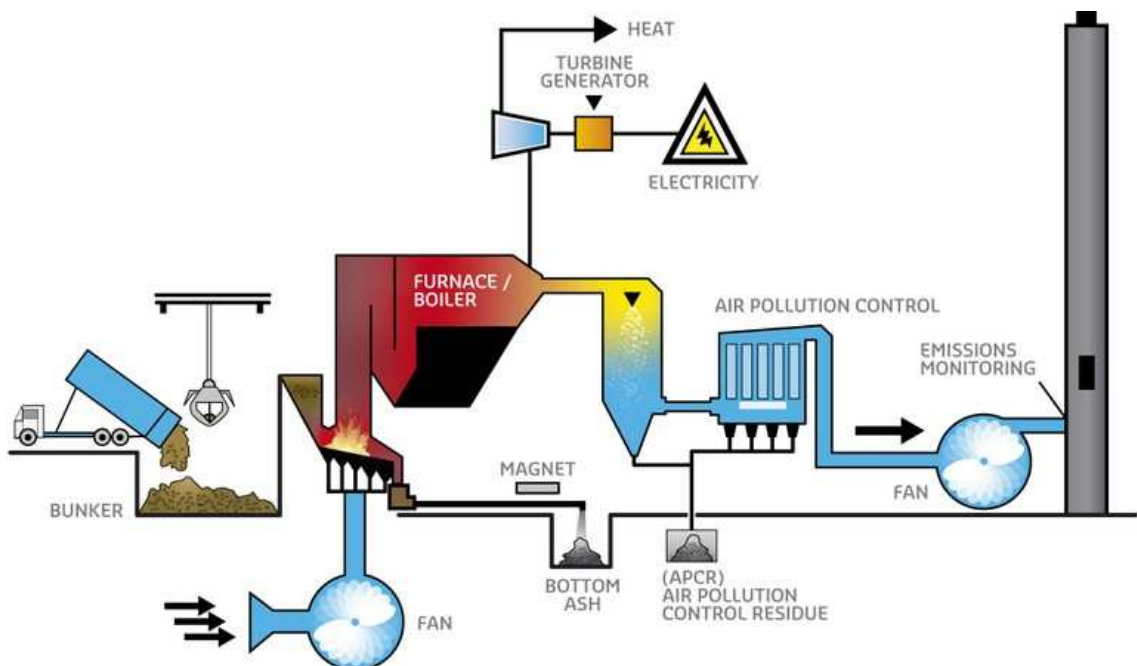


Figure 1. Schematic figure of a waste incineration plant. [3]

Besides from thermal/electrical energy the process generates bottom ash/slag and flue gas. Magnetic metals, such as iron, are removed from the bottom ash, and it goes to further treatment. The flue gas is purified in a multi-step process, in which solid particles are removed and contaminants are removed. The solid dust and heavy metal particles are removed using cyclones, electrostatic precipitators or fabric filters [5]. Problems with dust and SO₂ and NO_x removal already have satisfying solutions, but the heavy metals treatment is still an aspect to develop further [6].

The temperature of the incineration process should be at least 850 °C, and the residence time at least 2 s to ensure complete combustion and avoid formation of dioxins and carbon monoxide. However, in order to avoid dioxin/furan formation, the combustion temperature should be above 1000 °C, and the combustion chamber turbulence should have a Reynolds number greater than 50 000. Also, the MSW feed should be properly prepared and the feed rate controlled. After the combustion, a very rapid gas cooling from 400 to 250 °C should be achieved. [2]

3 Waste incineration ash

The ashes from waste incineration can be divided into ashes from the first and from the second phases of incineration. A third, small group, is the boiler slag. In this thesis, the focus lies on ashes from the second phase, separated from flue gas and dust from the waste gas purification processes.

3.1 Typical components in waste incineration ash

The major components of the ashes from municipal waste incineration are usually similar. They consist of calcium, alkali metals such as potassium and sodium, aluminum, iron, lead, and zinc. The typical minor components that are not always included are arsenic, cadmium, and copper [7]. However, metal species present in the ash depend on the type of waste and incineration furnace used, which varies between localities and municipalities.

The main solid wastes from waste management point of view generated in the incineration process are bottom slag and ash from the first phase of incineration, fly ash that is separated from the flue gas, dust from the waste gas purification processes (air pollution control residue, APC residue), and mixtures of these. Additionally, some relatively small amounts of boiler slag is produced in the boiler. 15 to 25% of the weight, and 5 to 15% of the volume, of the original waste becomes ash in incineration. Typically, 10 to 20 % of the ash weight is fly ash. [8]

Fly ash refers to fine particles that are separated from the flue gas using air pollution control equipment, such as cyclones, electrostatic precipitators, fabric filters, or scrubbers. The scrubber types are dry, half dry, or wet. The composition of the dust depends on the used equipment and method, the temperature window, and additives. [9]

In general, fly ash has a higher level of heavy metals than bottom ash, since some of these metals (e.g. Pb, Zn, As, Cd) vaporize during combustion, and also adsorb on the surface of already formed fly ash particles. Also the relative amount of chloride is higher in fly ash than in bottom ash, conceivably due to the lime scrubber in the air pollution control system. This scrubber removes acidic gases such as HCl, which leaves the fly ash with a higher chloride content after the APC system. [2]

3.2 Treatment of waste incineration ash

In this work the focus of the experimental part is on leaching of metals, which usually is the first important step in ash treatment processes. Special focus was put on the deep eutectic solvent, ethaline. Leaching is the method of choice when looking for metal recovery and recycling [10].

The treatment methods for fly ash or air pollution control residues can be divided into three classes: separation processes, solidification/stabilization, and thermal methods [11]. These can be further divided into washing, leaching, electrochemical processes, flocculation/filtration, ion exchange, crystallization/evaporation, vitrification, sintering, fusion, stabilization, S/S with binders, macro-encapsulation etc. The classes of treatments and their subgroups are shown in Figure 2. The process often starts with separation treatments followed by thermal or solidification/stabilization (S/S) treatments.

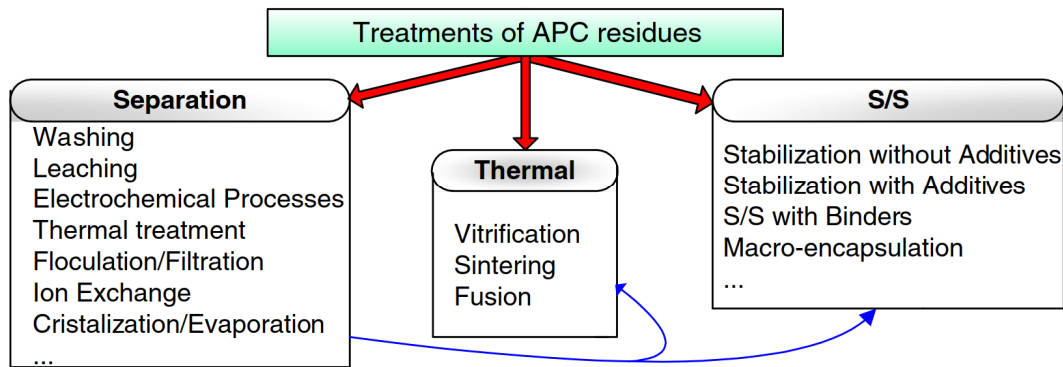


Figure 2. Treatments of air pollution cleaning (APC) residues. Separation is usually followed by thermal or solidification/stabilization treatments. [12]

3.2.1 Separation methods

Methods that aim at extracting some species from the ash, improving the quality of the residue and/or recovering the species are separation methods. Washing is used to remove salts that are soluble in water, such as calcium. A problem might be that part of the heavy metals are released at the same time. However, this can be avoided by using chemical additives, such as phosphates [12]. In leaching the goal is to get high enough concentrations of species in solution in order to further separate or recover them. Extraction efficiency of each metal of interest is determined by leaching process parameters such as temperature, pH, leaching time, the used leaching solution, oxidizing agents used and the liquid/solid ratio.

Most leaching reactions of metals are electrochemical in nature. This means that there is oxidation and corresponding reduction reaction(s) with electron transfer involved. If electrolysis i.e. electrochemical cell with external current/potential source is applied, the reactions are driven by the potential difference between the electrodes. The advantage is that no chemical additions are needed. The effectivity of these processes depends on the current density, distance between the electrodes, mixing conditions, pH of the solution, and temperature. Thermal treatment utilizes evaporation processes to remove heavy metals with relatively low boiling point. The main metals recovered by evaporation are Zn, Pb, Ca and Cd.

Commonly used lixiviants in leaching are mineral acids and or organic acids. However, there are also some relatively low cost ionic liquids such as ethaline. Deep eutectic solvents are a relatively new field of research, with the first article in the topic published in 2001 [13]. These solvents contain large, asymmetric ions with low lattice energy and hence low melting points. They are usually produced by complexing a quaternary ammonium salt with a metal salt of hydrogen bond donor [14]. In the case of ethaline, the ammonium salt is choline chloride (ChCl , $[\text{Me}_3\text{NC}_2\text{H}_4\text{OH}]\text{Cl}$) and the hydrogen bond donor is ethylene glycol, which are mixed in a 1:2 ratio. The complex anions that form when combining the salt and the hydrogen donor reduce the lattice energy, which in turn reduces the freezing point of the system [15]. Reasons for choosing choline chloride as the quaternary salt are its non-toxicity, biodegradability and low cost.

The absence of hydroxide may provide a way to avoid hazardous reagents to solubilize metal salts. The current efficiency can be improved by eliminating side electrode reactions involving water and its ionic constituents (H^+ and OH^-). In addition, the electrochemical window in ionic liquids is wider than in aqueous solutions, which means that the potential range is wider and electrowinning of more reactive metals is possible [14]. Another advantage of avoiding aqueous liquids is that in water-free ionic liquids, much higher metal concentrations are possible, since the solubility of metals is not limited by the tendency for water to combine with metal ions and precipitate oxides and hydroxides [16]. Also, by using an ionic solvent, the cationic and anionic components can be carefully chosen, and the solvent can be tailored to meet the requirements of the system in question [17]. Furthermore, the production of strong acids or bases, which are often needed in hydrometallurgical processes, need energy to produce, whereas production of deep eutectic solvents usually does not require much energy [17].

Ethaline is a deep eutectic solvent, which is a type of ionic liquid. Ionic liquids are solvents which consist solely of ions [14]. They have a high solving ability and good electrolytic properties. Ionic liquids also have potential for high selectivity in both recovery and dissolution. [16] Eutectic mixtures of salts are used to decrease the temperature for applications with molten salt. Even ambient temperature molten salts can be achieved by using deep eutectic solvents [18].

3.2.2 Residue thermal treatment

Thermal methods help reduce the volume of APC residues that are going to landfilling. Thermal processes are one of the most effective processes for destroying highly toxic dioxins, furans and other trace organic compounds [12]. However, the processes can be costly due to the high energy requirements.

Vitrification means melting the ash together with glass precursor to create a solid phase where the contaminants are fixed in a matrix. Sintering is usually performed in increasing temperatures of up to 900 – 1000 °C [12], until a chemical reconfiguration of the species of interest and a denser product is achieved.

In Fusion the ash is melted without glass precursor, creating a more heterogeneous product. If the incinerator is in a waste-to-energy plant, the created electrical energy may be utilized for the melting, otherwise a fuel-burning melting system might be applied.

3.2.3 Residue solidification/stabilization (S/S) treatment

In solidification processes a liquid or a sludge is transformed into a solid with or without using additives or binders, reducing the mobility of the contaminants. A common method is to bind the contaminants in cement. Stabilization means converting contaminants into other chemical forms that are less toxic or less soluble. The most effective procedure is to first stabilize and then solidify the material.

The immobilization of heavy metals depends on redox potential control, pH and the chemical speciation of metal. For organic compounds the immobilization can be achieved by reactions destroying or altering organic structures or by physical processes. This is a low cost and well established technology, but S/S methods include a risk for significant mass and volume increase with some of the used binders. This leads to increased transportation and landfill costs. Another drawback is that this method is ineffective for treating soluble salts, and those should therefore, if possible, be removed before adding binders. Also, this method does not support circular economy of metals as the elements

present in the ash are not taken as raw material but as a waste to be stabilized and landfilled. [12]

3.3 Fly ash properties

In this chapter, fly ash properties and leaching data from public domain is reviewed. In Table 1 fly ash properties from literature are presented. In the study of Nagib & Inoue [6], the fly ash was collected by the electrostatic precipitator at NKK Japan, whereafter it was digested by aqua regia and analyzed. Taiheiyo Cement Corp. Japan donated the fly ash to Huang *et al.* [7 & 10]. It was digested in aqua regia and analyzed by Shimadzu model ICP8100 inductively coupled plasmas–atomic emission spectrometry (ICP/AES) spectrometer. The fly ash in study of Zhang & Ma [19] came from ONE MSWI incineration plant in Shanghai China. It was dried at 105 °C in the oven and then content and leaching toxicity analysis was performed. The data ranges presented by Chandler *et al.* [11] are from a data base of data from mass burn incinerators in 7 countries and 39 different facilities.

The most common elements in fly ash from these sources are calcium (2270 – 250000 ppm), aluminum (2000 – 90000 ppm), chlorine (17000 – 380000 ppm), iron (1500 – 97000), potassium (12100 – 79500 ppm), magnesium (600 – 170000 ppm), sodium (720 – 114800 ppm), lead (2000 – 107000 ppm), sulfur (1400 – 45000 ppm), silicon (36000 – 210000 ppm) and zinc (7000 – 70000 ppm). Of these, zinc, calcium, chlorine, potassium, sodium and sulfur have low boiling points, which is why they are evaporated in the burning process and commonly end up in the gas purification stage. The high calcium content in the ashes are due to large amounts of calcium added in the process in order to remove acid gases such as SO_x and NO_x and hydrogen chloride from the waste gas [7].

Table 1. Published chemical composition of Fly ash. All values are in ppm.

	Nagib & Inoue, 2000 [6]	Huang et al., 2011 [10] & [7]	Zhang & Ma, 2012 [19]	Chandler et al., 1997 Fly Ash (mg/kg) [11]	Chandler et al., 1997 Dry/Semi dry APC System Residues [11]	Chandler et al., 1997 Wet APC System Residue without Fly Ash [11]	Chandler et al., 1997 Wet APC System Residue/Fly Ash Mixture [11]
Al	18500	2000	19210	49k - 90k	12k - 83k	21k - 39k	71k - 81k
As				37 - 320	18 - 530	41 - 210	130 - 190
Ba			539	330 - 3100	51 - 14k	55 - 1600	330 - 1900
Ca	2270	288800	258k	74k - 130k	110k - 350k	87k - 200k	93k - 110k
Cd			95	50 - 450	140 - 300	150 - 1400	220 - 270
Cl				29k - 210k	62k - 380k	17k - 51k	48k - 71k
Co			14	13 - 87	4 - 300	0.5 - 20	14 - 22
Cr			72	140 - 1100	73 - 570	80 - 560	390 - 660
Cu			570	600 - 3200	16 - 1700	440 - 2400	1000 - 1400
Fe	21190	1500	5240	12k - 44k	2600 - 71k	20k - 97k	15k - 18k
Hg				0.7 - 30	0.1 - 51	2.2 - 2300	38 - 390
K	79500	12100	23k	22k - 62k	5900 - 40k	810 - 8600	35k - 58k
Mg	600		10820	11k - 19k	5100 - 14k	19k - 170k	18k - 23k
Mn			309	800 - 1900	200 - 900	5000 - 12k	1400 - 2400
Na	114800	45700		15k - 57k	7600 - 29k	720 - 3400	28k - 33k
Ni			22	60 - 260	19 - 710	20 - 310	67 - 110
Pb	107000	22100	2000	5300 - 26k	2500 - 10k	3300 - 22k	5900 - 8300
S				11k - 45k	1400 - 25k	2700 - 6000	11k - 26k
Si				95k - 210k	36k - 120k	78000	120000
Sb				260 - 1100	300 - 1100	80 - 200	
Sn				550 - 2000	620 - 1400	340 - 450	1000
Sr			151	40 - 640	600 - 500	5 - 300	200
Ti			3496	6800 - 14k	700 - 5700	1400 - 4300	5300 - 8400
Zn		58k		9000 - 70k	7000 - 20k	8100 - 53k	20k - 23k

Also some mineralogical analysis was found in literature. Romero *et al.* investigated fly ash from domiciliary solid waste incineration was by SEM [20]. Andreola *et al.* used X-fluorescence (Philips PW 2004), of the insoluble fraction of fly ash from municipal recycling program [21]. Haiying *et al.* analyzed MSWI fly ash from Pudong MSW Incineration Plant, Shanghai, China. The chemical composition was analyzed by XRF on a SRS 3400 fluorescent X-ray spectrometer, and the mineral composition was analyzed by XRD on a Philips powder diffractometer. [22] Cheng & Chen analyzed fly ash from a municipal solid waste incinerator in Taipei by inductively coupled plasmas–atomic emission spectrometry (ICP-AES) [23].

Ginés *et al.* investigated air pollution control fly ashes from a single municipal solid waste incinerator in Tarragona, Spain [24]. Pan *et al.* analyzed MSWI ash obtained from the

municipal solid waste incinerator of the Hsinchu City in Taiwan. The chemical compositions were determined X-ray fluorescence spectrometry (XRF). [25] Yang *et al.* had fly ash from a MSWI plant in southern China and analyzed it by XRF on a SRS 3400 fluorescent X-ray spectrometer to detect chemical composition [26]. Cobo *et al.* analyzed bag filter (BF) fly ash from a hazardous waste incinerator located in Medellín, Colombia by X-ray fluorescence using a Philips model PW1480 [27]. In Table 2 it can be observed that the usual main components in fly ash are SiO₂, CaO and Al₂O₃, except for the fly ash investigated by Cobo et al. [27], where the main components are Cl⁻, Na₂O, and ZnO.

Table 2. Fly ash mineralogy from literature. All values are in wt-%.

Authors	[20]	[21]	[22]	[23]	[24]	[25]	[26]	[27]
CaO	29.3	37.5	35.8	19.7	43.05	24.9	16.6	2.3
SiO ₂	11.5	18.5	20.5	19.4	6.35	30.7	27.5	6.5
Al ₂ O ₃	5.8	7.37	5.8	10.1	3.5	22.3	11.0	0.4
SO ₃	-	14.4			4.64	5.2		2.9
K ₂ O	7.0	2.03	4.0	8.1	4.59	1.5		5.7
Fe ₂ O ₃	1.3	2.26	3.2	1.8	0.63	3.6	5.0	3.3
MgO	3.0	2.74	2.1	2.8	1.38	4.3	3.1	
TiO ₂	0.9	1.56		1.9			1.9	0.2
P ₂ O ₅	1.7	1.56						4.2
Na ₂ O	8.7	2.93	3.7	8.9	5.80	1.7		15.1
MnO	0.2	0.129						
BaO		0.139						
CuO		0.281						0.4
ZnO					1.41			12.1
Na ₂ O + K ₂ O							8.2	
Cl ⁻							10.3	33.2
SO ₄ ⁻							8.3	
Cr ₂ O ₃								0.1
NiO								0.1
PbO								2.4
Sb ₂ O ₃								8.8

In addition to Table 2, Bodog et al. [28] reported of fly ash from a municipal waste incinerator in Hungary, which had the main components syngenite (K₂Ca(SO₄)₂ *H₂O), apththitalite ((K,Na)₃Na(SO₄)₂) and anhydrite (CaSO₄). They also investigated fly ash from a dangerous waste incinerator in Switzerland with the main components montmorillonite ((Na,Ca)_{0.33}(Al,Mg)₂(Si₄O₁₀)(OH)₂·nH₂O) and illite (K,H₃O)(Al,Mg,Fe)₂(Si,Al)₄O₁₀[(OH)₂,(H₂O)]. In addition, a high amount of amorph phases were also found. These morphological investigations were carried out by X-ray powder diffraction (XRD, Philips M-1051, USA).

Fly ash in itself is very heterogeneous, and it should be noted that differences in partitioning depend strongly on the operation conditions and the properties of the raw material. This means that investigating fly ash samples from different sources usually gives different results. The x-ray diffraction of fly ash is quite complex [6], which can also be seen in the work of Haiying *et al.* [22], where it was found by XRD analysis of the fly ash that the major mineral constitutions were SiO_2 , $\text{K}_2\text{Al}_2\text{Si}_2\text{O}_8 \cdot 3.8\text{H}_2\text{O}$, $\text{AlCl}_3 \cdot 4\text{Al}(\text{OH})_3 \cdot 4\text{H}_2\text{O}$, $\text{Ca}_3\text{Si}_2\text{O}_7$, $\text{Ca}_9\text{Si}_6\text{O}_{21} \cdot \text{H}_2\text{O}$ and $\text{Ca}_2\text{SiO}_4 \cdot 0.35\text{H}_2\text{O}$, in addition to the XRF results in Table 2.

This means that, in the framework of this thesis, it is difficult to say much about the general dissolution mechanisms of fly ash, since (i) the mineralogy of fly ash varies remarkably and (ii) the analysis of mineralogy is very challenging due to the heterogeneous nature of the raw material, amorphous phases present, complex compounds present and difficulties in mineralogical analysis. However, some general phenomena are valid as the metals present in the ash fraction are leached into the solution. According to Wu & Ting, the high solubility of Fe in oxalic acid is due to the highly soluble FeC_2O_4 , whereas the leaching of lead was low in sulfuric acid and oxalic acid due to the low solubility of PbSO_4 and PbC_2O_4 [29]. Furthermore, according to Cobo *et al.* [27] heavy metals are fixed in the net structure of SiO_2 , which leads to resistance to leaching.

4 Leaching of fly ash

A variety of acids have been tested for leaching of air pollution control residue by Huang *et al* [7]. Table 3 shows extraction of Al, Ca, Fe, Cu, Zn, and Pb into citric, malic, acetic, lactic, oxalic, tartaric, sulfuric, hydrochloric, and nitric acid. At 0.1 M concentration, 40:1 liquid/solid (L/S) ratio, 25 °C temperature, and 1 h contact time, citric acid and malic acid were the most effective lixiviants, for all metals, except for calcium, for which citric acid had lower extraction than acetic, lactic, sulfuric, hydrochloric and nitric acids. Generally, Table 3 shows that high extractions can be achieved in several different leaching media. Lower acidity with pH above 3 restricts the leaching of Fe, keeping it in solids in sulfuric acid, hydrochloric acid and nitric acid. Oxalic acid and tartaric acid show the lowest efficiency on Pb leaching. However, the extractions of metals depend highly on the form in which minerals or compounds metals are present as well as temperature, lixiviant concentration, pH, temperature and solid/liquid ratio. This emphasizes the need of observing the process parameters in more detail.

Table 3. Extraction (%) of Al, Ca, Fe, Cu, Zn, and Pb into citric, malic, acetic, lactic, oxalic, tartaric, sulfuric, hydrochloric, and nitric acids. L/S ratio = 40:1, acid concentration 0.1 M, $T = 25\text{ }^{\circ}\text{C}$, $t = 1\text{ h}$. [7]

Leaching reagent	Final pH	Al	Ca	Fe	Cu	Zn	Pb
Citric acid	3.13	100	93.1	67.0	100	100	96.9
Malic acid	3.07	99.7	100	80.2	100	100	97.0
Acetic acid	3.02	88.4	100	23.2	100	100	70.1
Lactic acid	3.06	92.2	100	40.7	100	100	62.0
Oxalic acid	3.09	43.3	0.41	46.5	45.8	44.9	2.7
Tartaric acid	2.98	30.3	6.7	24.4	32.7	35.7	4.0
Sulfuric acid	3.03	44.2	100	5.8	52.4	57.9	28.3
Hydrochloric acid	3.10	42.5	100	2.9	50.2	54.3	14.8
Nitric acid	3.01	41.6	100	2.2	52.8	56.9	25.3

4.1.1 Effect of concentration

The effect of acid concentration in HCl on fly ash dissolution was investigated by Nagib & Inoue [6]. In Figure 3 the effects of increasing HCl concentration on different metals dissolution varied. Concentration had the greatest impact on Zn extraction, whereas it did not affect K or Na extraction almost at all. Zn, Mg, Ca and Na extractions into solution increased from almost no extraction at 5% to their respective maximum levels at 10%. Pb and Fe extractions are increasing with increasing concentration at all tested concentrations in Figure 3 (up to 20% HCl concentration). Magnesium extraction increases from 5 to 10% HCl concentration, and decreases from 10 to 20% concentration.

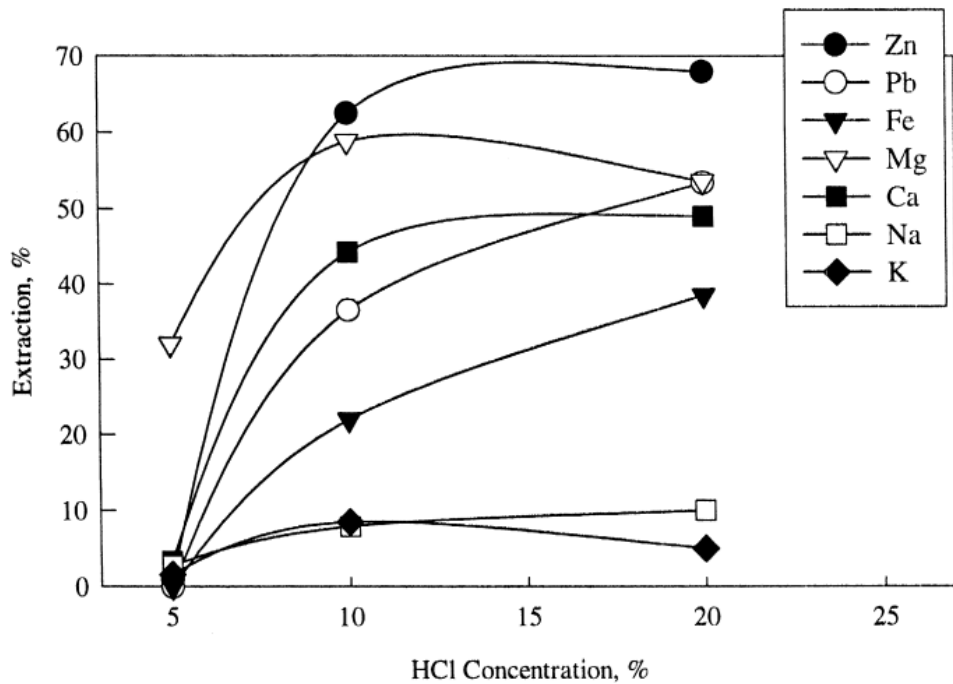


Figure 3. Extraction of Ca, Fe, K, Mg, Na, Pb, and Zn into HCl from fly ash as a function of concentration. $T = 30\text{ }^{\circ}\text{C}$, L/S ratio = 7 mL/g, contact time = 1 h. [6]

The effect of sulfuric acid concentration on leaching of Al, Ca, Fe, K, Mg, N, and Zn from fly ash was evaluated by Nagib & Inoue [6]. Figure 4 clearly shows the effect of sulfuric acid concentration on the extraction of Zn, Al, Mg, and Fe. The extraction of these metals is low (<10% for Zn, Al and Fe and ca. 25% for Mg) at 5% H_2SO_4 concentration. Zn, Mg and Fe extractions reach a maximum point at 10% extraction, whereas Al extraction still increases slightly between 10 and 20% acid concentrations. The extractions of Ca, K, and Na showed similar behavior to HCl leaching (Figure 3), as the increase in acid concentration was shown to increase metal extraction only slightly.

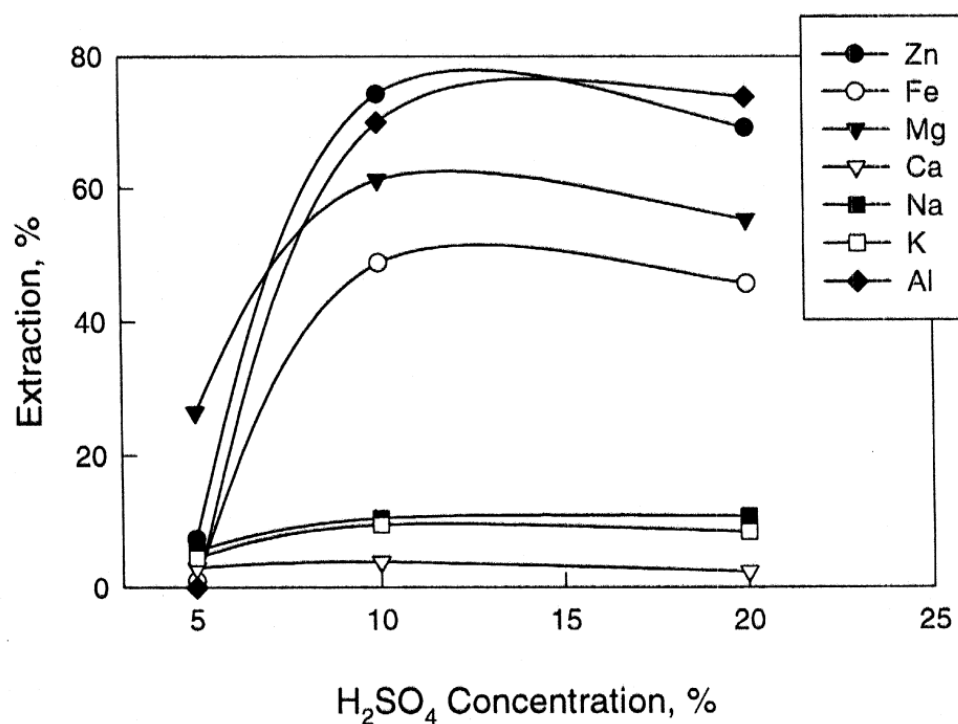


Figure 4. Extraction of Al, Ca, Fe, K, Mg, N, and Zn into H₂SO₄ from fly ash as a function of concentration. $T = 95\text{ }^{\circ}\text{C}$, L/S ratio = 7 mL/g. Contact time was 1 h. [6]

Also Zhang & Ma [19] studied the effect of concentration on metal extraction from fly ash into solution in H₂SO₄. Figure 5 displays the effect of sulfuric acid concentration on Cd, Cu, Pb and Zn extraction. It can be observed that the extraction of Pb was below 20% at all sulfuric acid concentrations and the extraction of Zn below 5%.. Pb is known to form insoluble lead sulfate which prevents Pb extraction into the sulfuric acid solutions. Cd had extractions between 75 and 85% at all concentrations, extraction decreasing slightly with increasing acid concentration above 4.7 M. Cu had a maximal extraction of 62 % at 3.7 and 9.3 M, and a minimum extraction of 42 % in 4.7 M.

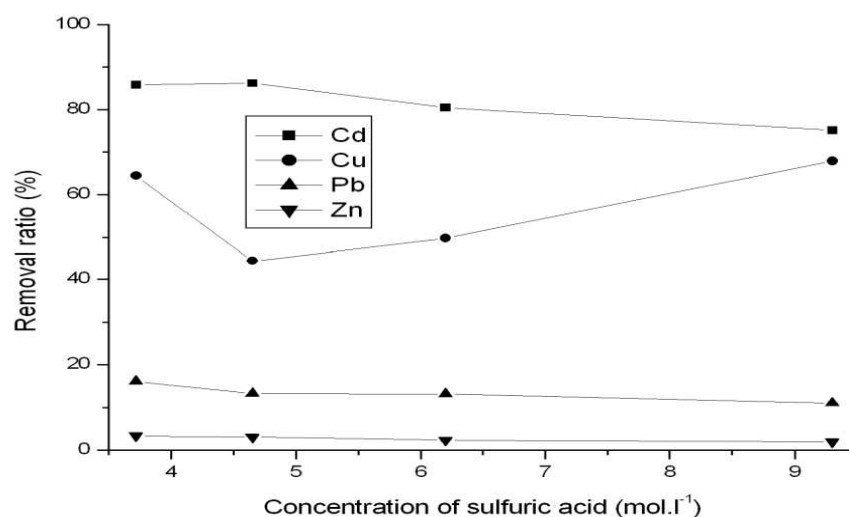


Figure 5. Removal ratios i.e. extraction of Cd, Cu, Pb, and Zn into H₂SO₄ from fly ash a function of concentration in H₂SO₄. $T = 25\text{ }^{\circ}\text{C}$, contact time = 4 h. [19]

From Figure 6 it can be seen that the extraction of Al, Ca, Cu, Fe, Pb, and Zn into citric acid was strongly dependent of acid concentration. Up to the concentration 0.2 M the extractions were increasing with increased concentration, after which the maximum extraction level into the citric acid solution was reached. In the article by Huang *et al.* [7], using 0.1 M concentration was recommended for economic reasons for MWI fly ash leaching. Figure 6 shows that Al, Ca, Cu, Zn and Pb can be extracted into the citric acid solution at high recovery. At low concentration, recoveries for Al, Zn and Cu are the highest whereas with increasing concentration up to 0.1M, also extraction of Pb increases to close to 100%. Figure 6 suggests some selectivity of Cu and Zn leaching (80% yield to solution) towards Pb and Fe leaching (<40% yield to solution) at very low citric acid concentration. This suggests that leaching with very dilute citric acid solution solutions, at room temperature with 1 hour contact time, Zn and Cu extraction can become one attractive option, keeping Fe and Pb in solution at lower level.

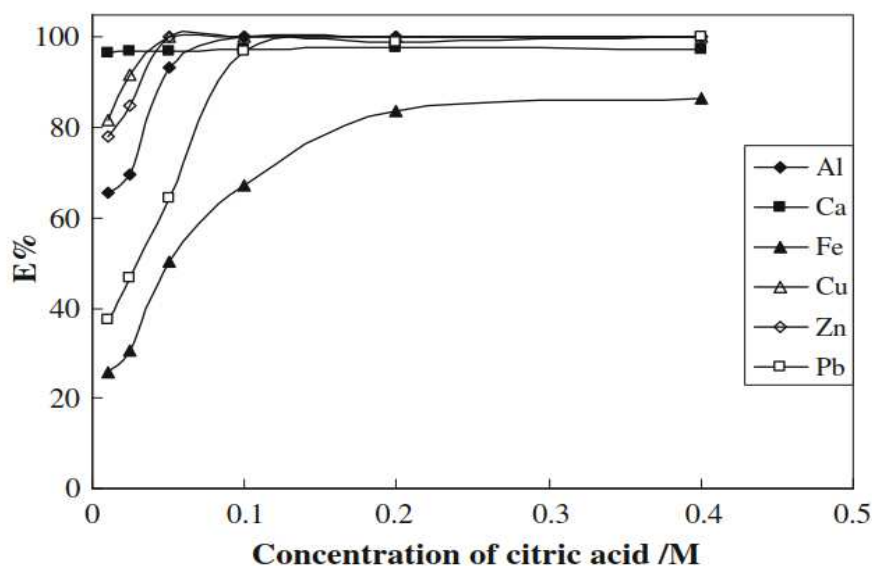


Figure 6. Extraction of Al, Ca, Cu, Fe, Pb, and Zn into citric acid as a function of concentration. $T = 25^{\circ}$, contact time = 1 h, final $pH = 3.0$, L/S ratio 40:1. [7]

In the study of Hu & Ting [29], the extraction of Al, Cu, Fe, Mn, Pb, and Zn into solutions from 1% (w/v) fly ash was tested in nitric acid, sulfuric acid, citric acid, oxalic acid and gluconic acid at 0.1 and 0.5 M concentrations. The results are shown in Figure 7. In general, the extraction percentage of metals was about the same at both concentrations for sulfuric acid and citric acid. On the other hand, the extraction of metals into nitric and gluconic acid increased with increasing concentration. The leaching of metals into oxalic acid was unchanged (for Cu) or slightly decreased (for Al, Fe, Mn, and Zn) with increasing concentration, except for Pb extraction, which increased. The temperature of the experiments was 30°C , and the solution was mixed at 120 rpm.

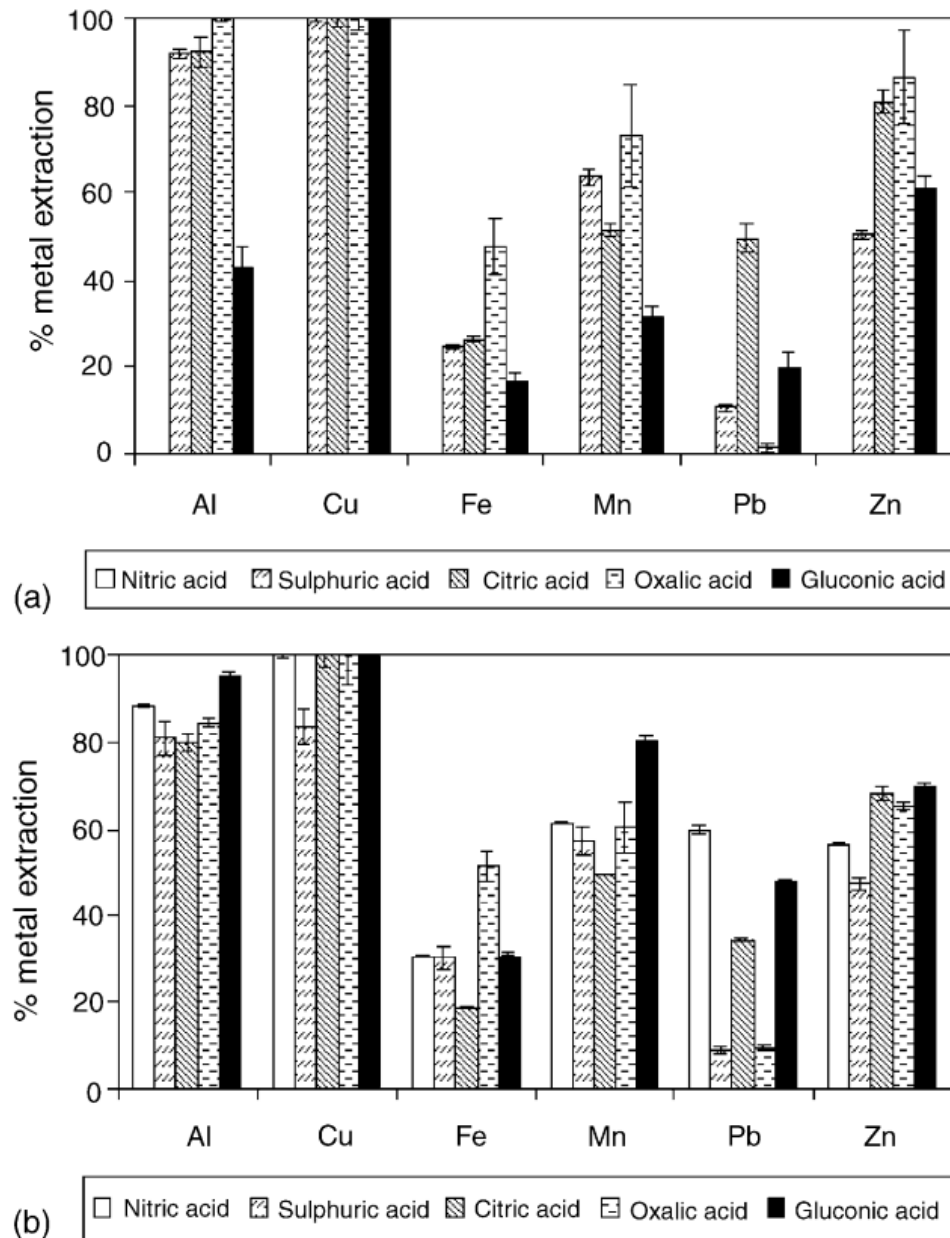


Figure 7. Extraction (%) of Al, Cu, Fe, Mn, Pb, and Zn from MSW fly ash into nitric acid, sulfuric acid, citric acid, oxalic acid, and gluconic acid. The temperature was 30 °C and stirring was set to 120 rpm. [29]

4.1.2 Effect of temperature

The effect of temperature on Al, Ca, Fe, K, Mg, Na, and Zn extraction from primary fly ash in 10% H₂SO₄ was investigated by Nagib & Inoue [6]. Sulfuric acid is one of the most investigated leaching media. The leaching time was 1 h and the L/S ratio used 7 ml/g. Increase in temperature did not increase the extraction of Zn, Fe, Mg, Ca, Na or Al from primary fly ash into sulfuric acid. However, increase up to 95 °C was shown to

increase Zn, Al, Mg and Fe extraction whereas elements typically remaining as salts (Na, K and Ca) were leached equally poorly at all investigated temperatures. None of the metals extractions into sulfuric acid were shown to increase up to 80%. Figure 8 illustrates the metal yields into the solution as a function of temperature.

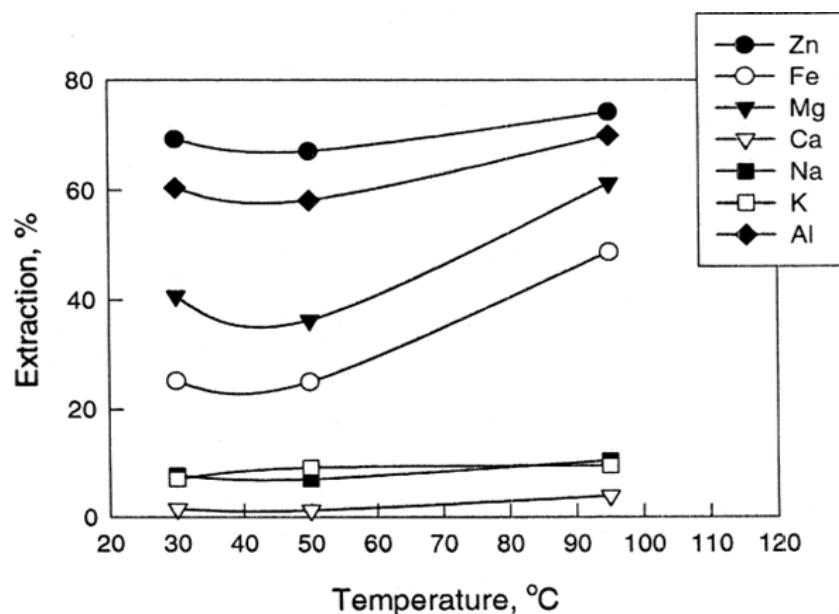


Figure 8. The extraction of Al, Ca, Fe, K, Mg, N, and Zn in H₂SO₄, concentration 10%, L/S ratio = 7 mL/g. Contact time was 1 h. [6]

Also citric acid has been investigated as a potential lixiviant for water-washed fly ash by Huang *et al.* [7]. In citric acid solution it was observed that effect of temperature on Al, Ca, Fe, Cu, Zn and Pb dissolution was negligible in 0.1 M citric acid solution, with the leaching time of 1 h (Figure 9). The investigated temperature range was 25 – 50 °C. Figure 9 shows also that citric acid resulted in almost 100% extraction for Al, Ca, Cu, Zn and Pb, and over 60% extraction for Fe.

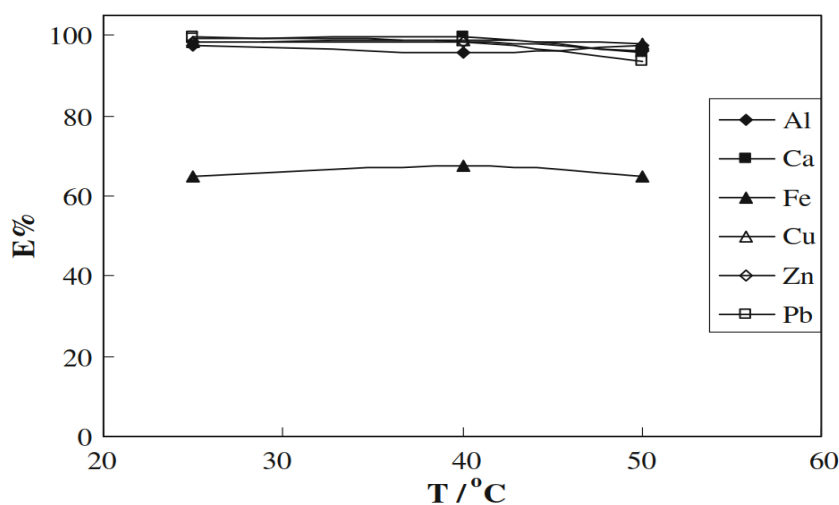


Figure 9. Extraction of Al, Ca, Cu, Fe, Pb, and Zn into citric acid. L/S ratio 40 mL/g, concentration 0.1 M. The final pH was 3.0 and the contact time 1 h. [7]

Hydrochloric acid is also one generally used leaching solution. Leaching of Al, Cd, Cu, Fe, Pb, and Zn from fly ash into HCl was investigated by Huang *et al.* [10]. As can be seen in Figure 10, temperature had only a slight effect on the extraction efficiency in the investigated range of 30 – 50 °C. Overall, the temperature did not have a large impact on the metal extraction from investigated fly ash in any of the experiments found in literature at lower temperatures up to 50 °C. However, increase up to 95 °C increased specifically Fe and Mn extraction in sulfuric acid media. A slightly decreasing trend was observed for the extraction of all metals (Pb, Zn, Cu, Fe, Cd, Al) into HCl solution in Figure 10. Also, most metals investigated could be extracted at temperatures close to room temperature. However, the typically used solid/liquid concentrations are relatively low, and in terms of industrial processing, higher solid/liquid ratios must be investigated.

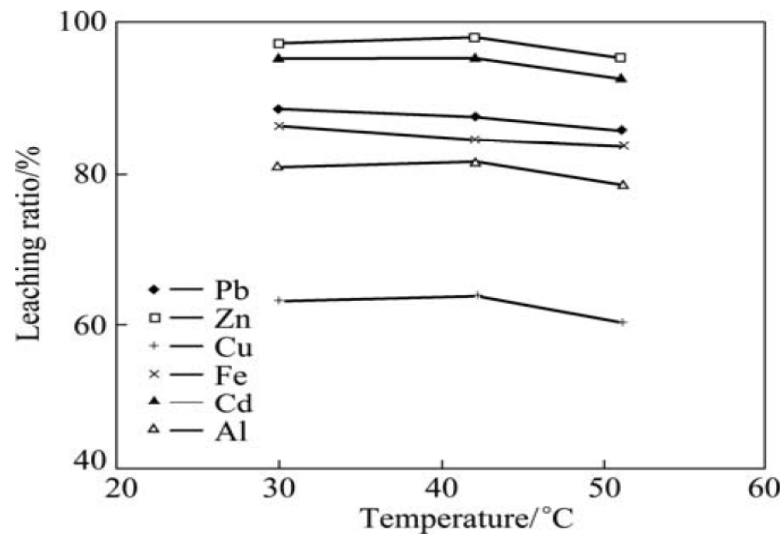


Figure 10. Leaching of Al, Cd, Cu, Fe, Pb, and Zn into HCl. $pH = 1.0$, L/S ratio = 50:1, contact time = 15 min. [10]

4.1.3 Effect of retention time

Huang *et al.* [10], found that the maximum metal extraction from MSW fly ash was reached at 20 min. Overall, time had very little effect on metal extraction rate. In Figure 11, the extraction rates of Al, Cd, Cu, Fe, Pb, and Zn into HCl are shown. Cu reached an extraction level slightly over 60%, the other metals had extractions between 80 and 100%, with the highest extraction efficiency for Cd, >95%.

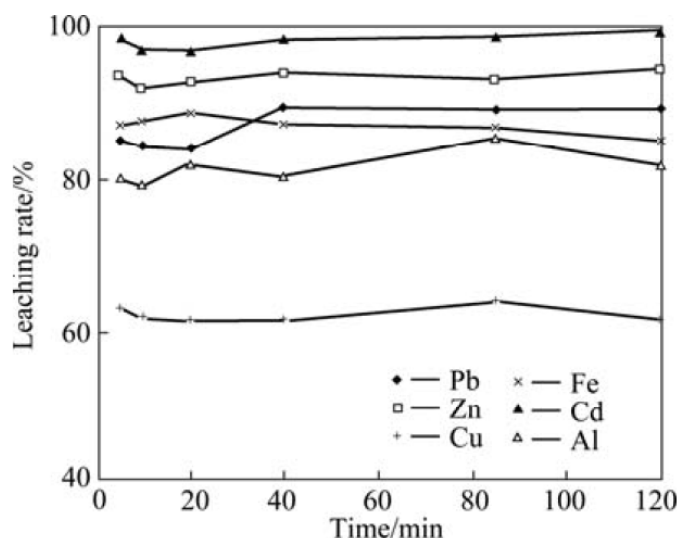


Figure 11. Leaching rate as a function of time. Al, Cd, Cu Fe, Pb, and Zn leaching to HCl. $pH = 1.0$, $T = 25\text{ }^{\circ}\text{C}$ L/S ratio 50:1. [10]

Figure 12, from the article by Nagib & Inoue [6], shows the extraction of Al, Ca, Fe, K, Mg, N, and Zn from MSW fly ash H_2SO_4 (20% concentration, $T = 95\text{ }^{\circ}\text{C}$, L/S ratio = 7:1). As it can be seen, the extraction of all metals is as good as constant after 100 min for all metals. Al, Fe, and Mg show an increase in extraction until ca. 50, 100 and 100 min respectively, the rest of the metals have as good as constant extraction over time.

Figure 12. Extraction of Al, Ca, Fe, K, Mg, N, and Zn into H_2SO_4 . H_2SO_4 concentration was 20%, $T = 95\text{ }^{\circ}\text{C}$, L/S ratio = 7 mL/g [6].

In an article by Huang *et al.* [7], the effect of time was investigated in 0.1 M citric acid at $25\text{ }^{\circ}\text{C}$ with L/S ratio 40 mL/g. As can be observed in Figure 13, all extractions increase in the beginning and have reached a maximum level at the latest after 50 min. Iron reached an extraction level of $>60\%$, whereas the extraction of other metals reached levels of $>90\%$. The results suggest that generally metals present in the ash fractions are available for leaching, the maximum extraction being achieved commonly already during 1 h contact time.

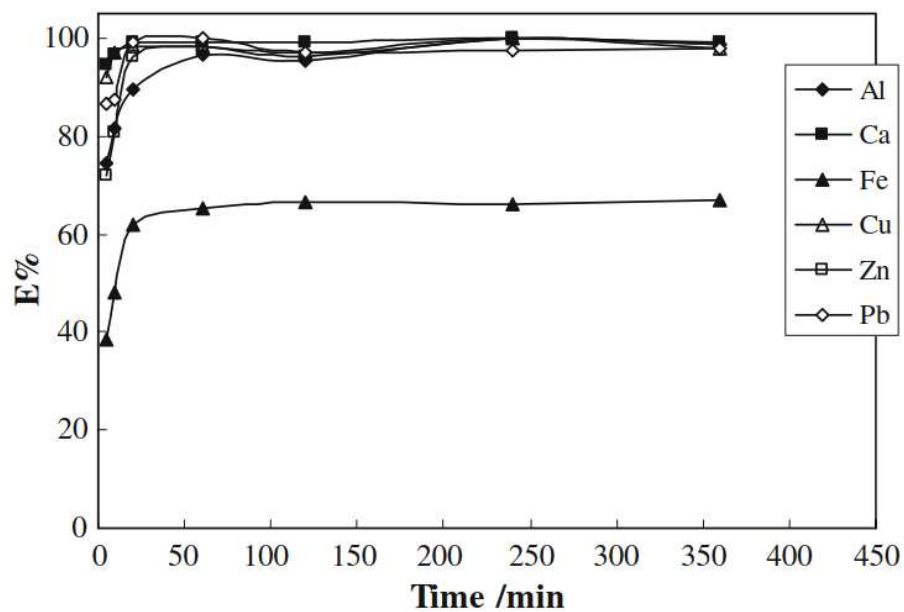


Figure 13. Extraction of Al, Ca, Cu, Fe, Pb, and Zn from MSW fly ash in citric acid as a function of time. Concentration = 0.1 M, final *pH* 3.0, *T* = 25 °C, L/S ratio 40 mL/g. [7]

II EXPERIMENTAL PART

5 Experimental methods and materials

Experiments were conducted at the Laboratory of Hydrometallurgy and Corrosion at Aalto University in Espoo, Finland. The waste gas purification dust (WGPD) was leached in different solvents in order to map out the most effective solution for batch leaching tests. The chosen lixiviants were then tested in WGPD batch leaching tests.

5.1 Waste gas purification dust

The waste gas purification dust used in the experiments was supplied by Ekokem Oyj. Previous experiments by Ekokem showed that the average size of the particles in the WGPD was 30 μm , additionally, 10% of the particles were below 5 μm [30]. The smallest detected particle size was 1-2 μm . The WGPD had previously also been analyzed with an x-ray fluorescence (XRF) device, and the results are shown in Table 4. Additionally, the characterization of the undivided WGPD made by total dissolution revealed the fractions of metals shown in Table 4. The total dissolution analysis was carried out by Milomatic Oy and the metal concentrations were determined using either Atomic absorption spectroscopy (AAS) Varian AA240 or ICP Perkin Elmer Optima 7100 DV. A comparative third characterization of the WGPD was performed by Labtium Oy. This characterization was made by total leaching and using inductively coupled plasma optical emission spectrometry (ICP-OES). The results are shown in Table 4. The results show that the major components in the WGPD raw materials were S (>34 000 ppm), Fe (>14 000 ppm) and Zn (>10 000 ppm). Additionally, there were remarkable amounts of lead (>6000 ppm), arsenic >1500 ppm and copper (>500 ppm). The minor elements present were Cr (>240 ppm), Ni (>250 ppm) and Sb (>220 ppm).

Table 4. Chemical analysis of the investigated raw material WGPD, analyzed at Ekokem Oyj (XRF), Milomatic (total dissolution and AAS/ICP-OES) and Labtium (total dissolution and ICP-OES).

METAL	XRF (Ekokem Oyj) ppm	Total dissolution AAS/ICP (Milomatic) ppm	Total dissolution ICP-OES (Labtium) ppm	Mean ppm	Standard deviation
As	1537	2700	3760	2666	908
Cd	<23	-	-	23	-
Co	<12	-	-	-	-
Cr	385	300	246	310	57
Cu	554	1100	568	741	254
Fe		14100	15400	14750	650
Hg	<20	-	-	20	-
Ni	368	300	251	306	48
Pb	8481	6800	7250	7510	711
S	-	-	34050	34050	-
Sb	223	400	377	333	79
Zn	10956	10500	11300	10919	328

Clearly, the most notable difference of the WGPD used in this thesis compared to literature, is that it contains more arsenic (As), 1537 – 3760 ppm, depending on the analysis method, vs. a maximum of 530 ppm in Dry/Semi dry systems in the work of Chandler *et al.* [11]. The amount of iron and lead in the dust used in this thesis was similar to the amount in wet APC system residue [11]. Zinc (Zn) fraction corresponded to the ranges in experiments by Chandler *et al.* [11], except for wet APC system, but were in the lower end of the ranges. Zinc content in both articles by Huang *et al.* [7 & 10] was higher. The copper (Cu) percentage was about same as in literature. Nickel (Ni) concentration corresponded to concentrations in experiments by Chandler *et al.* [11]. Sulfur (S) content in the studied WGPD was higher than contents found in literature, 34050 ppm vs. a maximum of 26000 ppm [11]. Antimony (Sb) content was similar as in dry/semi dry and wet APC system residue, and higher than in wet APC system residue without fly ash [11]. Chromium (Cr) percentage corresponded to the ranges found by Chandler *et al.* [11], whereas Zhang & Ma [19] found a lower content. Cadmium (Cd) content in WGPD was low, <23 ppm, literature showed values between 50 and 1400 [11], [19]. Cobalt (Co) and mercury (Hg) were found at similar concentrations (<12 and <20, respectively) as in literature, but some literature sources displayed higher maximum levels (300 ppm Co and 2300 ppm Hg [11]).

A further characterization of the WGPD was made with Scanning electron microscope – energy dispersion X-ray spectroscopy (SEM-EDS), Leo 1450 VP INCA Software. Samples were created by pressing pellets in a hydraulic press manufactured by Compac. The pressure was 17.7 kPa. The pellets were sealed in carbon powder using a press manufactured by Struers (Prontopress 2). The prepared samples, which can be seen in Figure 14, were ground using silica paper of decreasing roughness (manufacturer: Mirka), with the finest surface roughness of 2000 grid.



Figure 14. Investigated WGPD SEM samples as pellets sealed in carbon.

The Scanning electron microscope (SEM) analyses revealed that the WGPD is mostly of amorphous character, which is indicated by the total sums of recognized points, which should be $100 \pm 10\%$ for reliable analysis. In tables in Appendix A, many measuring points outside of the error margin can be observed. This means that no exact analysis of the composition can be made, but the analysis revealed that the WGPD consists of at least Na, Mg, Al, Si, S, Cl, K, Ca, Ti, Mn, Fe, Cu, Zn and Pb. A micrograph from the SEM analysis is presented in Figure 15, in which the major elements of the bright spectra 2, 4, and 5 are lead and chlorine. Spectra 6 – 18 consist in general mainly of chlorine, calcium, and oxygen. The major elements vary between spectra and phases. SEM micrographs also suggest that the ash particles vary in size and shape, dimensions varying from micrometer size to $>60 \mu\text{m}$. The rest of the micrographs and their spectra are presented in more detail in Appendix A.

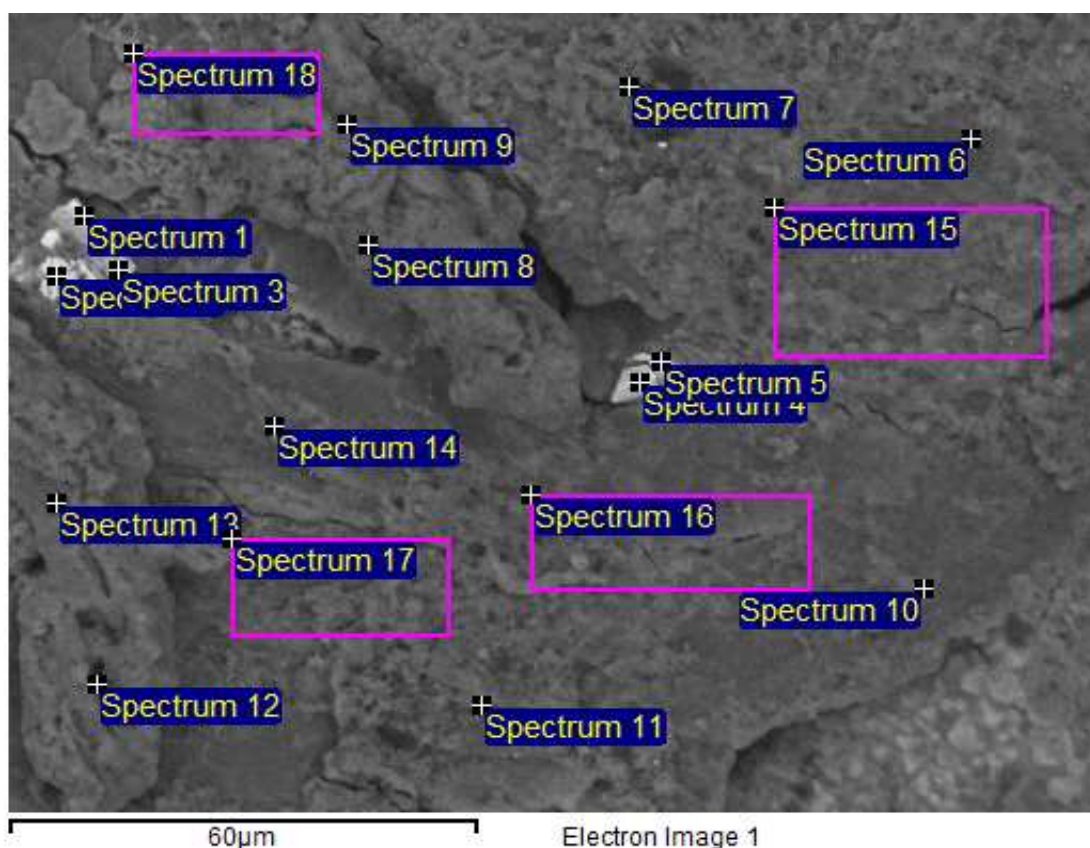


Figure 15. Micrograph from SEM-EDS analysis of waste gas purification dust (Leo 1450 VP INCA Software).

5.2 Studied leaching solutions

In order to find the most suitable lixiviant for WGPD metal leaching, 2 mineral acids, hydrochloric acid (HCl) and sulfuric acid (H₂SO₄), 3 organic acids, acetic acid (C₂H₄O₂), citric acid (C₆H₈O₇) and oxalic acid (C₂H₂O₄), and one ionic liquid, ethaline, were investigated. The studied leaching solvents and their concentrations are presented in Table 5, and the chemicals used for preparing the solutions are shown in Table 6.

Table 5. Mapping test; the solutions and concentrations studied for WGPD leaching

SOLUTION,	c (M)	SOLUTION,	c (M)	SOLUTION,	c (M)
C ₂ H ₄ O ₂	0.5	Ethaline	-	H ₂ SO ₄	0.2
	1	HCl	0.2		0.5
	2		0.5		1
	3		1		2
	5		2		3
	7		3		5
C ₆ H ₈ O ₇	0.5		5		7
	1		7	H ₂ O	-
	2	C ₂ H ₂ O ₄	1	HCl + H ₂ SO ₄	0.2
	3		0.5		
	4				

Table 6. Detailed information of the chemicals used in the experimental part.

REAGENT	SUPPLIER	PRODUCT NUMBER	GRADE
C ₂ H ₄ O ₂ (96 vol%)	VWR	20099.290	Analysis grade
C ₂ H ₂ O ₄ * 2 H ₂ O	Merck	1.00492.1000	Emplura®
C ₅ H ₁₄ CINO	MP Biomedicals	101386	Cell culture reagent
C ₆ H ₈ O ₇ (99.8 %)	VWR	20282.293	Pharmacopoeia Grade
H ₂ SO ₄ (95-97 vol%)	Merck	1.00731.2511	Analysis grade
HCl (37 vol%)	Merck	1.00317.1000	Analysis grade
HOCH ₂ CH ₂ OH (99.5%)	Merck	1.09621.1000	Analysis grade

All solutions, except for ethaline, were aqueous solutions. Ethaline was prepared by measuring 1 part choline chloride (C₅H₁₄CINO), and 2 parts 1,2-ethanediol in a beaker. The beaker was heated to 80 °C and stirred with a magnetic stirrer (IKA® RT 10) until the solution was clear, then it was cooled. No purging of gases was conducted for any of the solutions.

The measured pH and redox-potentials in the solution mapping tests carried out in 6 different solutions, water and one mixture solution, displayed in Table 5. From the results the extraction percentages of metals to the solution were calculated using Equation (1),

$$E = \frac{c_E * V_E}{M_T * m_T} * 100\% \quad (1)$$

, where E is the extraction to the solution (%), c concentration (mg/L), V volume (L), M metal concentration (mg/g), m mass (g), and the index E stands for values from the extraction samples and T for the values in the original WGPD, based on total leaching by Milomatic, shown in Table 4.

5.3 Equilibrium potentials

The equilibrium potentials of Cu, Fe, Ni, Pb and Zn were calculated. The reactions were assumed to be similar to equation (2)



, where Me is the metal species, n is the number of electrons, and e^- is the electron.

Nernst equation (3) was used to calculate the reduction potential under non-standard conditions (E) for the reduction reactions

$$E = E^0 - \frac{RT}{nF} \ln \frac{a_{red}}{a_{ox}} \quad (3)$$

a_{ox} is the activity of the electron donor and a_{red} activity of the electron acceptor. The metal solutions were all dilute (≤ 0.01 M), which means it can be assumed that the activity of the species is numerically equal to its molar concentration [31]. The activity of a pure metal is unity.

Table 7 shows the standard reduction potentials [31], and the calculated equilibrium under non-standard conditions, which are the minimum potentials required for the reactions to go in the direction of oxidation (right to left). Only lowest and highest calculated values are shown to represent the potential window. It should be note that these calculations consider an ideal system, in reality many different interactions play their part. As can be seen later, in Table 9 and Table 10 and 11, all the measured redox potentials i.e. the oxidative power of the solution was higher that the equilibrium of metals investigated, which means the oxidation reaction of the metal was thermodynamically possible.

Table 7. Standard reduction potentials at 25 °C (modified after [31]) and calculated reversible electrode potentials of oxidation reactions for Cu, Fe, Ni, Pb, and Zn.

REACTION	E^0 (mV) vs. SHE	Lowest analysed concentration of metal in solution (M)	Highest analysed concentration of metal in solution (M)	Lowest calculated value for E (mV) vs. SHE	Highest calculated value for E (mV) vs. SHE
$\text{Cu}^{2+} + 2\text{e}^- \rightleftharpoons \text{Cu(s)}$	340	$7.87 \cdot 10^{-6}$	0.0009	189	250
$\text{Fe}^{2+} + 2\text{e}^- \rightleftharpoons \text{Fe (s)}$	-440	$8.95 \cdot 10^{-6}$	0.01	-589	-495
$\text{Ni}^{2+} + 2\text{e}^- \rightleftharpoons \text{Ni (s)}$	-270	$8.52 \cdot 10^{-6}$	0.0003	-419	-374
$\text{Pb}^{2+} + 2\text{e}^- \rightleftharpoons \text{Pb (s)}$	-130	$2.41 \cdot 10^{-6}$	0.01	-296	-188
$\text{Zn}^{2+} + 2\text{e}^- \rightleftharpoons \text{Zn (s)}$	-760	0.0005	0.01	-857	-813

5.4 Experimental setup and leaching procedure

5.4.1 Preparations

The WGPD was homogenized and divided to the portions of about 5 g each using a spinning riffler manufactured by Microsal Ltd.

In order to take into account the evaporation of the liquid during mapping tests, a 24-hour evaporation test was performed with H₂O. The solution was heated to 33 °C and 50 °C and mixed with magnetic stirrer at 300 rpm. In evaporation tests, the volume of water was 100 and 200 mL, and the beakers were sealed with parafilm. The loss of volume was found to be 2.5% in both temperatures.

When adding solids into solution the volume will increase, therefore, the addition of volume when adding 5 g of WGPD to 100 mL H₂O was tested and found to be $\leq 5\text{mL}$, which is 5%. In both, evaporation test and volume increase test, the error of the measuring cylinder was $\pm 2\text{ mL}$, which is 2%. Therefore, it can be reasoned that the loss of 2.5% via evaporation and the gain of 5% via volume increase, with the error margin of 2% might as well cancel each other out within a 100 mL volume. If the volume is increased and the error is not, then this has to be taken into consideration.

Prior to the batch leaching tests, evaporation tests were performed. The glass reactor with 0.4 L (± 5 mL) water, was put in a water bath for one hour at 30, 50, 60, 70 and 90 °C. The obtained evaporations were 7.5 mL (1.9%), 8 mL (2%), 9 mL (2.25%), 10 mL (2.5%), and 35 mL (8.8%), respectively. Thus, corresponding volumes of water were added during the leaching, as it was assumed that the majority of the evaporated volume consisted of water.

The volume increase due to the added WGPD was tested for the batch leaching by adding 40 g WGPD in 400 mL water. The volume increased by 14.5 ± 0.5 mL. This was accounted for in the experiments, where 20 g WGPD was added to 371 mL of water, in order to obtain the chosen solids concentration of 50 g/L.

Mixing was used in the batch leaching tests in order to maintain the suspension, therefore, the mixing speed was investigated. It was found out that 300 rpm was the minimum rotating speed to maintain suspension.

5.4.2 Solution mapping tests

The purpose of the mapping test was to investigate the leaching behavior of WGPD for a variety of solutions in a small scale. All solutions listed in Table 4 were tested in mapping tests, with a total of 41 different leaching conditions (different leaching media with different conditions). Of these mapping tests, 30 were performed at 33 °C, and 11 at 50 °C. The solution volume used was 100 mL. Prior to leaching, the solution was pre-heated in a water bath. The leaching was conducted in a beaker on a heated magnetic stirrer (300 rpm). The pH and the redox potentials were measured from the pure solutions prior to WGPD was exposed to the solution. The used solids concentration of WGPD was 50 g/L. The beakers were sealed with parafilm in order to prevent evaporation. There was no oxygen/air purging during mapping tests. The experimental setup is displayed in Figure 16. A polypropen box acts as protection against spill on the stirrer. In the figure, the beakers are empty and only one beaker is sealed.



Figure 16. Mapping tests were performed in 10 glass beakers on a magnetic stirrer IKA® RT 10. Each beaker contained 100 mL of a solution and the used solids concentration of WGPD was 50 g/L. The stirring was set to 300 rpm. Investigated temperatures were 33 and 50 °C.

After 24 h of leaching, the solutions were filtered. In the first mapping round, every solution was vacuum filtered using double filter paper (Munktell, grade 10, size Ø 90 mm) in a Buhner funnel, and if the solution still looked turbid, they were gravity filtered a second time in funnel using a single filter paper (Whatman cat no. 1001-110). In the second and third mappings, the solutions were filtered once in the vacuum setup and the samples to be analyzed were filtered through a single filter paper in a funnel. Next, the pH and redox-potentials were measured from the leached solution. Finally, samples of 10 mL were made acid resistant by adding 3 drops of HNO₃ sent for chemical analysis.

The redox-potentials were measured using a Mettler Toledo Inlab® saturated calomel electrode (SCE) vs. platinum (Pt) wire (242 mV vs. SHE [31]). The pH was measured with Hanna Instruments edge® Multiparameter pH Meter - HI2020.

The samples were analyzed using an atomic absorption spectroscope (AAS) manufactured by Varian (AA240) by Milomatic Oy. The spectroscope has an air-acetylene flame and the radiation source is a HCl-lamp.

5.4.3 Batch leaching tests for WGPD

The purpose of the batch leaching tests was to investigate WGPD leaching behavior in more detail in a bigger scale (compared to mapping tests) for selected leaching media. The solutions chosen for batch leaching tests were hydrochloric acid (HCl) and citric acid ($C_6H_8O_7$). Both solvents were tested with two variables (i.e. concentration and temperature) having three values each, seen in Table 8. Lower temperatures were used with citric acid due to its decomposition risk at higher temperatures (2 h at 80 °C) [32]. The batch leaching tests were named as N1-N9 in the HCl leaching and M1-M9 in $C_6H_8O_7$ leaching.

Table 8. Investigated factors and their values used in batch leaching experiments. N1 – N9 representing HCl leaching series and M1 – M9 $C_6H_8O_7$ leaching series.

c, M	T, °C	EXPERIMENT #	T, °C	EXPERIMENT #
0.15	30	N1	30	M1
0.15	60	N2	50	M2
0.15	90	N3	70	M3
0.30	30	N4	30	M4
0.30	60	N5	50	M5
0.30	90	N6	70	M6
0.60	30	N7	30	M7
0.60	60	N8	50	M8
0.60	90	N9	70	M9

The batch leaching tests were carried out in a glass reactor, schematics presented in Figure 17. The reactor was submerged in a warm water bath (Lauda aqualine AL 25) in order to keep the temperature stable. A four-bladed teflon propeller ($\varnothing = 50$ mm) was used to mix the solution (300 rpm) and air was brought to the solution via an aeration sinter, with the air flow rate 1 L/min. First, the solution was heated to the desired temperature. Thereafter, the solid WGPD was added to the reactor, and the mixing and the aeration sparge were turned on. The pH and redox potential were measured in the beginning, and with every sampling. Samples were taken at $t = 0.5, 1, 2,$ and 4 h. The total leaching time was 4 h. In the batch leaching tests, the samples were gravity filtered through a single filter paper (Whatman cat no 1001-110).

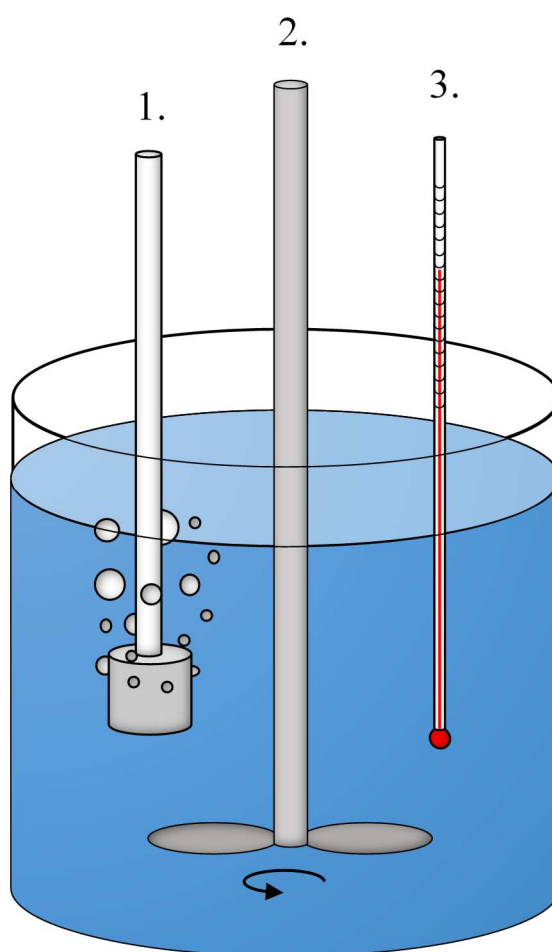


Figure 17. A schematic illustration of the batch leaching reactor, in which 1. presents an aeration sparge sinter, 2. a propeller for mixing the solution, and 3. a thermometer [33].

6 Results and Discussion

6.1 Mapping test results

The extraction of copper, iron, nickel, lead and zinc to the solution as a function of lixiviant concentration for all the investigated solutions are shown in Figures 18 – 22. The temperature used was 33 °C, but HCl and H₂SO₄ were also tested at higher temperature (50 °C). There was no oxygen/air purging into the solution. It can be seen that highest metal extractions (Cu, Fe, Ni, and Zn) were achieved with mineral acids at all concentrations. For Pb the highest extractions were achieved with HCl, but also C₂H₂O₄ gave high extraction at concentration 3M or above. Ethaline was shown to extract over 50% of lead into solution at 33 and 70% at 50 °C. Extractions of copper and zinc into ethaline were around 25%, and the extractions of nickel and iron were as low as 10%, at both 33 and 50 °C. Metal extractions from WGPD to water were low, 6% and 3% for nickel, 14% and 7% for zinc, 2% and 1% for copper, and less than 1% for iron and lead at 33 °C and 50 °C respectively.

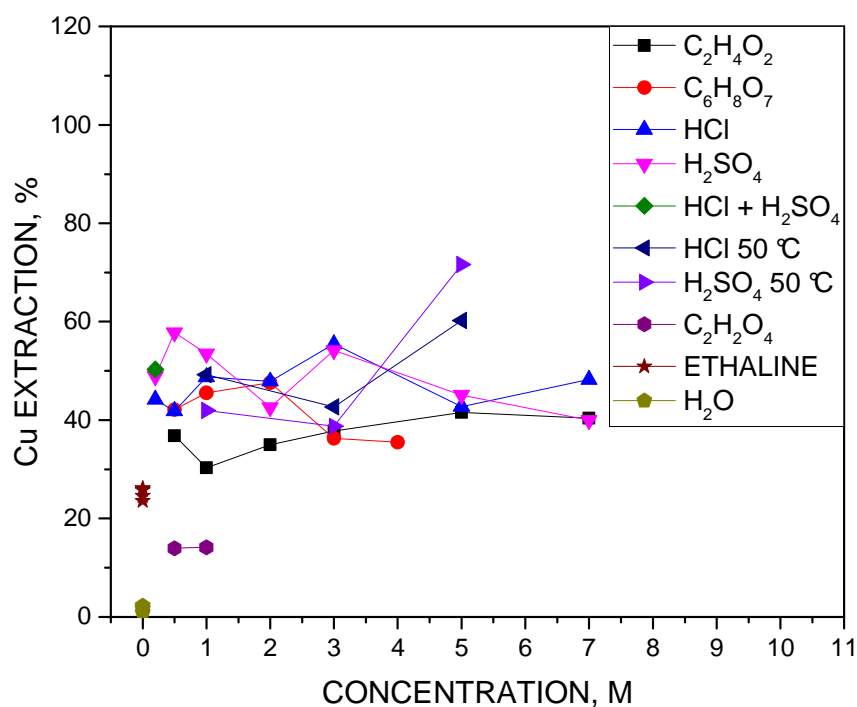


Figure 18 Extraction of copper from WGPD as a function of lixiviant concentration in all tested solutions in mapping tests. $T = 33\text{ }^{\circ}\text{C}$, additionally, HCl and H₂SO₄ were tested in 50 °C.

In Table 9, the pH and redox potentials measured before and after solution mapping tests are shown.

Table 9. Measured pH and redox-potentials (mV, vs. SCE and converted to SHE) from the solutions used in the mapping tests. The times of measurement are at 0 h and at 24 h. The gray cells indicate increased values. *c* stands for concentration and redox for redox potential.

SOLUTION	<i>c</i> , M	<i>pH</i> <i>t</i> = 0 h	<i>pH</i> <i>t</i> = 24 h	REDOX (mV) vs. SCE <i>t</i> = 0 h	REDOX (mV) vs. SCE <i>t</i> = 24 h	REDOX (mV) vs. SHE <i>t</i> = 0 h	REDOX (mV) vs. SHE <i>t</i> = 24 h
C ₂ H ₂ O ₄	0.5	0.8	0.6	405	300	647	542
C ₂ H ₂ O ₄	1	0.7	0.5	419	263	661	505
C ₂ H ₄ O ₂	0.5	3.5	4.1	410	252	652	494
C ₂ H ₄ O ₂	1	2.4	3.7	423	369	665	611
C ₂ H ₄ O ₂	2	2.3	3.6	411	361	653	603
C ₂ H ₄ O ₂	3	1.9	3.1	457	377	699	619
C ₂ H ₄ O ₂	5	1.7	2.7	455	400	697	642
C ₂ H ₄ O ₂	7	1.5	2.5	457	432	699	674
C ₆ H ₈ O ₇	0.5	1.7	2.3	435	285	677	527
C ₆ H ₈ O ₇	1	1.4	1.8	443	325	685	567
C ₆ H ₈ O ₇	2	0.9	1.3	529	403	771	645
C ₆ H ₈ O ₇	3	0.6	0.8	449	428	691	670
C ₆ H ₈ O ₇	4	0.2	0.2	512	425	754	667
H ₂ O	-	6.8	7	0	149	242	391
H ₂ O	-	7.8	7	0	154	242	396
H ₂ O	-	5.4	7	215	279	457	521
H ₂ SO ₄	0.2	0.7	1.1	523	477	765	719
H ₂ SO ₄	0.5	0.5	0.5	435	492	677	734
H ₂ SO ₄	1	0.1	0.2	445	500	687	742
H ₂ SO ₄	1	0.1	0.2	519	506	761	748
H ₂ SO ₄	2	-0.3	-0.2	510	520	752	762
H ₂ SO ₄	3	-0.4	-0.4	502	511	744	753
H ₂ SO ₄	3	-0.5	-0.2	560	506	802	748
H ₂ SO ₄	5	-0.9	-0.9	499	505	741	747
H ₂ SO ₄	5	-0.9	-0.2	569	506	811	748
H ₂ SO ₄	7	-1.3	-1.1	592	525	834	767
HCl	0.2	0.7	2.9	474	393	716	635
HCl	0.5	0.5	0.8	415	476	657	718
HCl	1	0.2	0.2	444	498	686	740
HCl	1	0.1	0.3	505	506	747	748
HCl	2	-0.3	-0.2	507	512	749	754
HCl	3	-0.5	-0.5	440	500	682	742
HCl	3	-0.4	-0.3	520	502	762	744
HCl	5	-0.7	-0.9	427	488	669	730
HCl	5	-0.9	-0.7	512	513	754	755
HCl	7	-1.3	-1.2	535	521	777	763
HCl + H ₂ SO ₄	0.2	0.4	0.6	440	500	682	742

As was displayed in Table 3, the extraction of copper was much more effective in article by Huang *et al.* [7] than in this thesis into citric acid (100 vs. max. 48%), acetic acid (100 vs. max. 40%) and oxalic acid (46 vs. max. 14%). In their work, copper extraction into sulfuric acid and hydrochloric acid was at about at the same level as in this thesis. Like in article by Zhang & Ma [19], the extraction of copper into sulfuric acid decreased with increased concentration in this thesis between 3.7 and 4.7 M, but no increase was detected in concentrations higher than that.

In research by Wu & Ting [29], in Figure 7, the extraction of Cu into sulfuric acid decreased from ca. 100 to ca. 85% between 0.5 and 0.1 M solutions, when it decreased from 58 to 53% in this thesis. Like in this thesis, the extraction of copper into citric acid also increased from 0.5 to 0.1 M concentration, but Wu & Ting obtained higher extraction efficiencies, >90% vs. 42 to 46%. Oxalic acid extractions remained as good as unchanged in this thesis and in research by Wu & Ting, but the level was higher in their work >90% vs. 14%.

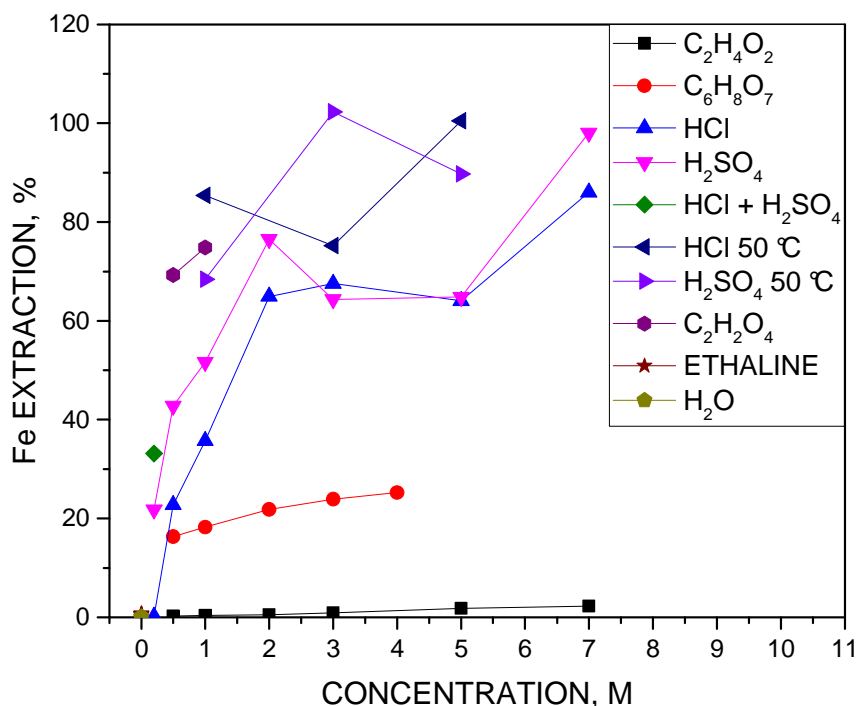


Figure 19. Extraction of iron from WGPD as a function of concentration for all tested solutions in mapping tests. $T = 33\text{ }^{\circ}\text{C}$, additionally, HCl and H₂SO₄ were tested in $50\text{ }^{\circ}\text{C}$.

Earlier, in Figure 7 [29], sulfuric acid, citric acid, and oxalic acid have also been tested in 0.5 and 1 M concentrations. As could be observed, the extraction of iron into sulfuric acid increased, like in this thesis, even if the values were a bit lower in their work (20 – 25% vs. 43 – 52% in this thesis). The iron extraction into citric acid decreased slightly in experiments by Wu & Ting [29] with increasing concentration, whereas in the current research, iron extraction increased slightly with increasing citric acid concentration, Figure 18, the extraction being ca. 20%. This is of the same magnitude with Wu & Ting [29] Both in the current research and in experiments by Wu & Ting, the extraction of oxalic acid increased, but the values in our research were much higher, 69 – 75% vs. >5 to 10%.

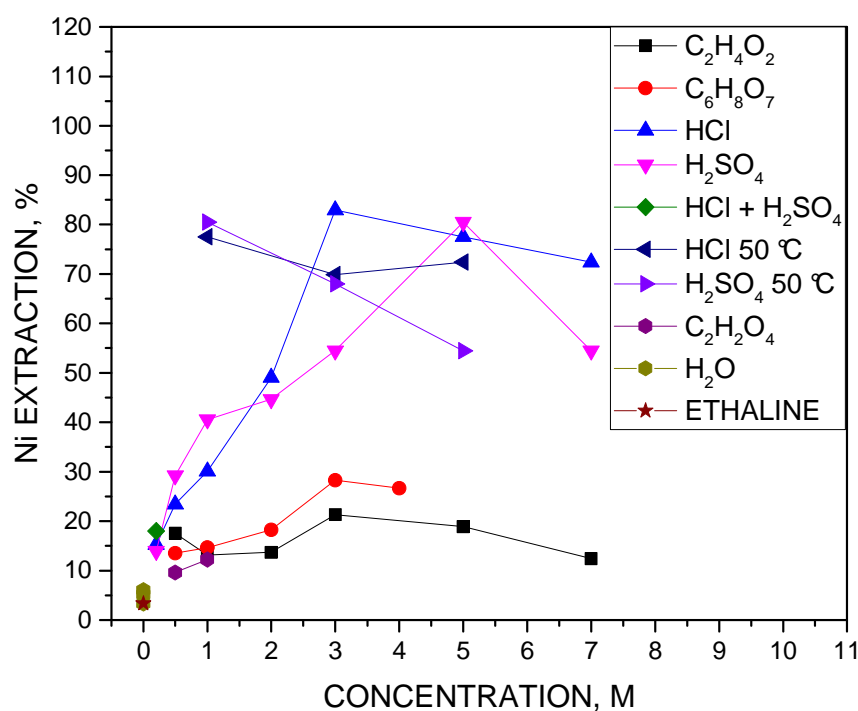


Figure 20. Extraction of nickel from WGPD as a function of concentration for all tested solutions in mapping tests. $T = 33\text{ }^{\circ}\text{C}$, additionally, HCl and H₂SO₄ were tested in $50\text{ }^{\circ}\text{C}$.

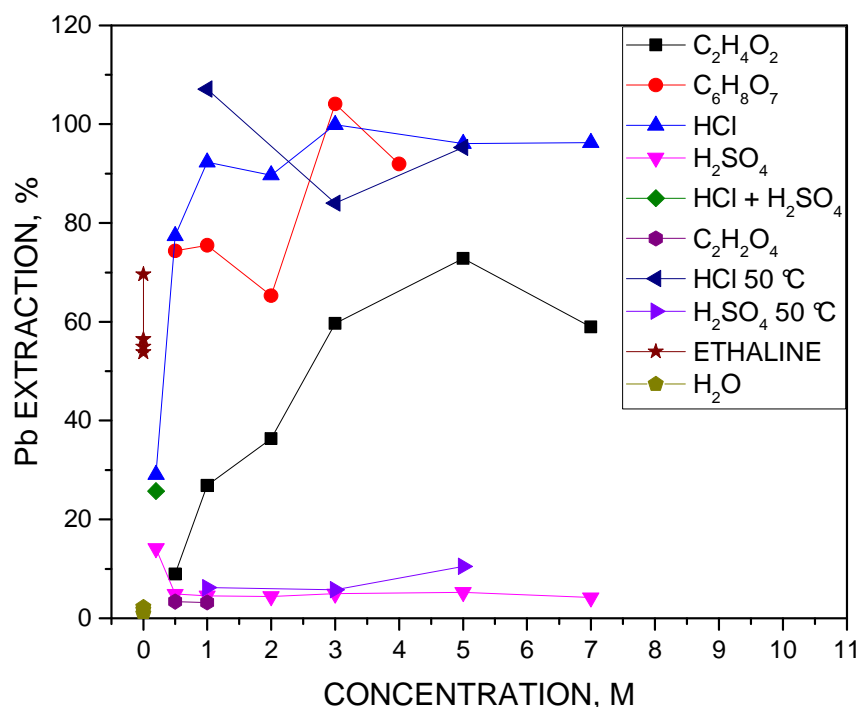


Figure 21. Extraction of lead from WGPD as a function of concentration for all tested solutions in mapping tests. $T = 33\text{ }^{\circ}\text{C}$, additionally, HCl and H_2SO_4 were tested in $50\text{ }^{\circ}\text{C}$.

The extraction of lead into citric acid, acetic acid and oxalic was found to be at a similar levels in both this thesis, Figure 21, and in the work of Huang *et al.* [7] (Table 3). Lead extraction from the raw material investigated in this study into sulfuric acid was shown to be lower (max 3%) compared to the study of Huang *et al.* [7] (28%) and Zhang & Ma [19] (ca. 15%), whereas into hydrochloric acid lead extraction was found to be higher (max 100%) in this study compared to study of Huang *et al.* [7]. Earlier, in Figure 7, Wu & Ting [29] also tested lead extraction into sulfuric acid, citric acid, and oxalic acid at 0.5 and 1 M concentrations. In their research, the extraction into citric acid decreased from 50% to below 40%, but stayed at 75% in the current research. In oxalic acid, the Pb extraction increased from <5% to around 10% in the study of Wu & Ting [29], but stayed low (3%) in this thesis. Lead had a decreasing extraction trend with increasing H_2SO_4 concentration also in Figure 5, from article by Zhang & Ma [19]. There, the extraction rate of lead (15%) was higher than in this thesis (5%), at 3.7 to 7 M concentrations.

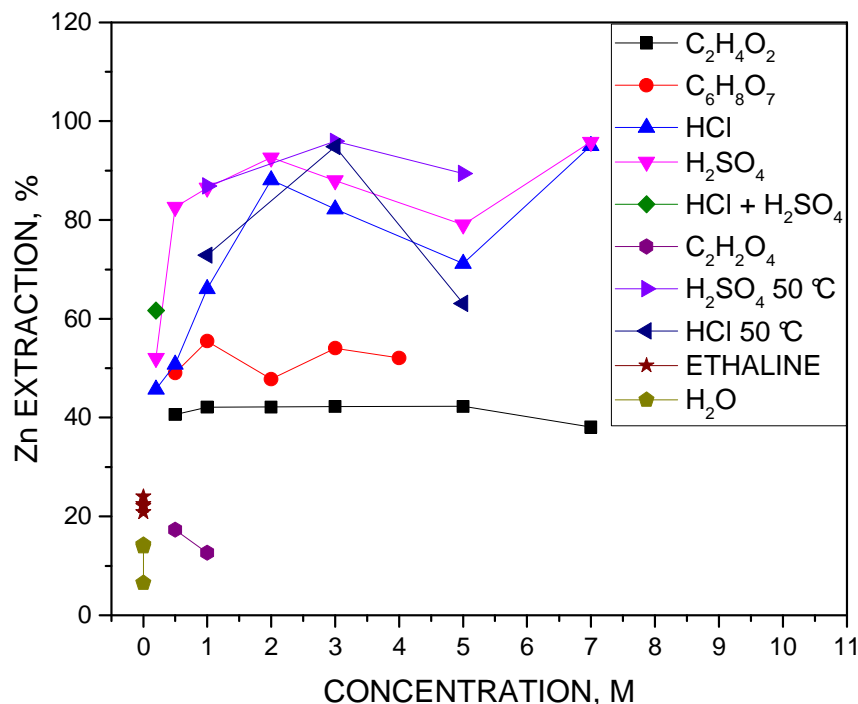


Figure 22. Extraction of zinc from WGPD as a function of concentration for all tested solutions in mapping tests. $T = 33\text{ }^{\circ}\text{C}$, additionally, HCl and H_2SO_4 were tested in $50\text{ }^{\circ}\text{C}$.

There was a clear difference in the efficiency of zinc extraction into HCl solution between this thesis and the article by Zhang & Ma (Figure 5) [19]. The extractions in the study of Zhang & Ma [19] were conducted for MSWI fly ash raw material and Zn extraction achieved in their study there was below 5%, whereas the extractions in this thesis reached levels higher than 90% (Figure 9). However, the leaching time for experiments conducted in this thesis was 24 h in solution mapping tests, whereas Zhang & Ma only had 4 h contact time. The temperature used by Zhang & Ma was $3\text{ }^{\circ}\text{C}$ lower.

Earlier, in Figure 7, Wu & Ting [29] also tested zinc extraction into sulfuric acid, citric acid, and oxalic acid at 0.5 and 1 M concentrations. The extraction into sulfuric acid stayed constant at 0.5 and 1 M concentrations in their experiments (ca. 50%), whereas in this thesis it increased slightly from 81 to 83% in this thesis (Figure 22).

In comparison with the current research, the extraction of zinc was higher in citric acid (100 vs. max 55%), acetic acid (100 vs. max. 42%) and oxalic acid (45 vs. max. 17%) in an experiment by Huang *et al.* (Table 3) [7]. Zinc extraction into sulfuric acid were lower in their work than in this thesis (58 vs. max 96%) and hydrochloric acid (54 vs. max. 89%). Sulfuric acid and hydrochloric acid had higher pH in their work than in this thesis

(3.1 and 3.0 vs. max. 1.1 and 2.9, respectively), so their results were lower for iron extraction, but lead was extracted more efficiently at lower pH into sulfuric acid.

In order to better visualize, the extractions of metals to the organic solutions are shown in Figure 23, for the inorganic solutions in Figure 24, and for ethaline in Figure 25. It can be seen that in general, Ni dissolved poorly in organic lixiviants, acetic acid had some selectivity towards iron, and the ethaline experiments showed a good reproducibility.

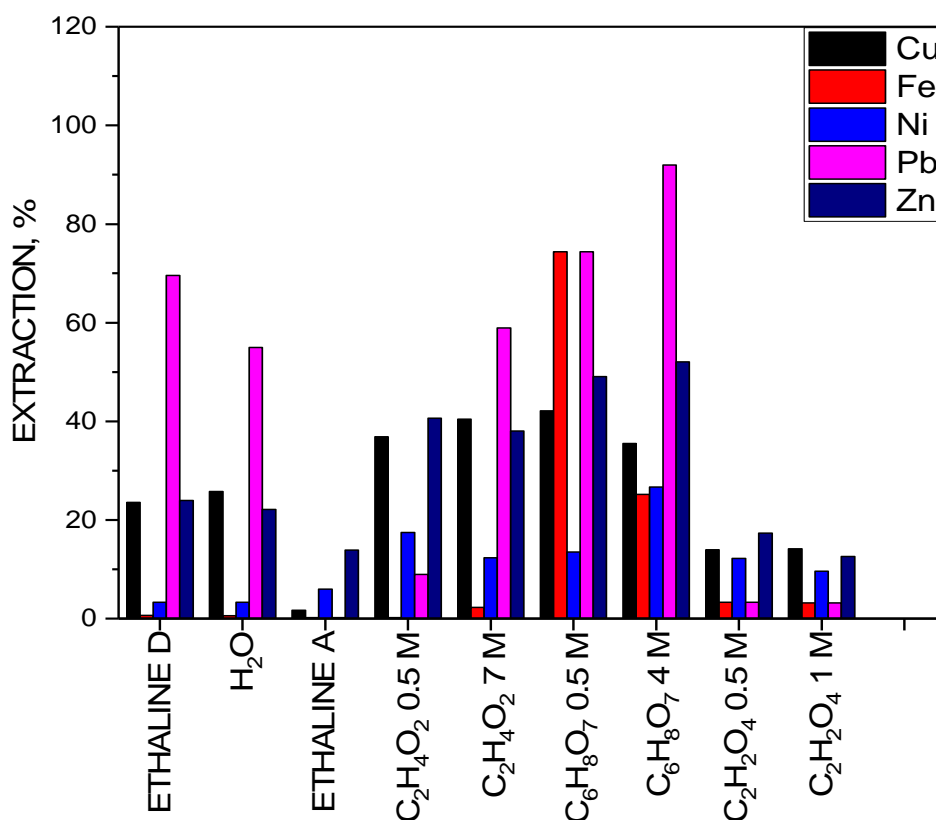


Figure 23. Extraction (%) of Cu, Fe, Ni, Pb and Zn from WGPD into the organic solutions investigated. Also extraction into the water is presented. The metal extraction after leaching at highest and lowest concentrations of each organic solution is presented. $T = 33\text{ }^{\circ}\text{C}$, leaching time 24 h, solid liquid ratio 50 g/L. Ethaline was also tested in $50\text{ }^{\circ}\text{C}$ (Ethaline D).

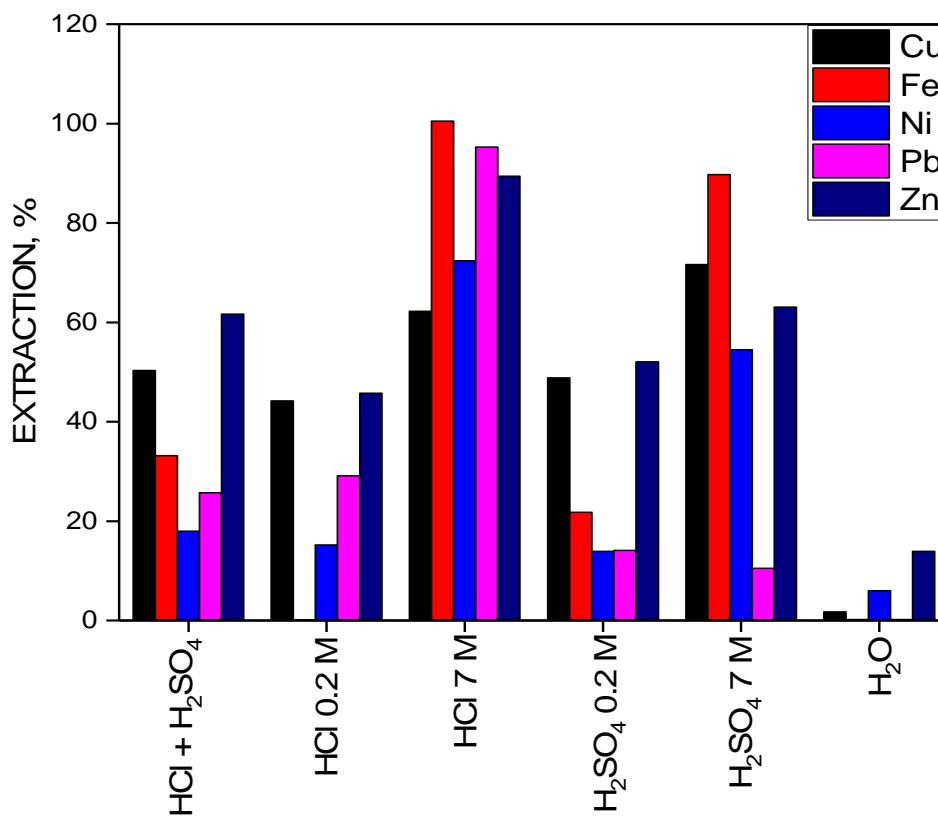


Figure 24. Extraction (%) of Cu, Fe, Ni, Pb and Zn from WGPD into inorganic solutions and water. The highest and the lowest concentrations of each solution are shown. $T = 33$ °C, leaching time 24 h, L/S ratio 20 mL/g.

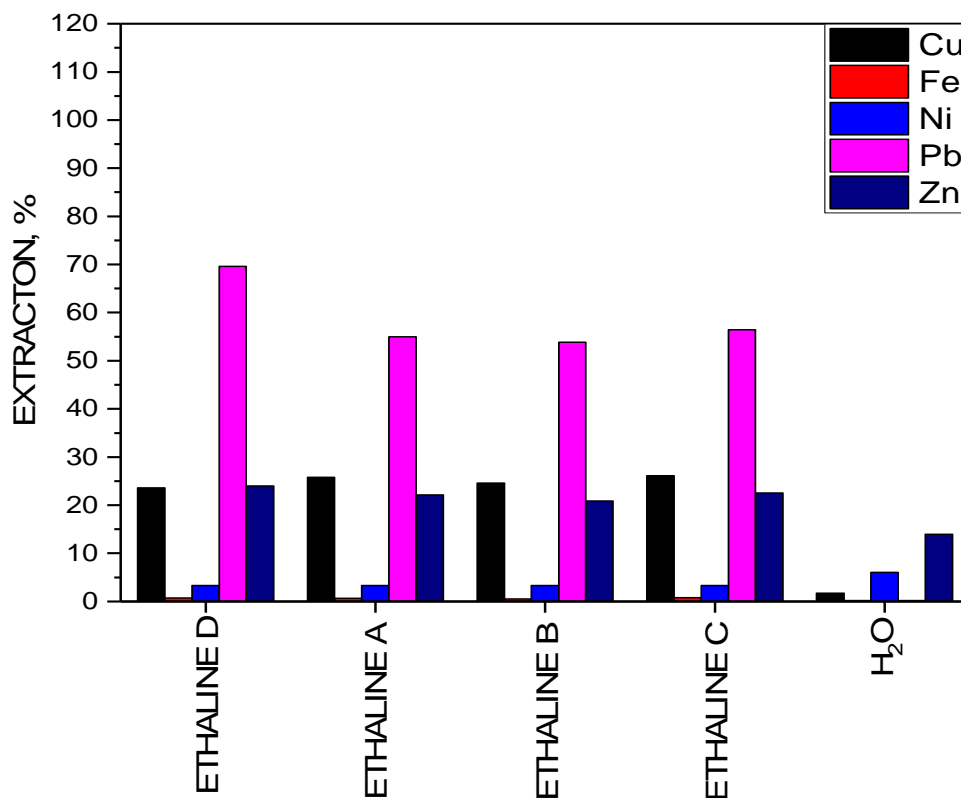


Figure 25. Extraction (%) of Cu, Fe, Ni, Pb and Zn from WGPD into ethaline. A, B and C were identical tests tested at 33 and D at 50 °C. Leaching time 24 h, L/S ratio 20 mL/g.

6.1.1 Effect of temperature

In the mapping tests, four solutions were tested at 50 °C: Ethaline, HCl, H₂SO₄, and water for reference. As could be observed in Figure 25, ethaline had a better extraction of lead to the solution at higher temperature ($T = 50\text{ °C}$). Temperature was shown not to have an impact for iron and nickel leaching in ethaline.

With HCl, the increase of temperature increased the extraction of zinc and decreased the extraction of lead. Copper and iron extraction showed an increase in extraction with increasing temperature at 3 M concentration, whereas the extraction decreased with increasing temperature at 1 and 5 M HCl solutions. Nickel extraction was shown to increase with increasing temperature at 1 M and decrease at 3 and 5 M HCl solutions. In Figure 26, the differences in extractions between 1, 3 and 5 M HCl in both temperatures ($T = 33$ and 50 °C) can be seen.

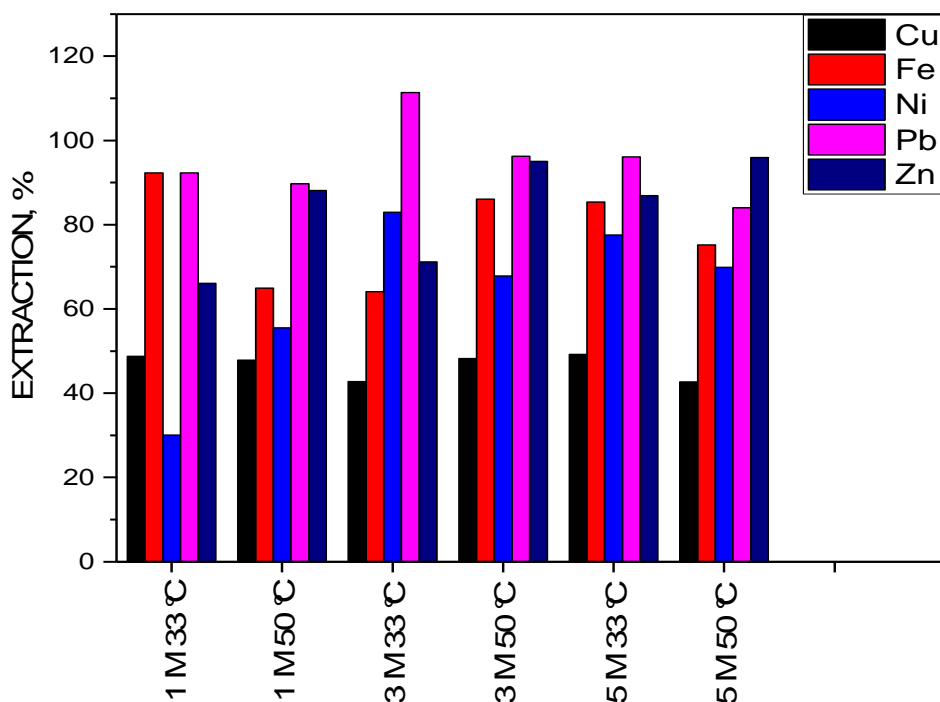


Figure 26. Extraction of Cu, Fe, Ni, Pb and Zn from WGPD to the solution in HCl at 33 and 50 °C.

H₂SO₄ was shown to leach copper almost equally efficiently at 33 °C and at 50 °C, whereas iron and zinc had higher extractions at 50 °C. Nickel extraction increased with increase in temperature in 1 M and 3 M sulfuric acid, but decreased in 5 M. The extraction of lead was not effective with H₂SO₄ due to insoluble lead sulphate formation. Figure 27 shows that the extractions of iron and zinc were generally higher than the extraction of

copper at 50 °C in sulfuric acid. The low efficiency for lead extraction is due to poor solubility of lead sulphate.

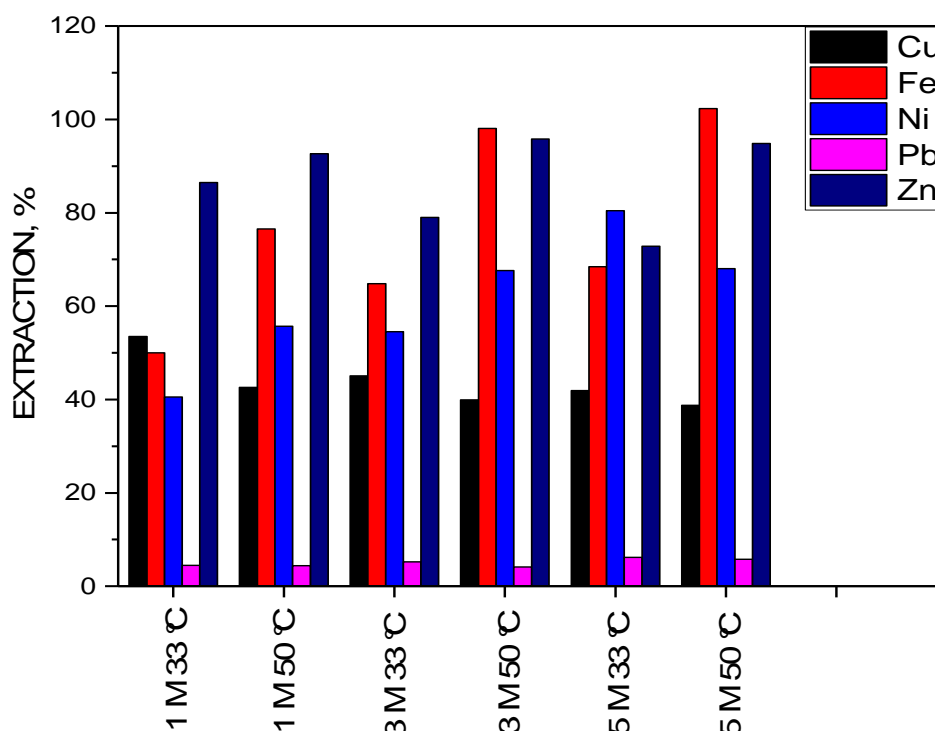


Figure 27. Extraction of Cu, Fe, Ni, Pb and Zn from WGPD to the solution in H₂SO₄ at 33 °C and 50 °C.

6.1.2 Effect of concentration

In acetic acid (C₂H₄O₂), the increase in concentration had no significant effect on the metal extraction, except for the extraction of lead, which increased in 0.5 M to 5 M from 9 to 73%, but decreased to 59% in 7 M. This trend can be observed in Figure 28. A clear selectivity towards lead compared to iron can also be observed in acetic acid.

As depicted in Figure 29, citric acid was an effective solvent of lead with an extraction into solution over 65% for all tested concentrations. The extractions into solution of Cu, Fe, Ni and Zn were all under 60%, with zinc extraction around 50%, copper decreasing from 48 to 35%, nickel increasing from 14% to 28% and iron increasing from 16% to 25% when concentration increased from 0.5 to 4 M.

In sulfuric acid, the increase of concentration had a positive effect on the extraction for iron, nickel and zinc. The increase was from 22% and 52% (0.2 M) to 77% and 93% (2 M) with iron and zinc respectively, and from 14% (0.2 M) to 96% (3 M) with nickel. With iron, there was also increase in extraction from 5 M (65%) to 7 M (98%). Nickel decreased

back to 54% at 7 M. Figure 30 illustrates the extractions as a function of concentration ($T = 33\text{ }^{\circ}\text{C}$).

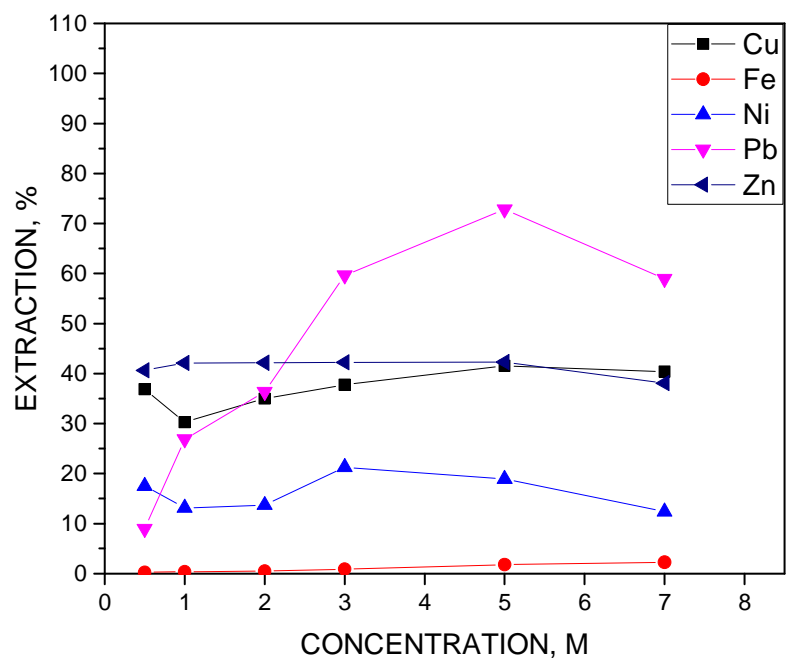


Figure 28. Extraction of Cu, Fe, Ni, Pb and Zn from WGPD to the solution in acetic acid ($\text{C}_2\text{H}_4\text{O}_2$). $T = 33\text{ }^{\circ}\text{C}$ leaching time 24 h, L/S ratio 20 mL/g.

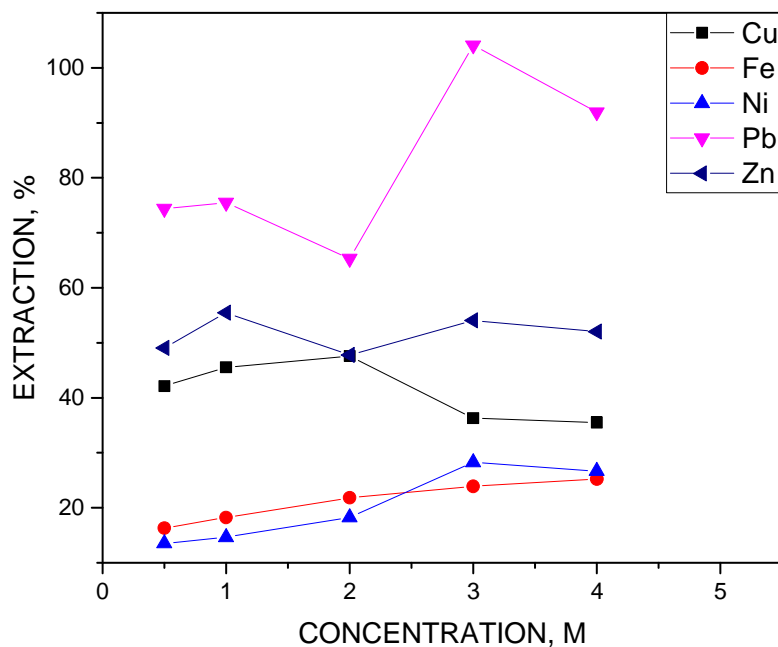


Figure 29. Extraction of Cu, Fe, Ni, Pb and Zn from WGPD to the solution in citric acid ($\text{C}_6\text{H}_8\text{O}_7$). $T = 33\text{ }^{\circ}\text{C}$ leaching time 24 h, L/S ratio 20 mL/g.

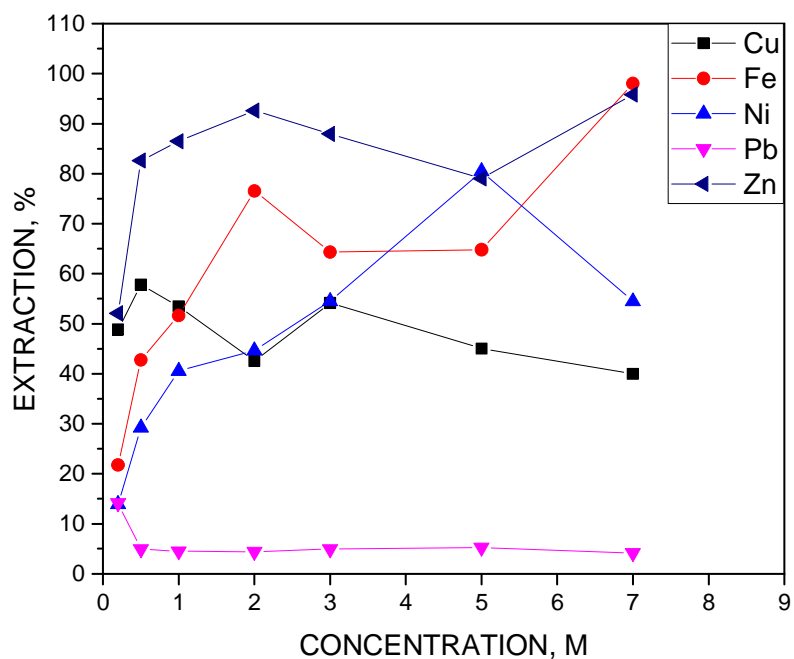


Figure 30. Extraction of Cu, Fe, Ni, Pb and Zn from WGPD to the solution in H_2SO_4 ($T = 33\text{ }^\circ\text{C}$, leaching time 24 h, L/S ratio 20 mL/g).

The extraction trends of zinc and iron into solution in H_2SO_4 as a function of increasing concentration look somewhat similar in this thesis (Figure 30) and in experiments by Nagib & Inoue [6] (Figure 4).

At $50\text{ }^\circ\text{C}$ in sulfuric acid, only nickel had a clear decreasing trend in extraction as a function of increase in concentration, which can be seen in Figure 31.

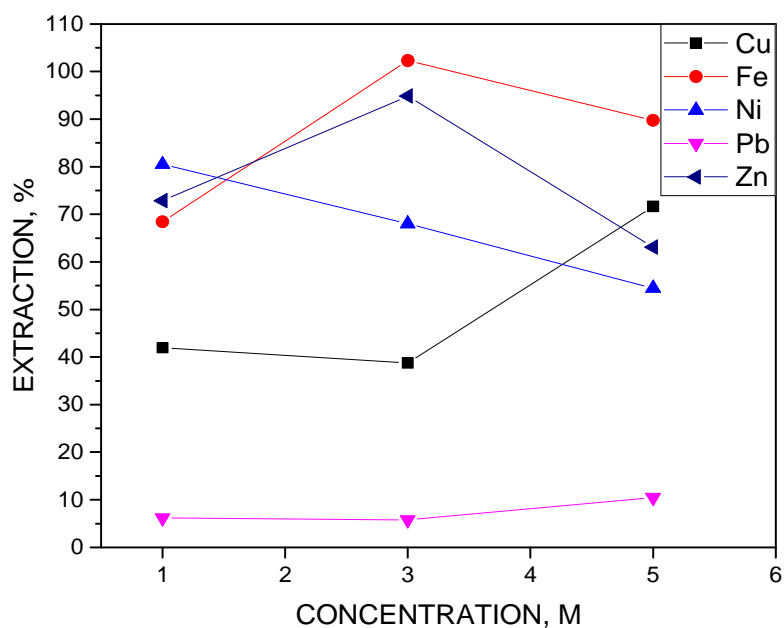


Figure 31. Extraction of Cu, Fe, Ni, Pb and Zn into solution as a function of concentration in H_2SO_4 ($T = 50\text{ }^\circ\text{C}$, leaching time 24 h, L/S ratio 20 mL/g).

In HCl, the maximum metal extraction was achieved in most of the solutions with 2 M concentration. For Pb and Zn almost complete dissolution was achieved and for Fe and Ni over 60% extraction. Final Cu extraction remained below 60% at all concentrations at 33 °C, Figure 32.

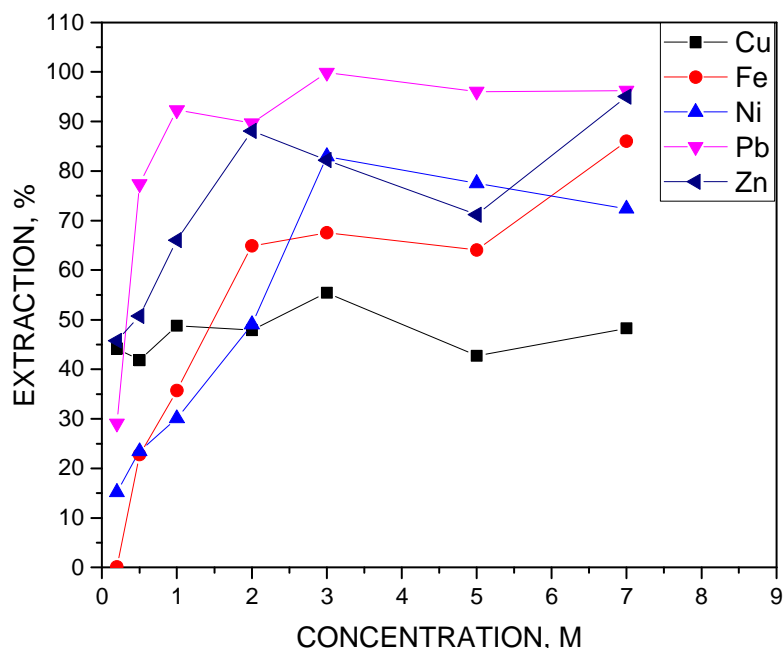


Figure 32. Extraction of Cu, Fe, Ni, Pb and Zn from WGPD to the solution in HCl ($T = 33$ °C, leaching time 24 h, L/S ratio 20 mL/g).

At 50 °C, the extractions of all metals into HCl, except for zinc, had a lower extraction at 3 M, and higher at 1 M and 5 M compared to 33 °C. The behavior of zinc was the opposite. However, the changes were not excessive and can be also due error margings in sample homogeneity or sampling. Figure 33 illustrates the metal extraction at 50 °C in HCl.

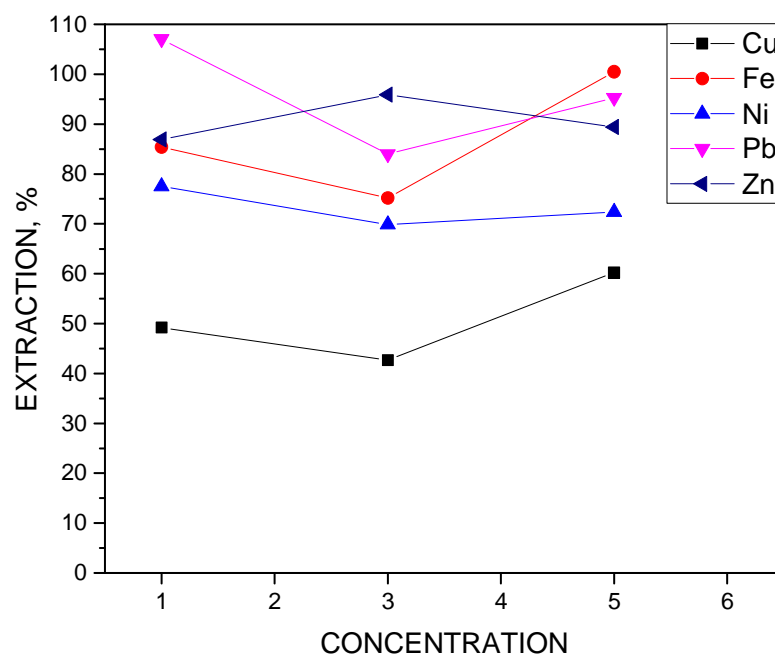


Figure 33. Extraction of Cu, Fe, Ni, Pb and Zn from WGPd to the solution as a function of concentration in HCl. ($T = 50\text{ }^{\circ}\text{C}$, leaching time 24 h, L/S ratio 20 mL/g)

Oxalic acid leaching could only be conducted at low concentrations due to its solubility. Thus, solutions of 0.5 and 1 M were made. The extraction stayed at the same level for copper (14%) and lead (3%), increased with concentration for iron (from 69 to 75%), and decreased for nickel (from 12 to 10%) and zinc (from 17 to 13%).

6.2 Batch leaching test results

The batch leaching experiments were carried out in HCl (N1-N9) and citric acid solutions (M1-M9). The measured pH and redox potentials during these experimental series are presented in Table 10 and 11. The final extractions after 4 hours of leaching of Cu, Fe, Ni, Pb, and Zn into HCl and citric acid are shown in Table 12. The extractions were calculated using equation (3).

Table 10. pH and redox potentials measured in experiments HCl (N1-N9) at times 0, 0.5, 1, 2, and 4 h. The redox potentials are vs. SHE. Test conditions are presented in more detail in Table 4.

TIME, h	pH N1	Redox N1 (mV)	pH N2	Redox N2 (mV)	pH N3	Redox N3 (mV)
0	1.1	729	1.2	784	1.1	692
0.5	4.2	614	4.3	637	4.0	598
1	4.3	618	4.3	612	4.0	565
2	4.2	608	4.6	564	3.5	543
4	4.2	581	4.6	578	3.0	545
	pH N4	Redox N4 (mV)	pH N5	Redox N5 (mV)	pH N6	Redox N6 (mV)
0	0.9	677	1.1	720	0.8	645
0.5	1.5	682	1.8	687	1.5	691
1	1.5	699	1.7	674	1.4	684
2	1.7	700	1.8	680	1.3	674
4	1.7	697	1.5	674	1.2	675
	pH N7	Redox N7 (mV)	pH N8	Redox N8 (mV)	pH N9	Redox N9 (mV)
0	0.69	704	0.6	736	0.6	710
0.5	0.81	754	0.9	727	0.7	720
1	0.81	748	0.9	721	0.5	712
2	0.8	746	0.8	719	0.6	715
4	0.84	742	0.8	717	0.5	716

Table 11. pH and redox potentials measured in experiments citric acid ($C_6H_8O_7$) (M1-M9) at times 0, 0.5, 1, 2, and 4 h. The redox potentials are vs. SHE. Test conditions are presented in more detail in Table 4.

	pH M1	Redox M1 (mV)	pH M2	Redox M2 (mV)	pH M3	Redox M3 (mV)
0	1.9	660	2.0	747	2.0	662
0.5	3.0	672	2.9	546	2.9	472
1	3.0	648	2.9	530	3.0	451
2	3.0	632	2.9	519	2.9	467
4	3.0	643	3.0	562	2.8	473
	pH M4	Redox M4 (mV)	pH M5	Redox M5 (mV)	pH M6	Redox M6 (mV)
0	1.7	773	1.8	775	1.7	721
0.5	2.6	680	2.4	521	2.3	597
1	2.6	629	2.4	505	2.3	536
2	2.6	630	2.4	502	2.2	551
4	2.6	480	2.4	523	2.1	572
	pH M7	Redox M7 (mV)	pH M8	Redox M8 (mV)	pH M9	Redox M9 (mV)
0	1.5	694	1.6	752	1.7	714
0.5	1.9	567	2.0	621	2.0	542
1	1.9	561	2.0	559	2.0	474
2	1.7	582	2.0	590	1.9	274
4	1.8	657	2.0	597	1.9	563

Table 12. Extractions (%) of Cu, Fe, Ni, Pb, and Zn into HCl and citric acid after 4 hours of leaching. Test conditions are presented in more detail in Table 8.

	E (%) N1	E (%) N2	E (%) N3	E (%) N4	E (%) N5	E (%) N6
Cu	19.6	20.6	20.6	47.8	53.6	98.8
Fe	0.1	0.1	0.1	10.7	13.3	26.8
Ni	12.6	21.7	21.7	23.1	25.4	41.2
Pb	1.6	2.5	2.5	52.2	92.7	202.6
Zn	38.6	44.4	44.4	49.2	59.0	125.8
	E (%) N7	E (%) N8	E (%) N9	E (%) M1	E (%) M2	E (%) M3
Cu	44.9	56.3	99.9	37.6	42.5	58.9
Fe	23.0	36.5	122.2	10.7	13.4	20.5
Ni	23.1	44.7	124.4	14.5	14.4	23.8
Pb	80.1	108.3	198.6	64.4	68.3	101.7
Zn	55.5	74.9	184.8	44.4	50.0	67.3
	E (%) M4	E (%) M5	E (%) M6	E (%) M7	E (%) M8	E (%) M9
Cu	39.4	47.4	46.9	41.4	44.9	68.1
Fe	12.0	17.3	16.2	14.9	17.6	32.2
Ni	13.1	17.1	13.1	15.4	16.6	32.0
Pb	69.5	82.6	79.4	70.5	77.1	128.1
Zn	45.2	52.4	50.3	47.5	51.2	80.3

Some of the obtained extractions are over 100%, which is probably due to the heterogeneity of the WGPD and/or sampling and analysis errors. All extraction results from batch leaching tests are shown in Appendix B.

As could be observed in Figure 9 from experiments by Huang *et al.* [7], the extraction of metals into solution in citric acid showed similar trends as results obtained in this thesis in experiments M1 – M9, but with higher extraction levels for lead (ca. 100%), iron (ca. 80%), copper (ca. 100%) and zinc (ca. 100%).

6.2.1 Effect of temperature

With the batch leaching test in HCl, it was found out that the connection between temperature and metals extraction was not unambiguous. For copper, the metal extraction into the solution was highest at 60 °C. For iron, lead and zinc, the extractions increased with increase in temperature, and for nickel it increased in all other solutions but not in 0.15 M HCl solution. In Figure 34, the increase in Zn extraction as a function of temperature can be seen.

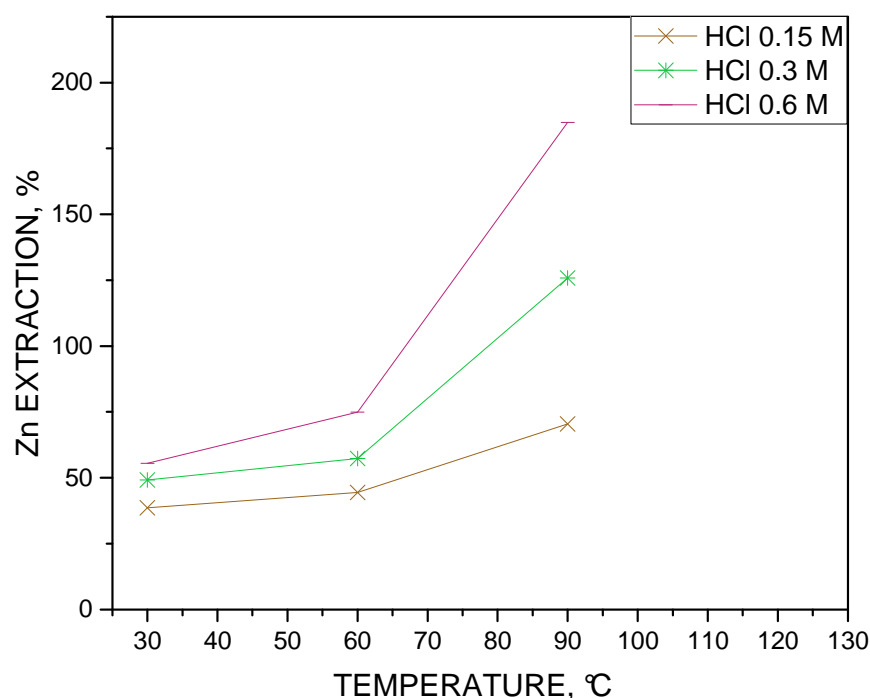


Figure 34. The extraction of zinc to HCl as a function of temperature after 4 hours of leaching. Analysis results from experiments N1 – N9.

In the study of Huang *et al.*, Figure 10 [10], the extraction of all metals into HCl solution were shown to decrease with increase in temperature from 30 to 50 °C. This was opposite to the results found in this study. In this study copper showed increasing trends from 30 to 60 °C in WGPD batch leaching tests, but had a slight general decrease in extraction into solution in mapping leaching tests when temperature increased from 33 to 50 °C. This could be explained by the more similar pH in batch leaching (initial pH in e.g. N6 was 1.1 and pH in experiments by Huang *et al.* [10] was 1.0).

In $C_6H_8O_7$ solution it was found out that the leaching efficiency increased with increasing temperature, with only exception in 0.3 M solution, where the metal dissolution was not shown to increase with increase of temperature from 50 to 70 °C. There might be an error in the test or analysis of the experiment M6. In Figure 35, the lead extraction into citric acid ($C_6H_8O_7$) solution is presented as a function of temperature.

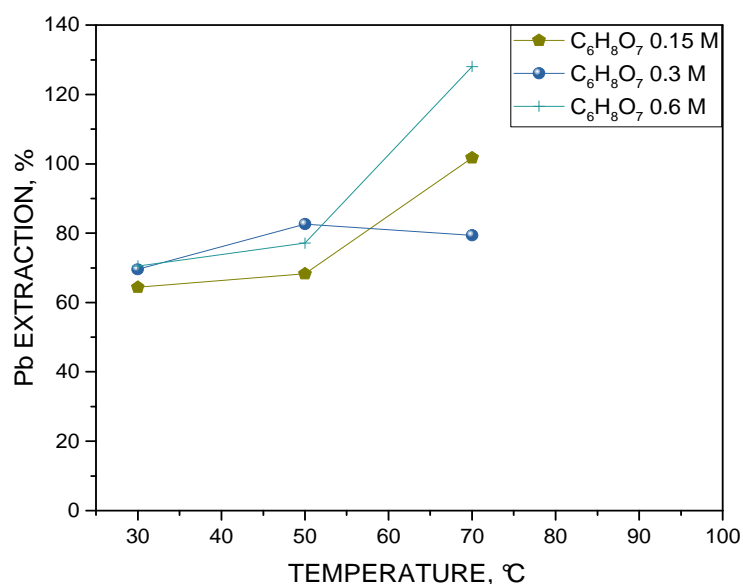


Figure 35. The extraction of lead from WGPD to citric acid (C₆H₈O₇) a function of temperature after 4 hours of leaching. S/L ratio 20 mL/g. Analysis results from experiments M1 – M9.

6.2.2 Effect of concentration

With HCl, there is some indication that a higher HCl concentration yields a higher extraction of metals. This was the case for Cu, Fe, Ni, Pb and Zn, with Zn shown in Figure 36. The only exceptions, or error points were found with Cu at 30 °C, ni at 60 °C, and Pb at 90 °C.

With citric acid (C₆H₈O₇), all the investigated metals showed a similar behavior. At 30 °C, there was a slight increase in the extraction percentage with increasing concentration and at 50 °C, the extraction increased with the concentration increase from 0.15 to 0.3 M, but decreased or plateaued from 0.3 to 0.6 M. At 70 °C, there was a clear dip in the extraction at 0.3 M concentration. This is thought to be a measurement error. The extraction as a function of concentration is illustrated by the extraction curve of lead in Figure 37. The graphs showed similar trends for all investigated metals.

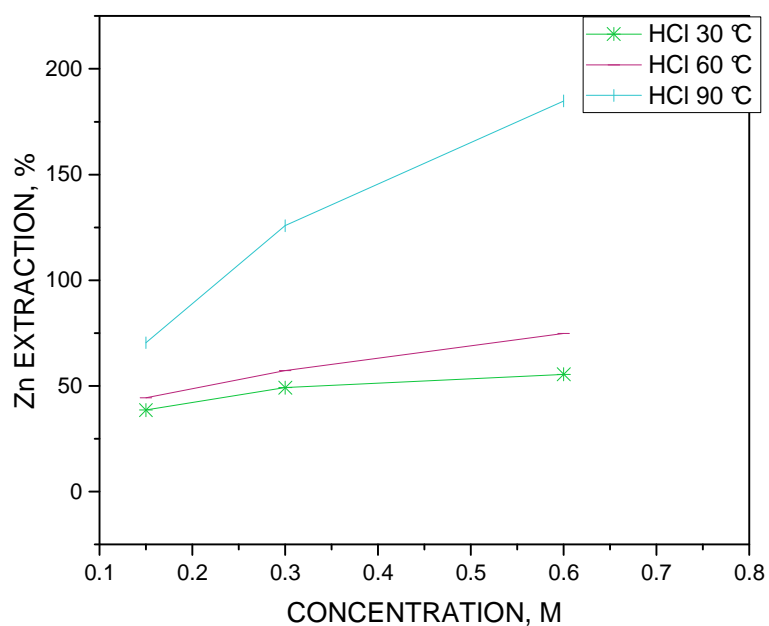


Figure 36. The extraction of zinc from WGPD as a function of concentration in HCl after 4 hours of leaching, L/S ratio 20 mL/g. Analysis results from experiments N1 – N9.

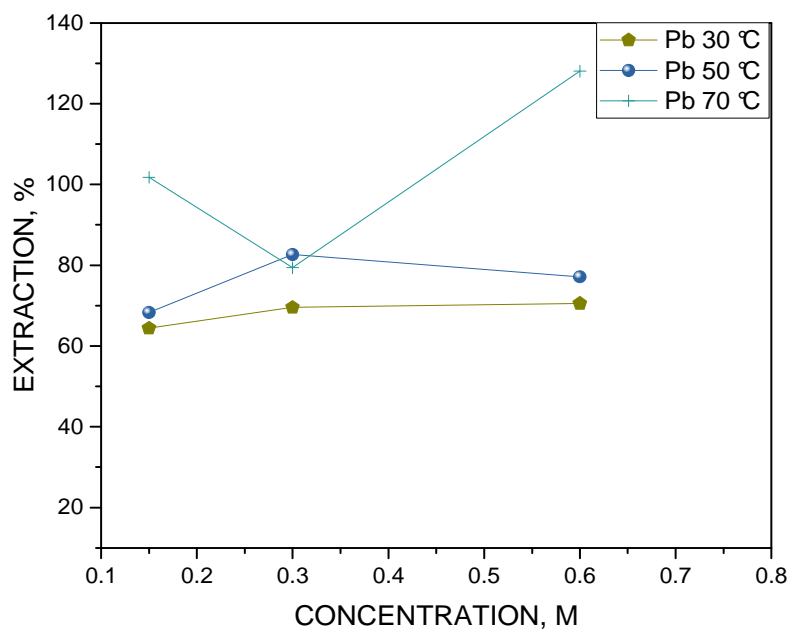


Figure 37. The extraction of lead to citric acid as a function of citric acid concentration after 4 hours of leaching. Analysis results from experiments M1 – M9.

6.2.3 Effect of leaching time

Extractions in HCl and $C_6H_8O_7$ with concentrations 0.15 and 0.6 M were compared at 30 °C, since this was the only common temperature for both solutions. The first sampling was made at 0.5 h. At that time, the leaching had already reached its maximal level, only minor changes can be seen between 0.5 and 4 h. The Cu extraction kinetics as a function of time (Figure 38, 0.15 M) suggests either (i) one error analysis at $t = 0.5$ h for 0.15 M HCl or (ii) that a back precipitation phenomenon of copper may occur. In general, at 30 °C the extraction efficiency did not change significantly after 0.5 h leaching time.

The extraction of metals from the WGPD into solution as a function of concentration for all experiments N1 – N9 and M1 – M9 are displayed in Appendix B. Also the final calculated extraction level at 4 h based on the residue analysis made by Ekokem (Table 12) is shown as a single point in the graphs. In general, there are not many changes in extraction after 1 h of leaching, except for experiments in at higher temperature, N6 (0.3 M, 90 °C), N9 (0.6 M, 90 °C) M3 (0.15 M, 70 °C) and M9 (0.6 M, 90 °C), where the extraction is directly dependent of temperature. In N3, the sudden peak at 1 h is probably analysis error. There is some variation in the final extractions based on solution or solid analysis. Differences up to 90 percentage can be observed for copper extraction, and lead extractions at higher temperatures (N6, N9, M3, M9) are quite far (>40%) from each other. The analysis based on solid analysis of other metals tend to be within 20% of the solution analysis based extractions.

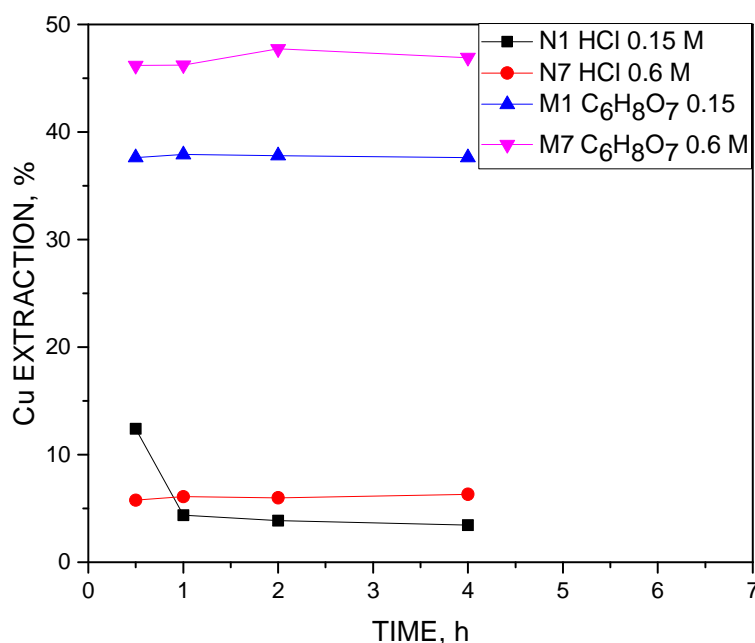


Figure 38. The extraction of copper to HCl (0.15 and 0.6 M) and $C_6H_8O_7$ (0.15 and 0.6 M) as a function of time at 30 °C after 4 hours of leaching. Test results presented from tests N1, N7, M1 and M7.

6.2.4 SEM analysis of the leaching residue of WGPD after batch leaching

A sample from the residue of leaching in HCl (0.3 M) at 30 °C was analyzed with SEM-EDS at GTK (Geological survey of Finland). It revealed that the insoluble material consisted of many different phases including Pb-Cl compounds and Fe- Zn oxides. These phases were found rimming the particles, but also inside precipitates. Zn and Fe, and sometimes Ni, Cu, and Cr were found in silicate phases. Figure 39 shows an oxide phase with Fe, Ni and Cr. Only small amounts of C were found in brass like phases. Some nickel was found together with Zr and with As. Figure 40 depicts the heterogeneous nature of the WGPD, with many different particle shapes and sizes and crystal structures, such as gypsum, fluorite, oxides with Pb, I and Cl, oxides with Fe, Si and oxides with Fe and Zn. Overall, the material was shown to be heterogenic with different ball, shell, and grain structures. Appendix C shows the chemical analysis more specifically.

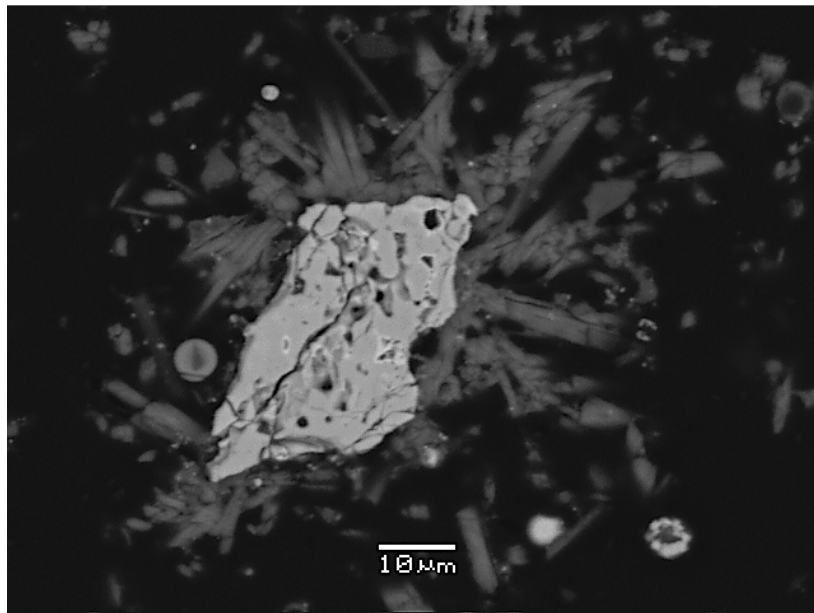


Figure 39. SEM analysis of WGPD leaching residue. Figure presents a oxide particle phase containing Fe, Ni, and Cr. SEM analysis made at GTK. The rest of the results from this analysis are shown in Appendix C. Test leach residue origins from test N4.

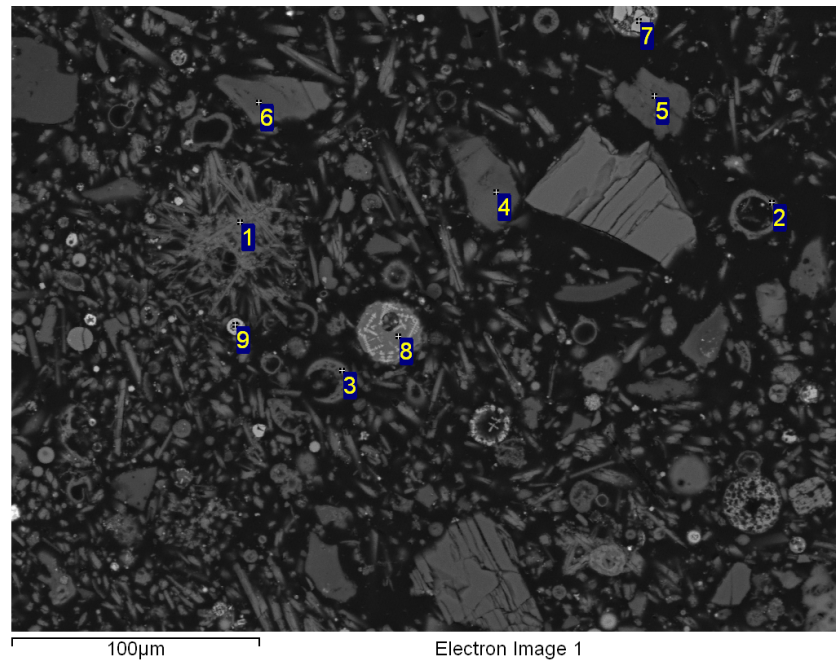


Figure 40. SEM analysis of WGPD leaching residue. Figure depicts the heterogeneous nature of the WGPD, with many different particle shapes and sizes and crystal structures such as gypsum (1), fluorite (2, 3), oxide with Pb, I and Cl (4, 5, 6), oxide with Fe (7), Si (8) and oxide with Fe and Zn (9). More results in Appendix C. Residue from test N4.

6.2.5 Batch leaching residue chemical analysis

The filtrated leaching residues of WGPD after batch leaching tests (N1-N9 and M1-M9) were sent for total leaching and ICP analysis to Ekokem Innolab. The results of this analysis are seen in Table 12 and 13. The filter papers used in the batch leaching test were weighed both before and after the filtration to find out the mass of the residue.

The residue percentage was compared to the metal leaching extraction to the solution (%), which was calculated similarly to equation (3). The sum of these percentages (mass balance) should in an ideal case be 100%. Table 12 shows that the mass balance was not ideal and varied depending on the leaching media and metal investigated. This is probably due to inaccurate analysis results or due to moisture in the filters when measuring the m_R , increasing the mass of the leach residue. The original WGPD mass added to the reactor was 20 g.

Table 13. The chemical composition of the leach residues (ppm) after batch leaching experiments N1-N9 in HCl. Analyses by Ekokem Innolab.

Metal fraction (ppm) in HCl	30 °C	60 °C	90 °C	30 °C	60 °C	90 °C	30 °C	60 °C	90 °C
	0.15 M	0.15 M N2	0.15 M	0.3 M	0.3 M	0.3 M	0.6 M	0.6 M	0.6 M
	M	*7.9 g	N3	N4	N5	N6	N7	N8	N9
leaching residue	N1		*7.4 g	*5.6 g	*5.1 g	*5.0 g	*3.4 g	*2.7 g	*2.9 g
	*9.0 g								
Cu	900	980	780	480	450	400	630	650	380
Fe	35k	34100	34k	49k	50k	40k	66k	76k	37k
Ni	600	610	550	900	980	750	1400	1600	790
Pb	18k	18k	13k	13k	7900	4100	10k	7700	4500
Zn	18k	18k	13k	22k	24k	18k	31k	32k	15k

*indicates WGPD mass after leaching experiments

Table 14. The chemical composition of the leach residues (ppm) after batch leaching experiments M1-M9 in citric acid ($C_6H_8O_7$). Analyses by Ekokem Innolab.

Metal fraction (ppm) in $C_6H_8O_7$ leaching residue	30 °C	50 °C	70 °C	30 °C	50 °C	70 °C	30 °C	50 °C	70 °C
	0.15	0.15 M	0.15 M	0.3 M	0.3 M	0.3 M	0.6 M	0.6 M	0.6 M
	M	M2	M3	M4	M5	M6	M7	M8	M9
	M1	*3.1 g	*5.7 g	*5.0 g	*4.5 g	* N/A	*6.1 g	*6.3 g	*7.1 g
	*4.7 g								
Cu	670	520	460	560	390	380	420	330	290
Fe	49k	45k	39k	48k	40k	40k	39k	35k	30k
Ni	750	710	620	720	560	610	610	530	450
Pb	13k	11k	9000	11k	6400	6900	8300	5700	4400
Zn	27k	24k	21k	25k	18k	20k	20k	17k	15k

*indicates WGPD mass after leaching experiments

6.2.6 Extraction modelling

The results from the batch leaching tests (N1-N9 and M1-M9) were processed with Modde 8.0® (Umetrics AB) software. Due to only having 9 batch leaching experiments in each solution (HCl and C₆H₈O₇) (see Table 8 for conditions), the results produced statistically only valid model for copper and not for the other metals. The validity of the factors is shown in Table 15, in which the direction of the arrows indicates a positive or negative effect on metal extraction. It seems that increase in temperature, concentration and in the combined effect of these parameters have a positive effect on all metal dissolution in HCl and C₆H₈O₇ solutions. The parenthesis around the arrow indicate a non-valid factor, which means the error margins were shown to exceed the range of the factor impact. All the resulting models (valid and non-valid) are presented in Table 16. It needs to be noted that only the model for Cu extraction in C₆H₈O₇ media was shown to be statistically valid.

Table 15. The validity of the effect of factors on the extraction by Modde 8.0 software. The direction of the arrow indicates a positive or negative effect, and the parenthesis indicate a non-valid factor. The investigated factors are temperature, concentration, and their product. T is temperature (°C) and c concentration (M).

HCl	T	c	T*c
Cu	(↑)	(↑)	(↑)
Fe	(↑)	(↑)	(↑)
Ni	↑	↑	(↑)
Pb	(↑)	(↑)	(↑)
Zn	↑	↑	(↑)
C ₆ H ₈ O ₇			
Cu	↑	(↑)	(↑)
Fe	↑	(↑)	(↑)
Ni	(↑)	(↑)	(↑)
Pb	↑	(↑)	(↑)
Zn	↑	(↑)	(↑)

Table 16. Models of the valid factors obtained from extraction analysis in the Modde 8.0 software. E stands for extraction (%), T for temperature ($^{\circ}\text{C}$), and c for concentration (M).

HCl	
Ni	$E = -3 + 0.3T + 43c$
Zn	$E = 15 + 0.5T + 47c$
C ₆ H ₈ O ₇	
Cu	$E = 24 + 0.5T$
Fe	$E = 4 + 0.3T$
Pb	$E = 39 + 0.9T$
Zn	$E = 29 + 0.5T$

The statistical validity of the models depend on their “goodness of fit” and “goodness of prediction”. The former is expressed by a value R^2 , and the latter by a value Q^2 . For a statistically valid model Q^2 should be greater than 0.5 and the difference between R^2 and Q^2 less than or equal to 0.3 [34]. Thus, only the model for copper leaching in citric acid is statistically valid, which is indicated by the values in Table 17. The reliability of the models is low because of the lack of the amount or repetitions of experiments. Further research is required to study the reproducibility of the data.

Table 17. Goodness of fit (R^2), goodness of prediction (Q^2), and their difference from analysis of leaching models of Cu, Fe, Ni, Pb, and Zn into HCl and citric acid.

	HCl			C ₆ H ₈ O ₇		
	R^2	Q^2	$R^2 - Q^2$	R^2	Q^2	$R^2 - Q^2$
Cu	0.5	0.1	0.4	0.7	0.5	0.2
Fe	0.9	0.3	0.6	0.5	0.3	0.2
Ni	0.7	0.3	0.4	0.4	0.1	0.3
Pb	0.5	0.1	0.4	0.5	0.4	0.1
Zn	0.7	0.3	0.4	0.6	0.4	0.2

7 Conclusions

These experiments aimed at finding the most effective lixiviant for leaching metals for WGPD, test it in batch leaching tests, and create a leaching model for it. Another objective was to reduce the total metal concentration in residue below 1000 ppm. A further interest was the selectivity of metal dissolution towards iron (Fe), with the goal of finding a solvent that would extract the metals of interest, but leave iron in the residue.

In the solution mapping tests pH and redox potentials were measured. During the mapping test, there was no pH control nor air feed into the solution. The redox potential (mV vs. SCE) and pH windows for all the solutions were the following: acetic acid 252 – 457 and 1.5 – 4.1, citric acid 285 – 529 and 0.2 – 2.3, HCl 393 – 535 and -1.3 – 2.9, H₂SO₄ 435 – 592 and -1.3 – 1.1 as well as HCl + H₂SO₄ 440 – 500 and 0.4 – 0.6.

The chosen solution for the batch leaching experiment was hydrochloric acid, because it gave the highest metal dissolution in the mapping tests (24 hour leaching tests). In addition, citric acid was selected for the batch leaching tests due to the fact that it was shown to be the most effective organic acid. In the mapping tests it was also found that acetic acid had a certain selectivity between lead and iron. Citric acid showed potential for being a good solvent of lead. Ethaline showed good reproducibility in tests.

In addition to extraction efficiency, the impact of concentration and temperature was evaluated in both mapping and batch leaching tests. The effects varied, which was also seen in the validity of model factors. Both temperature and concentration were valid for nickel and zinc extraction in hydrochloric acid. Temperature was shown to be a valid factor for copper, iron, lead, and zinc extraction in citric acid. Both temperature and concentration increase had a positive effect on extraction. Models were built for all investigated metals in both citric and hydrochloric acid. The model for copper in citric acid was shown to be valid.

The batch leaching tests were carried out in a bigger scale reactor (400 ml) and with air feed to the solution. However, there was no pH adjustment during the leaching tests. The objective to reduce metal concentrations in the residue below 1000 ppm was successful for copper in all batch leaching experiments (N1-N9 and M1-M9). The content of iron, nickel and zinc in solids (i.e. percentage in leach residue) increased in all batch leaching experiments. This increase of concentration is due fact that a major part (ca. 70 – 90 %) of the WGPD was dissolved during the leaching, decreasing solid mass remarkably. As a

consequence, the content per mass unit of solids increases. This makes it challenging to decrease the total metal content in the leach residue below 1000 ppm.

The lead concentration was shown to be reduced from the original concentration (ppm in WGPD) at 90 °C HCl (0.3 and 0.6 M) and in at 50 and 70 °C citric acid (0.6 M), regardless of the mass reduction during the leaching. This suggests that citric acid can be an effective leaching agent for lead removal from WGPD.

8 References

- [1] O. S. o. F. (OSF), "www.stat.fi," 2015. [Online]. Available: http://www.stat.fi/til/jate/2014/jate_2014_2015-12-01_tie_001_en.html. [Accessed 10 February 2017].
- [2] C. H. K. Lam, A. W. M. Ip, J. P. Barford and G. McKay, "Use of Incineration MSW Ash: A review," *Sustainability*, no. 2, pp. 1943 - 1968, 2010.
- [3] T. W.-t.-E. R. a. T. C. (WtERT), "The Waste-to-Energy Research and Technology Council (WtERT)," [Online]. Available: <http://www.wtert.eu/default.asp?Menu=12>. [Accessed 1 January 2017].
- [4] U. SUEZ recycling and recovery, "The energy-from-waste process," [Online]. Available: <http://www.suez.co.im/energy-recovery/the-energy-from-waste-process>. [Accessed 1 January 2017].
- [5] W.-t.-E. R. a. T. C. (WtEC), "Incineration," [Online]. Available: <http://www.wtert.eu/default.asp?Menu=12>. [Accessed 15 January 2017].
- [6] S. Nagib and K. Inoue, "Recovery of lead and zinc from fly ash generated from municipal incineration plants by means of acid and/or alkaline leaching," *Hydrometallurgy*, vol. 56, no. 3, p. 269–292, 2000.
- [7] K. Huang, K. Inoue, H. Harada, H. Kawakita and K. Ohto, "Leaching of heavy metals by citric acid from fly ash generated in municipal waste incineration plants," *Journal of Material Cycles and Waste Management*, vol. 13, no. 2, pp. 118-126, 2011.
- [8] Y. Zhang, J. Chen, K. Perthel, T. B. Edil and W. J. Likos, "Leaching Characteristics of Fly Ash from Municipal Solid Waste Incineration," 2014.
- [9] T. Kaartinen, J. Laine-Ylijoki and M. Wahlström, "Jätteen termisen käsittelyn tukien ja kuonien käsittely- ja sijoitusmahdollisuudet," VTT Technical Research Centre of Finland, Espoo, 2007.
- [10] K. Huang, K. Inoue, H. Harada, H. Kawakita and K. Ohto, "Leaching behavior of heavy metals with hydrochloric acid from fly ash generated in municipal waste incineration plants," *Transactions of Nonferrous Metals Society of China*, vol. 21, no. 6, pp. 1422 - 1427, 2011.
- [11] A. J. Chandler, T. T. Eighmy, J. Hartlén, O. Hjelm, D. S. Kosson, S. E. Sawell, H. A. van der Sloot and J. Vehlow, "Municipal Solid Waste Incinerator Residues," *Studies in Environmental Sciences*, vol. 67, 1997.

- [12] M. J. Quina, J. C. Bordado and R. M. Quinta-Ferreira, "Treatment and use of air pollution control residues from MSW incineration: An overview," *Waste management*, vol. 28, no. 11, p. 2097–2121, 2008.
- [13] A. P. Abbot, G. Capper, D. L. Davies, H. L. Munro, R. K. Rasheed and V. Tambyrajah, "Preparation of novel, moisture-stable, Lewis-acidic ionic liquids containing quaternary ammonium salts with functional side chains," *Chemical Communications*, no. 19, pp. 2010 - 2011, 2001.
- [14] E. L. Smith, A. P. Abbot and K. S. Ryder, "Deep Eutectic Solvents (DESs) and Their Applications," *Chemical Reviews*, pp. 11060 - 11082, 2014.
- [15] A. P. Abbott, D. Boothby, G. Capper, D. L. Davies and R. K. Rasheed, "Deep Eutectic Solvents Formed between Choline Chloride and Carboxylic Acids: Versatile Alternatives to Ionic Liquids," *Journal of the American Chemical Society*, vol. 126, pp. 9142 -9147, 2004.
- [16] G. R. T. Jenkin, A. Z. M. Al-Bassam, R. C. Harris, A. P. Abbot, D. J. Smith, D. A. Holwell, R. J. Chapman and C. J. Stanley, "The application of deep eutectic solvent ionic liquids for environmentally-friendly dissolution and recovery of precious metals," *Minerals Engineering*, vol. 87, pp. 18 - 24, 2016.
- [17] A. P. Abbot, R. C. Harris, F. Holyoak, G. Frisch, J. Hartley and R. T. G. Jenkin, "Electrocatalytic recovery of elements from complex mixtures using deep eutectic solvents," *Green Chemistry*, no. 4, pp. 2172 - 2179, 2015.
- [18] A. P. Abbott, G. Capper, D. L. Davies, R. K. Rasheed and V. Tambyrajah, "Novel solvent properties of choline chloride/urea mixtures," in *Chemical Communications*, 2002, pp. 70 - 71.
- [19] H. Y. Zhang and G. X. Ma, "Leaching of Heavy Metals from Municipal Solid Waste Incineration (MSWI) Fly Ash Using Sulfuric Acid," *Applied Mechanics and Materials*, Vols. 249 - 250, pp. 922 - 926, December 2012.
- [20] M. Romero, J. M. Rincón, R. D. Rawlings and A. R. Boccaccini, "Use of vitrified urban incinerator waste as raw material for production of sintered glass-ceramics," *Materials Research Bulletin*, vol. 36, no. 1 - 2, pp. 383 - 395, 2001.
- [21] F. Andreola, L. Barbieri, S. Hreglich, I. Lancellotti, L. Morselli, F. Passarini and I. Vassura, "Reuse of incinerator bottom and fly ashes to obtain glassy materials," *Journal of Hazardous Materials*, no. 153, pp. 1270 - 1274, 200.
- [22] Z. Haiying, Z. Youcai and Q. Jingyu, "Study on use of MSWI fly ash in ceramic tile," *Journal of Hazardous Materials*, vol. 141, no. 1, pp. 106 - 114, 2007.
- [23] T. W. Cheng and Y. S. Chen, "Characterisation of glass ceramics made from incinerator fly ash," *Ceramics International*, vol. 30, no. 3, pp. 343 - 349, 2004.
- [24] O. Ginés, J. M. Chimenos, A. Vizcarro, J. Formosa and J. R. Rosell, "Combined use of MSWI bottom ash and fly ash as aggregate in concrete formulation," *Journal of Hazardous Materials*, vol. 169, no. 1 - 3, pp. 643 - 650, 2009.

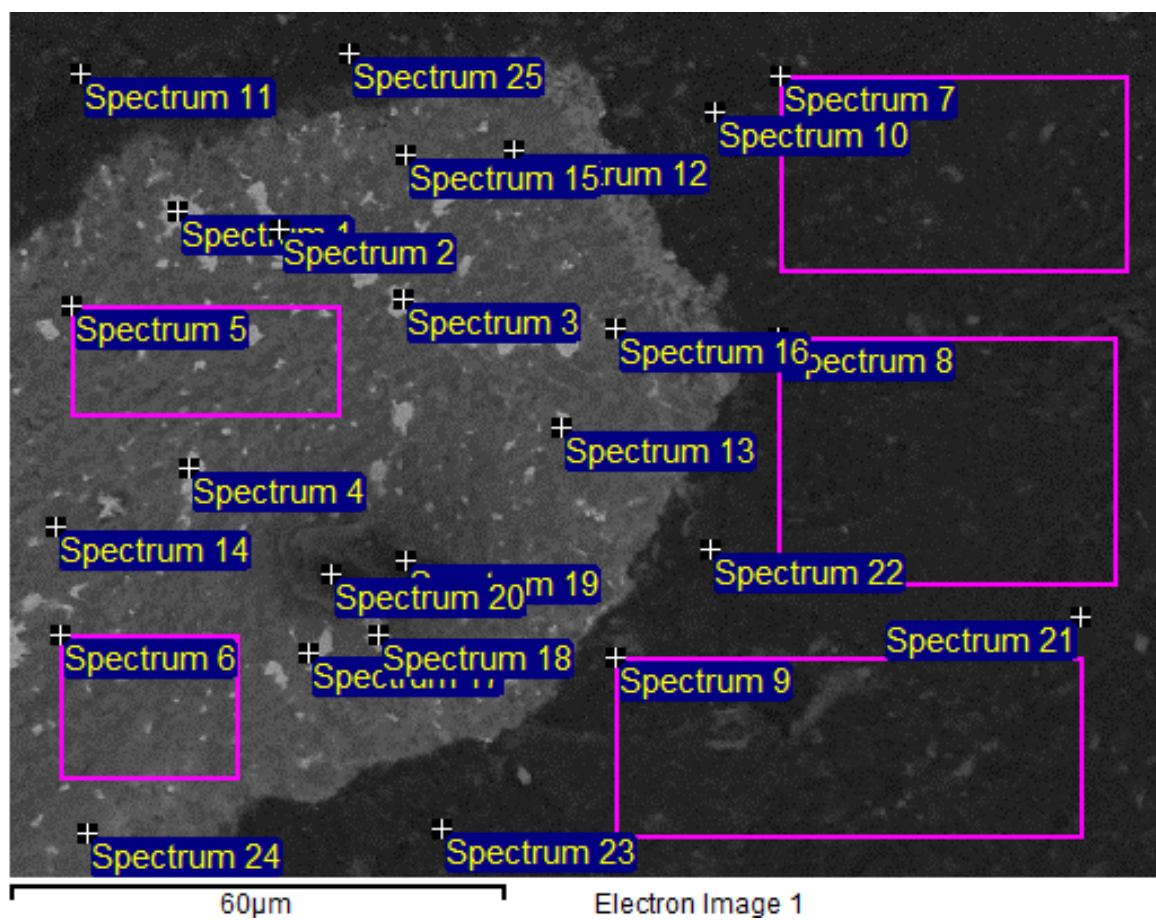
- [25] J. R. Pan, C. Huang, J.-J. Kuo and S.-H. Lin, "Recycling MSWI bottom and fly ash as raw materials for Portland cement," *Waste Management*, vol. 28, no. 7, pp. 1113 - 1118, 2007.
- [26] J. Yang, B. Xiao and A. R. Boccaccini, "Preparation of low melting temperature glass–ceramics from municipal waste incineration fly ash," *Fuel*, vol. 88, no. 7, pp. 1275 - 1280, 2009.
- [27] M. Cobo, A. Gálvez, J. A. Conesa and C. M. de Correa, "Preparation of low melting temperature glass–ceramics from municipal waste incinerator in Medellin, Colombia," *Journal of Hazardous Materials*, vol. 168, no. 2 - 3, pp. 1223 - 1232, 2009.
- [28] I. Bódog, K. Polyák, Z. Csikós-Hartyányi and J. Hlavay, "Sequential Extraction Procedure for the Speciation of Elements in Fly Ash Samples," *Microchemical Journal*, no. 54, pp. 320 - 330, 1996.
- [29] H.-Y. Wu and Y.-P. Ting, "Metal extraction from municipal solid waste (MSW) incinerator fly ash - Chemical leaching and fungal bioleaching," *Enzyme and Microbial Technology*, vol. 38, pp. 839 - 847, 2006.
- [30] P. c. w. J. Ö. Ekokem Oyj, 2016.
- [31] P. Hayes, *Process Principles in Minerals & Materials Production*, 3 ed., Brisbane: HAYES PUBLISHING CO, 2003, p. 734.
- [32] N. Habache, N. Alane, S. Djerad and L. Tifouti, "Leaching of copper oxide with different acid solutions," *Chemical Engineering Journal*, vol. 152, pp. 503 - 508, 2009.
- [33] R. Björkvall, *Thiosulfate leaching of metals from waste electric and electronic equipment and bottom ash*, Aalto University School of Chemical Technology, 2016.
- [34] L. Eriksson, E. Johansson, N. Kettaneh-Wold, C. Wikström and S. Wold, *Design of Experiments: Principles and Applications*, Umetrics AB, Umeå Learnways AB, 2000, p. 329.
- [35] C.-W. W. C.-J. S. Sue-Huai Gau, "Washing pretreatment to improve the quality during the regeneration of MSWI fly ash," in *3rd International Conference on Waste Management and Technology*, Beijing, 2008.
- [36] S. Sernuschi, M. Giugliano and I. de Paoli, "Leaching of residues from MSW incineration," *Waste Management & Research*, vol. 8, no. 6, pp. 419 - 427, 1990.
- [37] K. Karlfeldt Fedje, *Metals in MSWI fly ash - problems or opportunities?*, Göteborg: Chalmers University of Technology, 2010.
- [38] C. Fischer, "Municipal waste management in Finland," European Environment Agency, 2013.

- [39] S. Cernuschi, M. Giugliano and I. de Paoli, "Leaching of residues from MSW incineration," *Waste management & research*, pp. 419-427, 1990.
- [40] U. Bertocci and D. R. Turner, "6. Copper," in *Encyclopedia of Electrochemistry of the Elements*, Austin, Marcel Dekker Inc., 1974, pp. 384 - 499.
- [41] A. J. Arvía and D. Posadas, "3. Nickel," in *Encyclopedia of Electrochemistry of the Elements*, Austin, Marcel Dekker Inc., 1975, pp. 212 - 399.
- [42] A. Abbott, "Deep Eutectic Solvents," in *Leuven Summer School on Ionic Liquids*, 2010.

Appendix A. SEM analysis results of the WGPD.

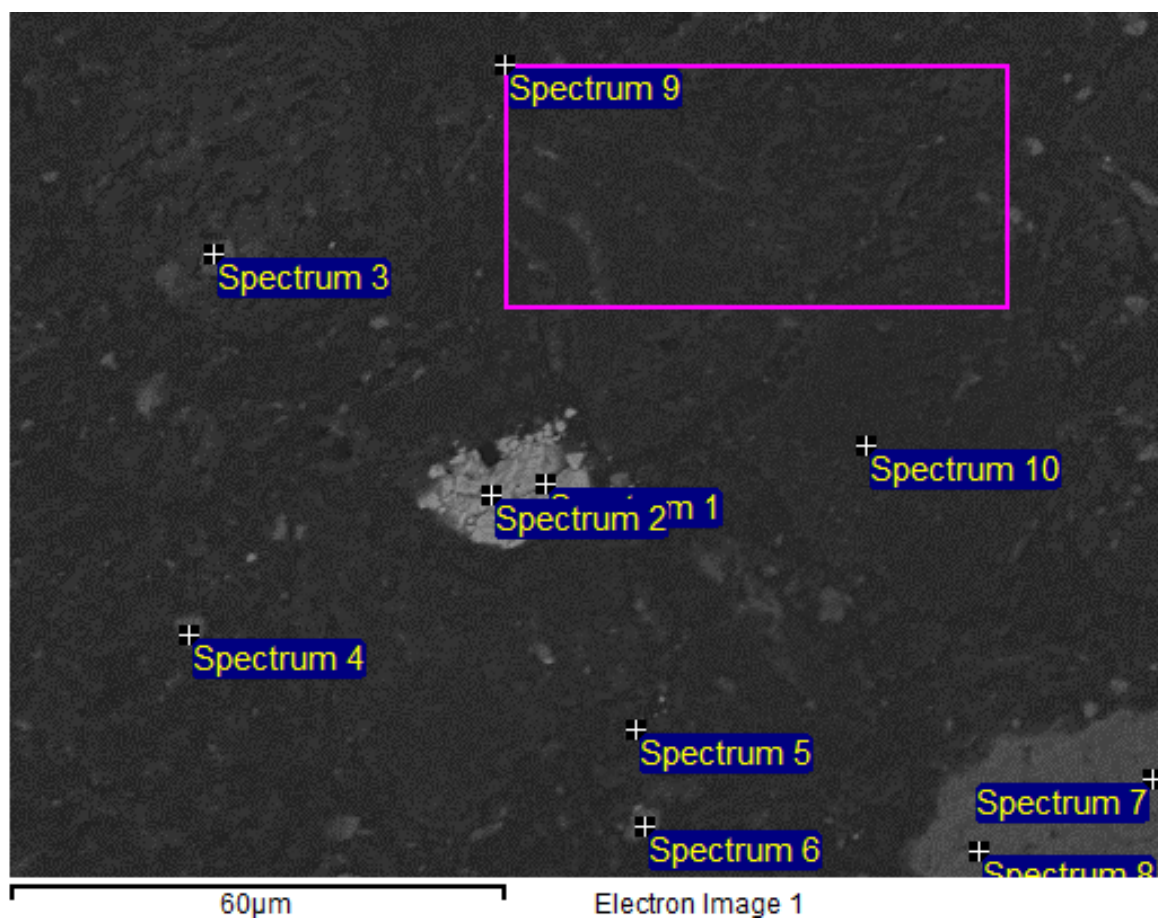
Spectrum	O	Na	Mg	Al	Si	S	Cl	K	Ca	Ti	Mn	Fe	Cu	Zn	Pb	Total
Spectrum 1							0.47		0.55			93.16	2.03			96.20
Spectrum 2	3.27		0.42		0.62		0.95		1.06			92.35	2.27			100.94
Spectrum 3	2.26				0.30		0.64		1.02			93.39	2.26			99.86
Spectrum 4	1.20						0.43		0.64			91.08	2.46			95.80
Spectrum 5	44.09		4.10	6.89	19.26		1.03		15.32	0.53		10.88				102.10
Spectrum 6	44.25		3.63	7.69	19.09		1.81	0.36	15.76	0.45		9.30				102.34
Spectrum 7	4.62		0.25	0.61	0.66	0.39	1.52	0.17	1.06			0.35				9.62
Spectrum 8	3.61		0.21	0.42	0.47	0.38	1.27	0.16	0.76			0.25				7.52
Spectrum 9	5.94		0.34	0.78	1.04	0.25	1.94	0.27	1.29			0.23		0.56		12.64
Spectrum 10	7.13		0.31	0.23	0.30		3.29	0.26	1.76			0.30				13.57
Spectrum 11	6.72	0.20	0.47	0.59	0.84	0.18	2.14	0.27	1.28			0.29				12.98
Spectrum 12	45.55		2.15	10.25	18.81		0.25		13.49	0.24		7.26				97.99
Spectrum 13	25.90		3.68	3.43	16.83		2.94	0.27	15.23	0.53		8.61	2.61			80.02
Spectrum 14	43.28		5.42	3.20	19.40		1.92		16.45	0.72	0.38	10.48	0.69			101.96
Spectrum 15	50.16		5.79	4.58	21.41		0.95		16.71	0.73	0.41	8.64				109.37
Spectrum 16	25.58		4.47	2.32	16.53		3.25	0.19	12.06	0.45	0.42	16.62	0.96			82.86
Spectrum 17	48.03	0.22	3.57	10.06	20.51		1.04	0.21	15.75	0.33		4.15				103.85

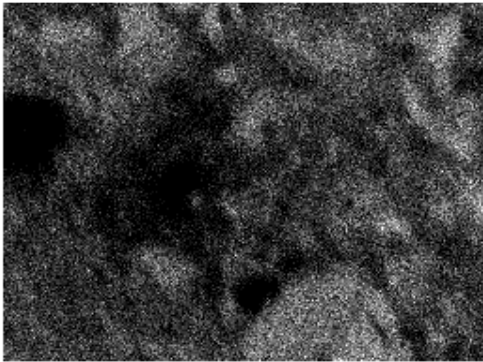
Spectrum 18	26.89	3.98	2.14	14.48	0.30	2.91	0.23	11.64	0.49	35.96	2.47	101.50
Spectrum 19	32.89	2.62	8.35	15.55		1.81		11.97		29.76	1.08	104.11
Spectrum 20	18.92	2.20	1.06	6.19		3.85	0.29	4.63		74.58	2.03	113.75
Spectrum 21	5.99	0.43	0.28	0.32		1.75		1.06				9.82
Spectrum 22	2.41	0.13	0.27	0.31	0.43	0.95		0.62		0.30		5.42
Spectrum 23	6.19	0.38	0.20	0.19		1.41	0.12	0.98		0.30	0.93	10.71
Spectrum 24	24.86	0.48	1.34	2.32	6.69	11.19	1.35	6.10		13.41		5.78
Spectrum 25	43.96	3.72	7.48	19.35		2.40	0.22	15.83	0.48	6.71	0.70	100.85
Max.	50.16	0.48	5.79	10.25	21.41	0.43	11.19	1.35	16.71	0.73	0.42	93.39
Min.	1.20	0.20	0.13	0.20	0.19	0.18	0.25	0.12	0.55	0.24	0.38	0.23
												0.69
												0.56
												5.78



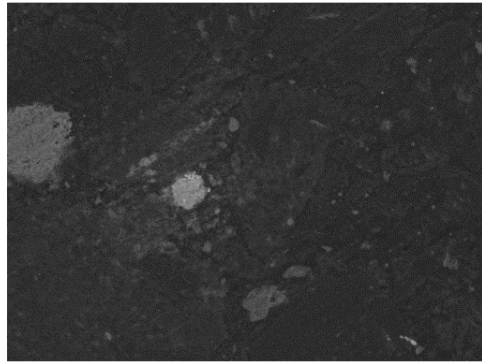
All results in weight%

Spectrum	O	Na	Mg	Al	Si	P	S	Cl	K	Ca	Ti	Mn	Fe	Zn	Total
Spectrum 1	29.44		0.84					0.28		0.29		0.41	70.10		101.37
Spectrum 2	8.88		0.84			0.13		0.46		0.96		0.74	64.19		76.21
Spectrum 3	1.94				15.18			5.50	0.43	3.16					26.21
Spectrum 4	4.44		0.33	0.54	0.69		0.18	1.74	0.16	1.01					9.10
Spectrum 5	7.26		0.73	0.79	1.06		0.11	0.64	0.16	2.55			0.22	0.37	13.88
Spectrum 6	6.97		0.39	0.25	0.30		0.22	1.74	0.16	1.57					11.60
Spectrum 7	46.86	0.97	0.63	15.22	22.57			1.53	3.44	1.01	0.82		0.70		93.73
Spectrum 8	51.93	1.00	0.57	16.05	24.58			2.48	3.68	1.61	1.10		0.99		104.01
Spectrum 9	4.10		0.21	0.46	0.48		0.34	1.68	0.21	1.20			0.22		8.88
Spectrum 10	1.79						0.46	1.26	0.13	0.78			0.24		4.65
Max.	51.93	1.00	0.84	16.05	24.58	0.13	0.46	5.50	3.68	3.16	1.10	0.74	70.10	0.37	
Min.	1.79	0.97	0.21	0.25	0.30	0.13	0.11	0.28	0.13	0.29	0.82	0.41	0.22	0.37	

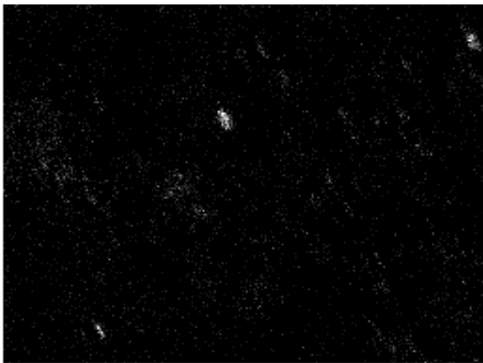




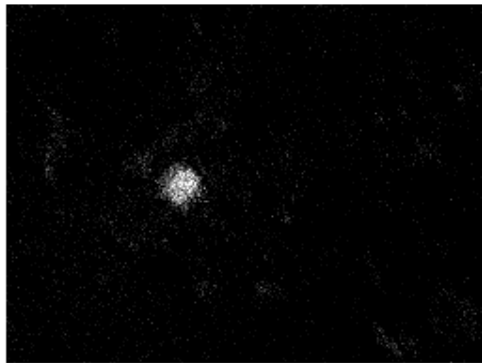
C Ka1_2



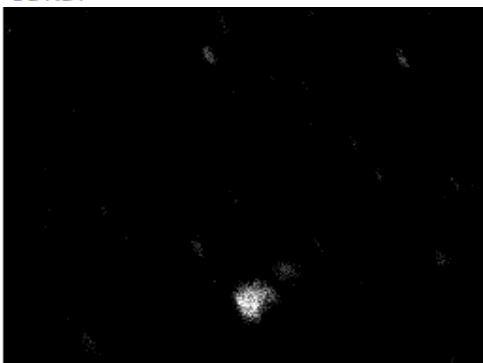
Electron Image 1



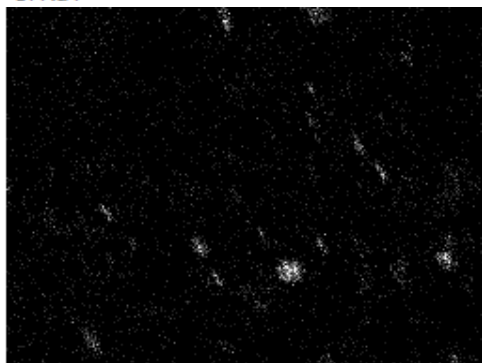
Ca Ka1



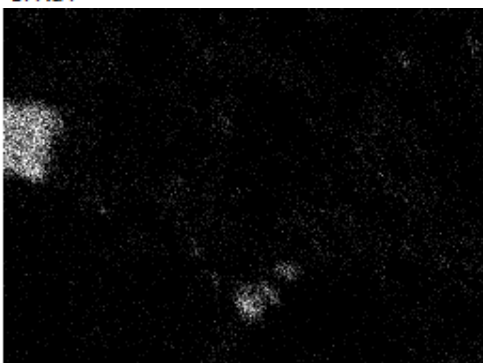
Cl Ka1



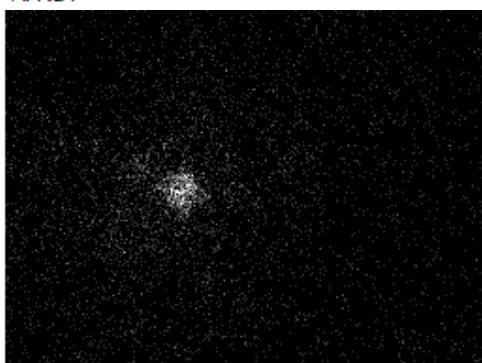
Si Ka1



Al Ka1



O Ka1

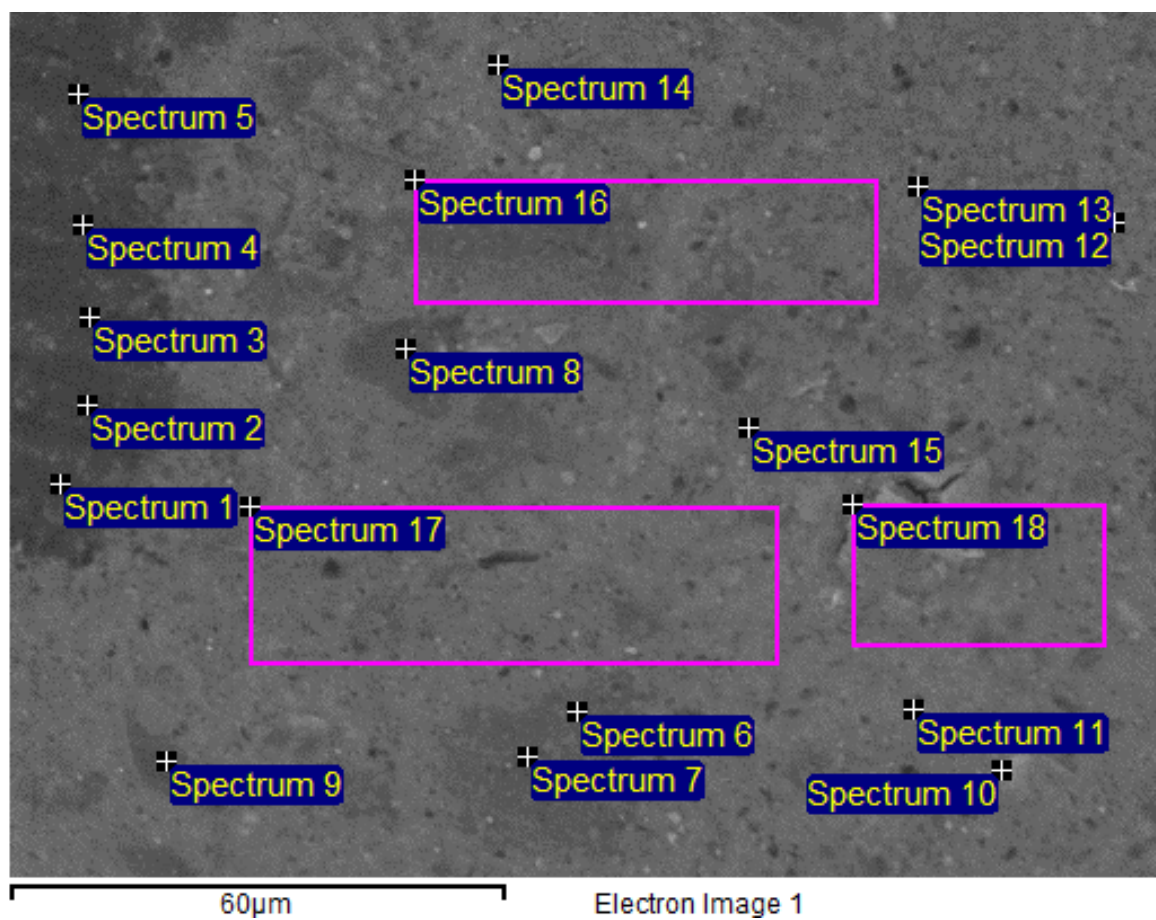


Cu Ka1

All results in weight%

Spectrum	O	F	Na	Mg	Al	Si	P	S	Cl	K	Ca	Cr	Fe	Cu	Zn	As	Br	I	Total
Spectrum 1	15.91				0.73	0.37		0.86	10.76	1.15	3.13		1.54	0.58	1.84			2.62	39.49
Spectrum 2	13.28	0.63			0.56			0.90	12.28	0.62	5.16			0.70	2.79			2.32	39.25
Spectrum 3	13.98	0.55			0.58			0.82	12.73	0.60	4.80			0.61	2.82			2.18	39.67
Spectrum 4	16.07	2.48		0.20	0.57			0.82	14.10	0.76	5.82			0.49	3.12			1.61	46.04
Spectrum 5	14.16				0.62			0.82	12.15	0.55	4.10			0.89	3.00			1.65	37.94
Spectrum 6	20.48	3.20	0.37	0.40		0.35	0.35	1.05	6.37	1.14	33.69		0.58		0.67	0.49			69.16
Spectrum 7	31.11	1.71		0.48				0.31	2.16	0.68	37.41				0.12				73.97
Spectrum 8	21.49	2.53				55.77		0.97	7.34	0.93	9.46		0.30		0.25				99.03
Spectrum 9	5.37	1.00				61.22		0.51	3.16	0.50	3.29								75.04
Spectrum 10	5.92	3.25			0.53	1.60		1.14	17.58	5.62	9.37	34.85	16.40		0.31				96.58
Spectrum 11	11.44	4.04	2.18	0.27	0.29	0.72		2.25	45.65	14.25	24.98		0.67						106.73
Spectrum 12	7.40	1.70	13.20			0.44		1.67	52.82	10.86	16.41		0.55						105.05
Spectrum 13	5.89	1.33	1.02	0.26	0.25	0.46		1.41	28.14	9.75	27.11		0.70						76.31
Spectrum 14	22.06	6.56	1.37			0.49		1.66	45.60	15.40	25.47		0.58						119.18
Spectrum 15	15.06	4.02	10.41	0.31		1.01		2.07	50.88	14.17	21.29		0.62				0.83		120.67
Spectrum 16	21.63	3.06	2.92		0.24	0.81		1.48	32.90	9.56	24.87		0.46						97.94

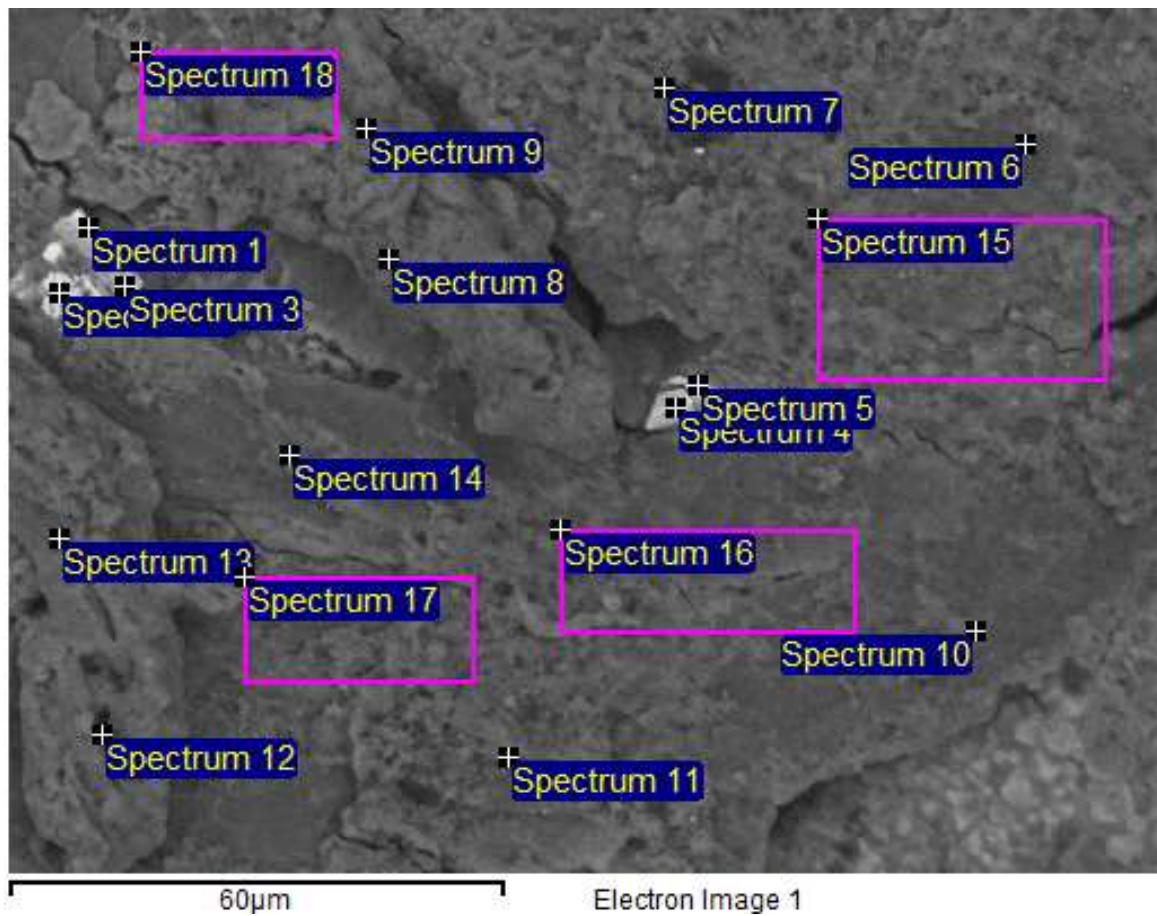
Spectrum 17	17.50	3.78	3.52	0.25	0.27	0.84	1.88	41.72	12.46	23.17	0.80	106.19					
Spectrum 18	13.85	3.93	2.54		0.20	1.44	1.81	47.25	14.73	22.04	0.70	108.49					
Max.	31.11	6.56	13.20	0.48	0.73	61.22	2.25	52.82	15.40	37.41	34.85	16.40	0.89	3.12	0.49	0.83	2.62
Min.	5.37	0.55	0.37	0.20	0.20	0.35	0.31	2.16	0.50	3.13	34.85	0.30	0.49	0.12	0.49	0.83	1.61



All results in weight%

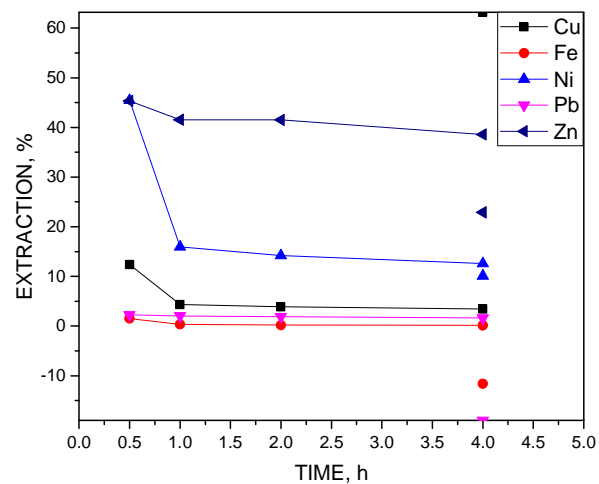
Spectrum	O	Na	Mg	Al	Si	S	Cl	K	Ca	Fe	Ni	Cu	Zn	As	Ba	Pb	Total
Spectrum 1	3.20			0.04			4.68	0.66	2.12				0.24		0.71	3.85	15.50
Spectrum 2	1.53						22.41	8.05	2.16						4.55	35.74	74.45
Spectrum 3	2.63			0.03			3.42	0.41	1.24						0.66	3.82	12.23
Spectrum 4	3.87			0.25			34.04	11.24	2.37					0.09	6.09	48.68	106.63
Spectrum 5	7.60			0.25			30.41	10.55	3.69						7.01	44.56	104.06
Spectrum 6	16.51		0.33	0.37			34.44	3.47	16.33	0.37			2.34				74.15
Spectrum 7	20.92		0.32	0.34	0.26	0.22	30.21	2.75	14.25	0.63			0.69				70.61
Spectrum 8	32.45		0.45	0.46	0.23	0.27	35.02	2.66	18.13	0.83			1.33				91.83
Spectrum 9	8.82		0.23	0.27	0.18	0.29	30.25	2.37	16.09	0.58			0.92				60.00
Spectrum 10	21.54		0.26	0.32			31.32	2.17	14.88				1.89				72.39
Spectrum 11	29.60		0.33	0.65	0.51	0.24	29.67	2.30	14.51	0.88			1.27				79.96
Spectrum 12	0.90		0.09	0.16	0.10	0.14	32.72	2.21	14.75	0.40	-0.01		1.32				52.79
Spectrum 13	19.49		0.27	0.41			28.24	1.68	13.41				1.72				65.21
Spectrum 14	15.34		0.16	0.24			23.60	1.11	11.50	0.30			1.74				53.99
Spectrum 15	25.28	0.68	0.25	0.36	0.27	0.22	32.50	3.56	16.14	0.49			1.15				80.90
Spectrum 16	26.99	2.20	0.24	0.30	0.19	0.26	31.78	2.30	13.14	0.63			1.10				79.13
Spectrum 17	18.61		0.23	0.35	0.40	0.26	29.44	2.49	14.12	0.61			1.14				67.64

Spectrum 18	22.84	1.75	0.18	0.30	0.49	0.17	26.44	1.84	15.33	0.43	0.47	0.67	70.91			
Max.	32.45	2.20	0.45	0.65	0.51	0.29	35.02	11.24	18.13	0.88	-0.01	0.47	2.34	0.09	7.01	48.68
Min.	0.90	0.68	0.09	0.03	0.10	0.14	3.42	0.41	1.24	0.30	-0.01	0.47	0.24	0.09	0.56	3.82

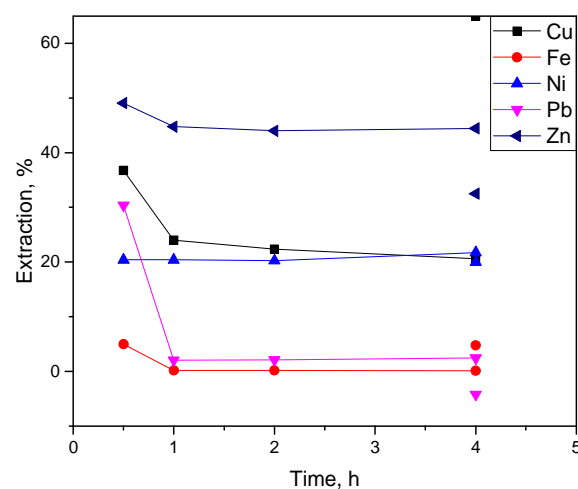


Appendix B. Extraction into solution in HCl and citric acid at $t = 0.5, 1, 2$ and 4 h and final extraction calculated from WGPLD mass on filters, displayed as single points.

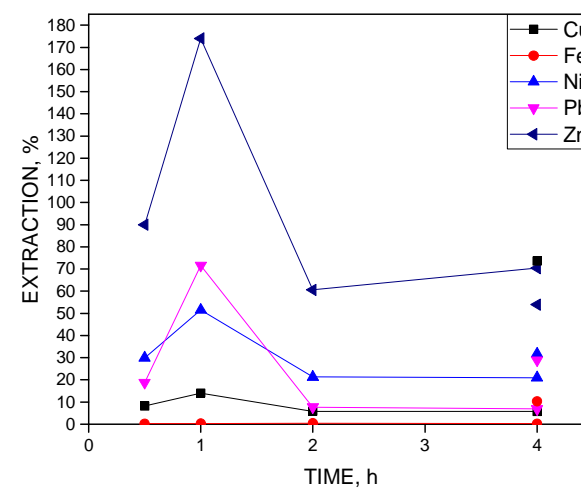
N1



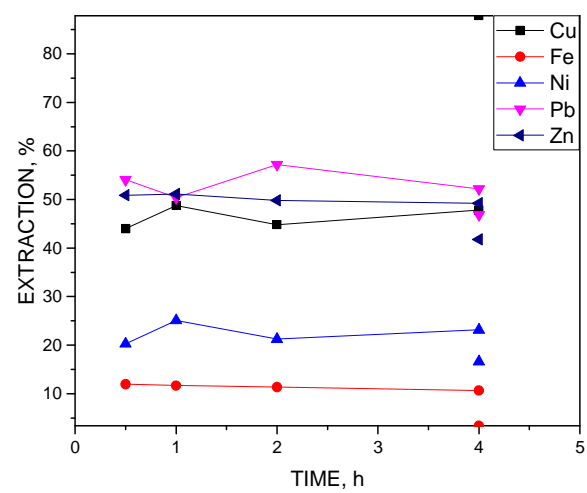
N2



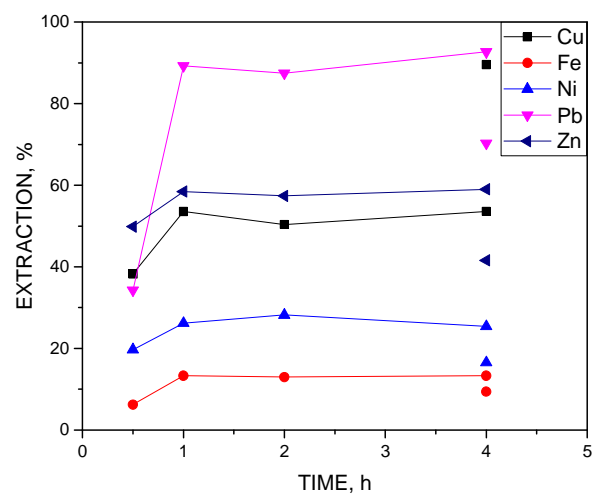
N3



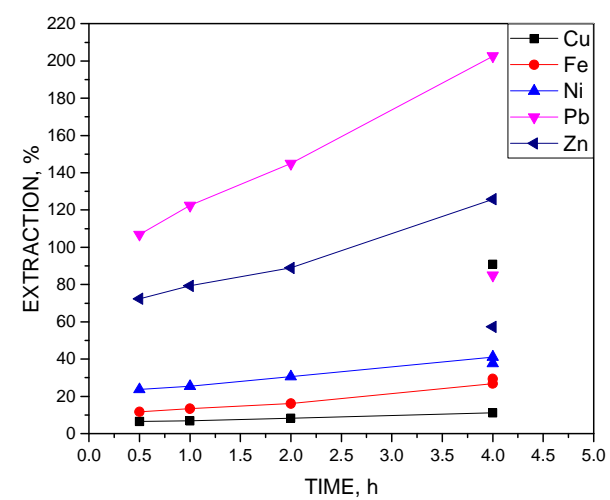
N4



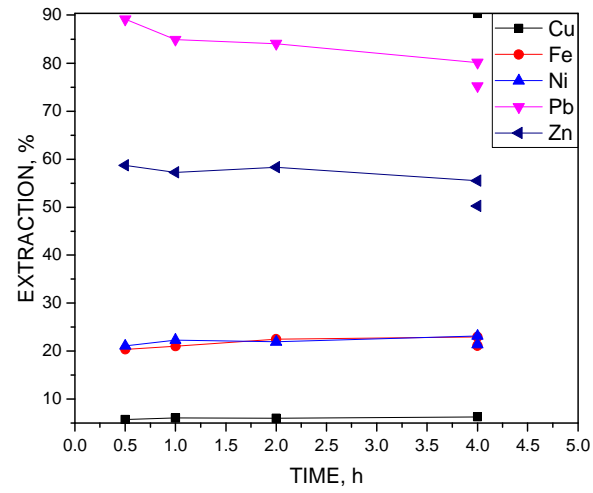
N5



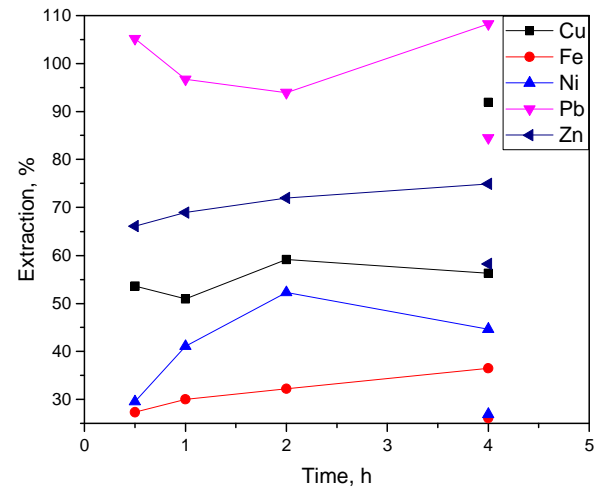
N6



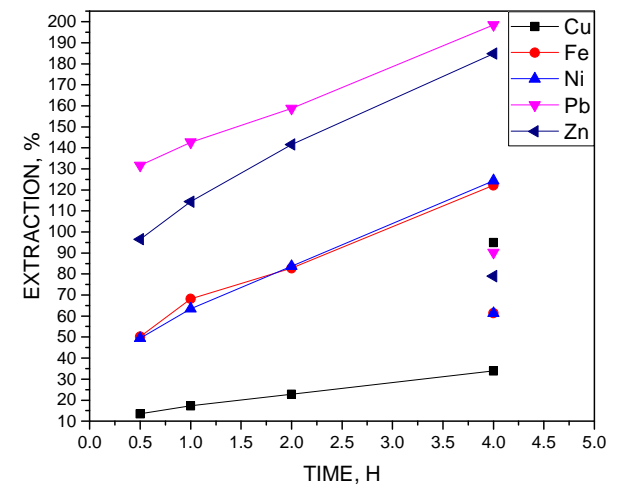
N7

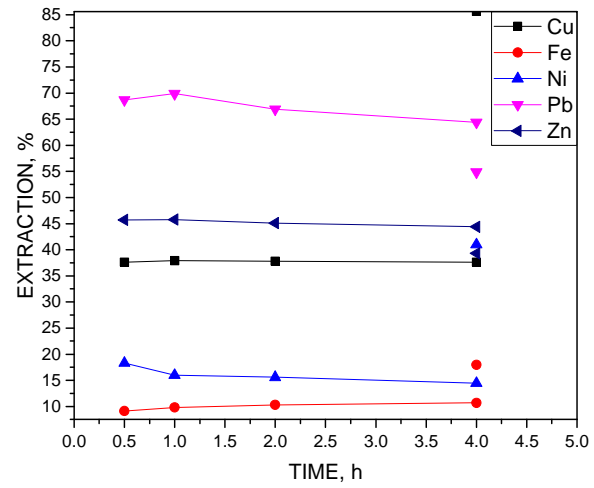
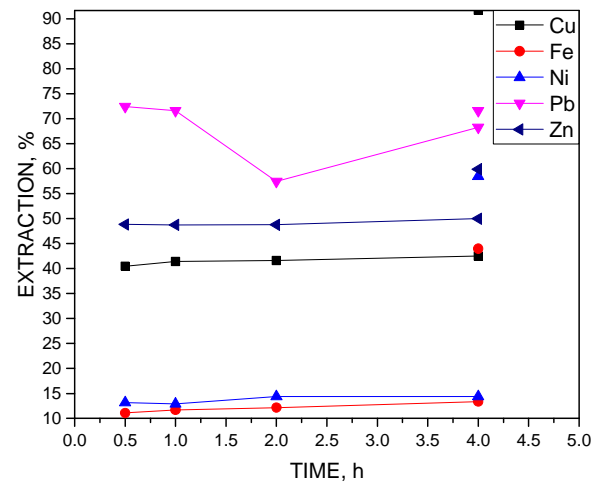
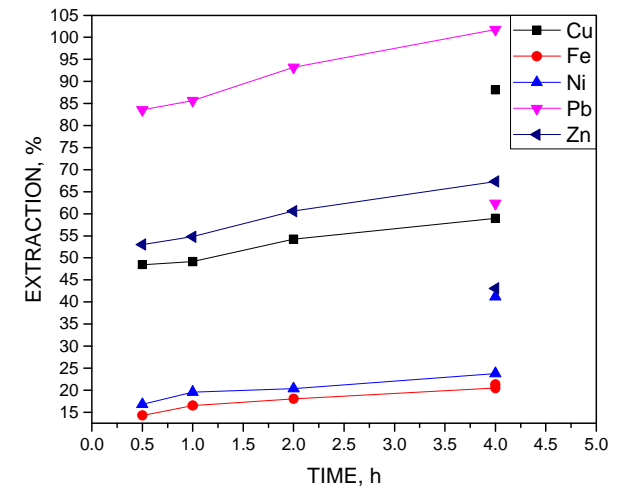


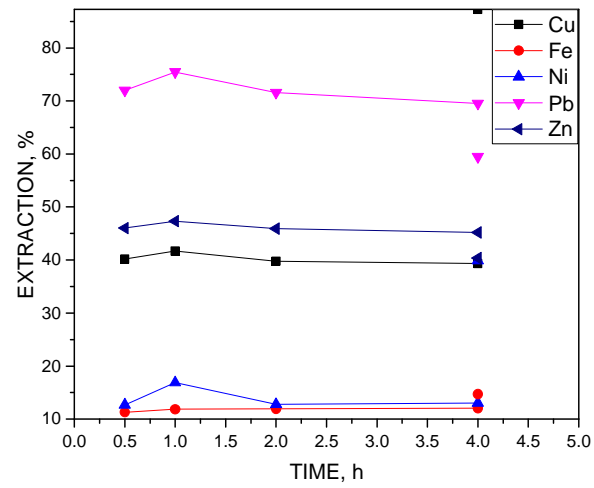
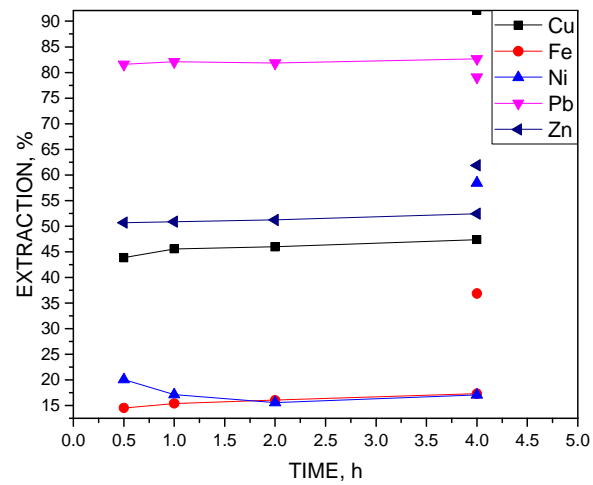
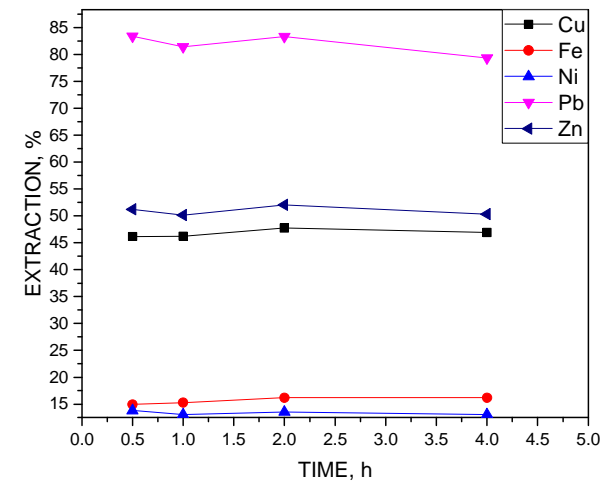
N8



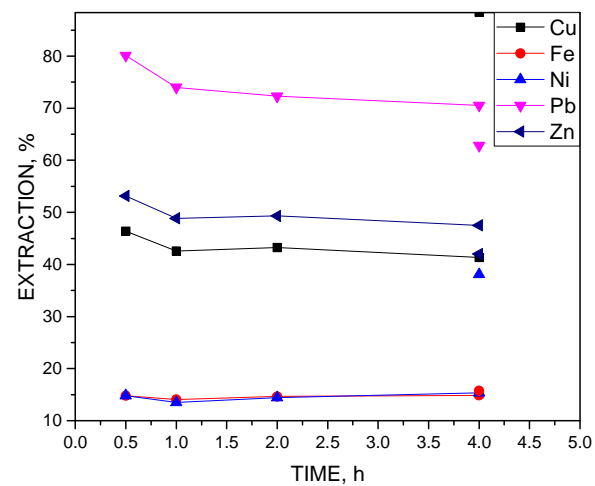
N9



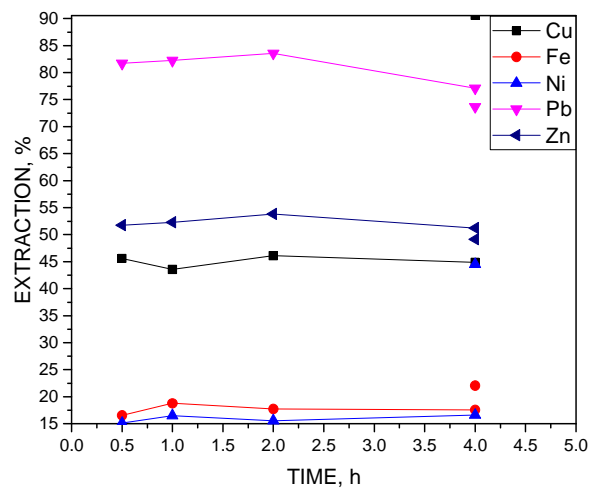
M1*M2**M3*

M4*M5**M6*

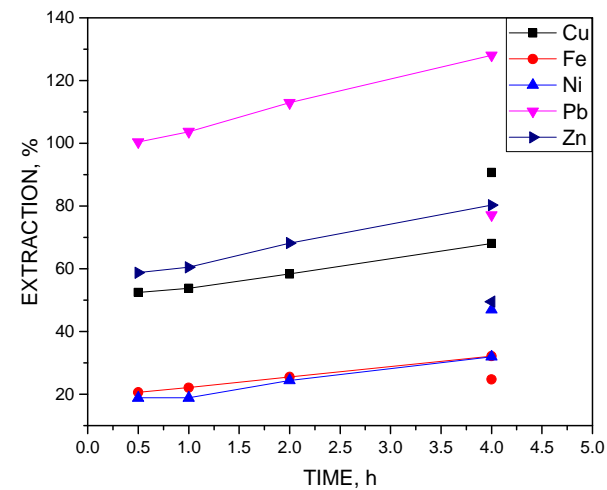
M7



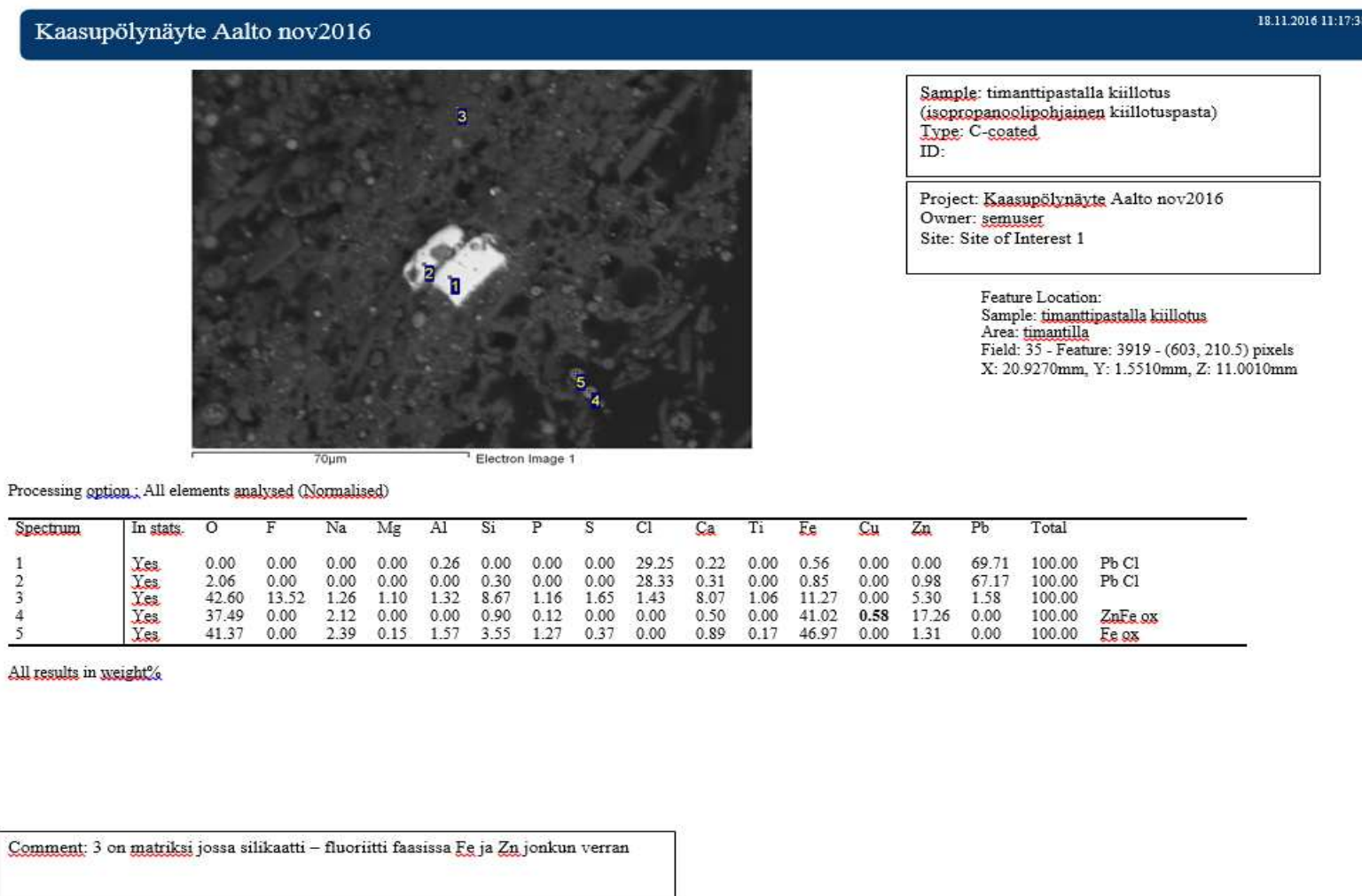
M8

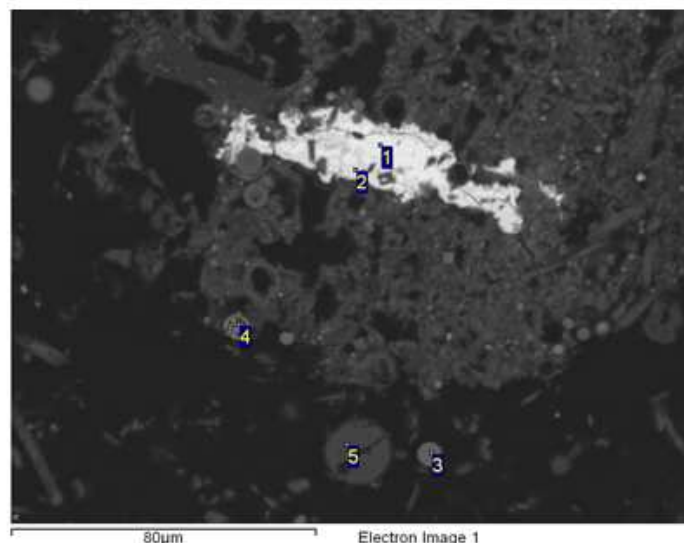


M9



Appendix C.





80µm

Electron Image 1

Sample: timanttipastalla kiillotusType: C-coated

ID:

Project: Kaasupölynäyte Aalto nov2016Owner: semuserSite: Site of Interest 2

Feature Location:

Sample: timanttipastalla kiillotusArea: timantilla

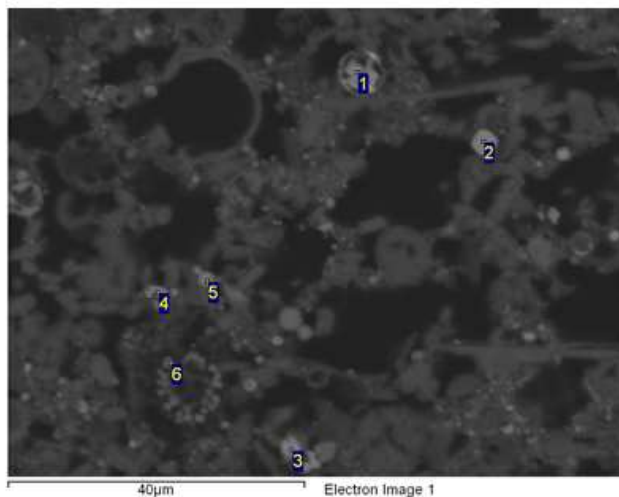
Field: 5 - Feature: 699 - (583.5, 112) pixels

X: 20.9440mm, Y: -0.7030mm, Z: 11.0010mm

Processing option: All elements analysed (Normalised)

<u>Spectrum</u>	<u>In stats.</u>	<u>O</u>	<u>Na</u>	<u>Mg</u>	<u>Al</u>	<u>Si</u>	<u>Cl</u>	<u>K</u>	<u>Ca</u>	<u>Ti</u>	<u>Cr</u>	<u>Fe</u>	<u>Ni</u>	<u>Zn</u>	<u>Pb</u>	<u>Total</u>
1	<u>Yes</u>	0.00	0.00	0.00	0.30	0.19	28.08	0.00	0.30	0.00	0.00	0.62	0.00	0.74	69.76	100.00
2	<u>Yes</u>	0.00	0.00	0.00	0.00	0.00	31.25	5.56	0.81	0.00	0.00	0.93	0.00	0.91	60.54	100.00
3	<u>Yes</u>	42.80	5.92	0.37	1.05	12.72	0.00	1.40	1.25	1.63	0.00	16.37	0.00	16.49	0.00	100.00
4	<u>Yes</u>	39.58	1.57	1.43	2.54	0.00	0.13	0.00	0.36	0.68	0.91	42.88	0.45	9.47	0.00	100.00
5	<u>Yes</u>	55.80	3.73	0.00	8.49	24.30	0.00	5.06	0.52	0.00	0.00	2.10	0.00	0.00	0.00	100.00

All results in weight%



Sample: timanttipastalla kiillotus
Type: C-coated
ID:

Project: Kaasupölynäyte Aalto nov2016
Owner: semuser
Site: Site of Interest 3

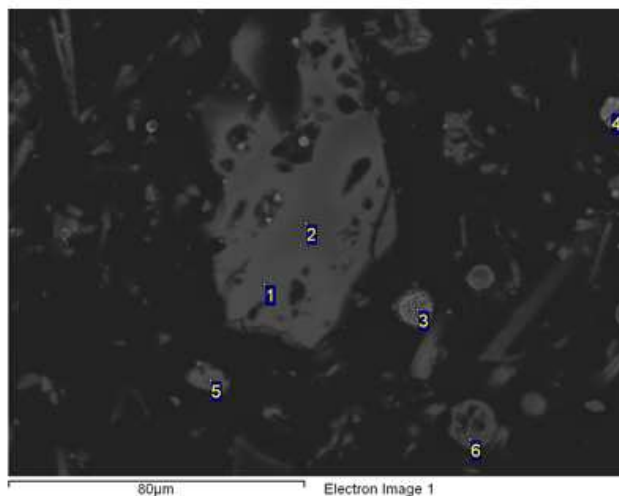
Feature Location:
Sample: timanttipastalla kiillotus
Area: timantilla
Field: 51 - Feature: 5582 - (625.5, 94.5) pixels
X: 17.0690mm, Y: 2.8910mm, Z: 11.0010mm

Processing option: All elements analysed (Normalised)

Spectrum	In stats.	O	Mg	Al	Si	P	S	Ca	Ti	Mn	Fe	Ni	Zn	Sb	Ba	Pb	Total
1	Yes	32.59	0.49	0.18	0.68	0.51	0.45	17.20	0.47	0.41	10.22	0.00	1.97	34.85	0.00	0.00	100.00
2	Yes	34.58	0.00	0.00	0.15	0.00	0.00	0.51	0.00	0.41	44.67	0.00	19.67	0.00	0.00	0.00	100.00
3	Yes	41.30	0.59	1.38	3.36	0.60	7.52	2.60	4.16	0.00	6.64	0.00	4.58	0.88	19.62	6.75	100.00
4	Yes	39.42	1.29	4.63	1.19	0.20	0.76	1.20	0.82	0.54	31.31	0.69	17.94	0.00	0.00	0.00	100.00
5	Yes	45.49	2.10	6.40	3.30	0.41	2.73	3.64	4.47	0.24	9.19	0.00	14.20	0.00	5.10	2.73	100.00
6	Yes	45.11	5.37	5.74	2.79	0.67	0.39	5.87	1.81	0.00	21.22	0.00	9.98	0.00	0.00	1.06	100.00

All results in weight%

Comment: 1. Antimoni oksidi.



Sample: timanttipastalla kiillotus
 Type: C-coated
 ID:

Project: Kaasupölynäyte Aalto nov2016
 Owner: semuser
 Site: Site of Interest 4

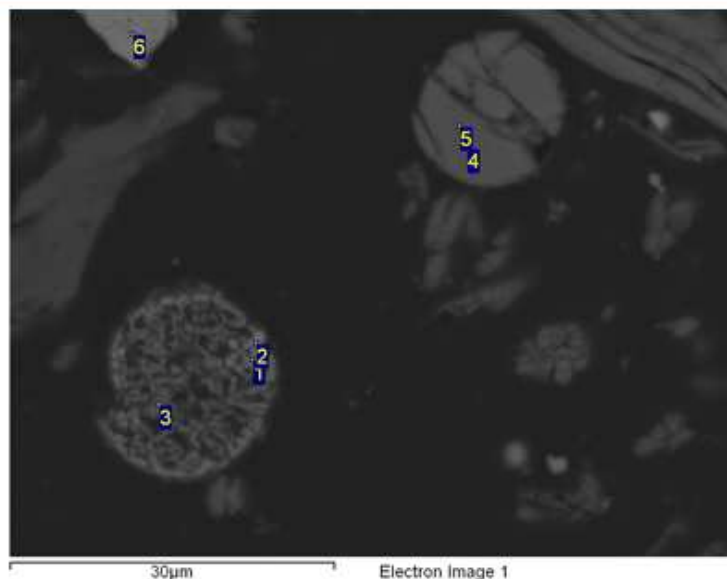
Feature Location:
 Sample: timanttipastalla kiillotus
 Area: timantilla
 Field: 11 - Feature: 1301 - (69, 337) pixels
 X: 17.5890mm, Y: 0.2310mm, Z: 11.0010mm

Processing option: All elements analysed (Normalised)

Spectrum	In stats	O	F	Na	Mg	Al	Si	S	Cl	Ca	Ti	Cr	Fe	Zn	I	Total
1	Yes	15.99	0.00	5.33	0.00	1.37	0.00	3.06	20.77	0.85	0.00	0.00	0.00	0.00	52.62	100.00
2	Yes	12.96	0.00	2.88	0.00	0.85	0.00	1.75	5.87	0.00	0.00	0.00	0.00	1.86	73.82	100.00
3	Yes	29.08	0.00	0.60	2.48	1.82	0.18	0.00	0.24	0.69	0.53	0.56	59.98	3.84	0.00	100.00
4	Yes	52.71	0.00	0.96	0.32	2.20	6.21	0.00	0.00	0.39	29.05	2.16	3.44	2.55	0.00	100.00
5	Yes	14.33	45.46	0.51	0.26	1.40	1.17	1.56	2.80	29.41	0.40	0.00	1.84	0.88	0.00	100.00
6	Yes	14.42	49.57	0.44	0.00	0.61	0.16	0.46	1.10	33.24	0.00	0.00	0.00	0.00	0.00	100.00

All results in weight%

Comment: 1-2. I Cl happi faasi? hiili ja typpi ei analysoitu - ehkä mukana yhdisteessä? 5-6 fluoriitti. Näytteessä myös hopea jodidia.



Sample: timanttipastalla kiillotus
 Type: C-coated
 ID:

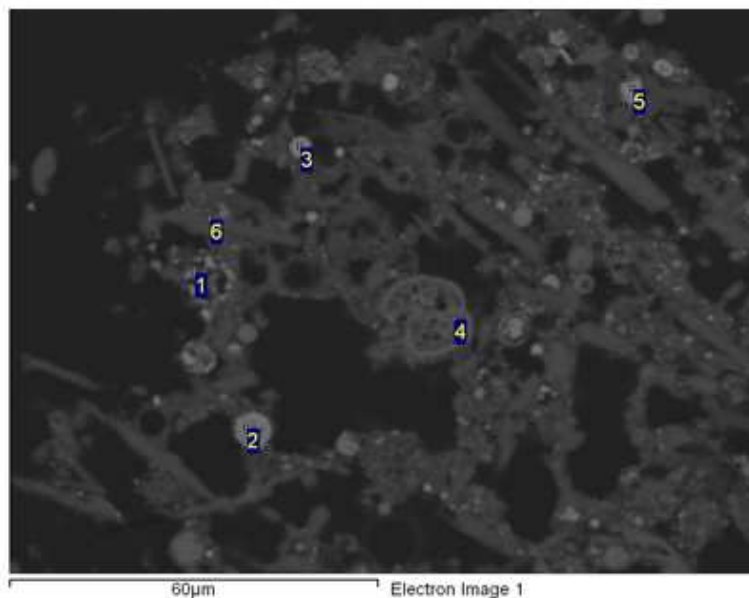
Project: Kaasupölynäyte Aalto nov2016
 Owner: semuser
 Site: Site of Interest 5

Feature Location:
 Sample: timanttipastalla kiillotus
 Area: timantilla
 Field: 13 - Feature: 1598 - (644, 466) pixels
 X: 18.9700mm, Y: 0.3660mm, Z: 11.0010mm

Processing option: All elements analysed (Normalised)

Spectrum	In stats.	O	Na	Mg	Al	Si	P	Cl	K	Ca	Ti	Mn	Fe	Zn	Pb	Total	
1	Yes	38.30	2.81	1.54	9.18	0.28	0.30	0.30	0.00	0.38	0.38	0.62	26.24	19.67	0.00	100.00	ZnFeAl ox
2	Yes	37.35	2.49	1.35	8.54	0.71	0.48	0.29	0.00	0.39	0.47	0.57	26.73	20.61	0.00	100.00	ZnFeAl ox
3	Yes	33.06	2.59	1.81	9.47	0.00	0.59	0.58	0.17	0.46	0.63	0.69	29.80	20.15	0.00	100.00	ZnFeAl ox
4	Yes	51.67	5.05	0.00	0.18	26.59	0.00	0.00	3.53	0.97	0.00	0.00	4.11	6.75	1.15	100.00	silikaattinen
5	Yes	52.18	5.48	0.00	0.16	27.05	0.00	0.00	3.62	1.04	0.00	0.00	3.55	5.79	1.12	100.00	silikaattinen
6	Yes	35.48	0.00	0.00	0.00	0.15	0.00	0.00	0.00	0.28	0.00	0.00	62.26	1.83	0.00	100.00	Fe ox

All results in weight%



Sample: timanttipastalla kiillotus
 Type: C-coated
 ID:

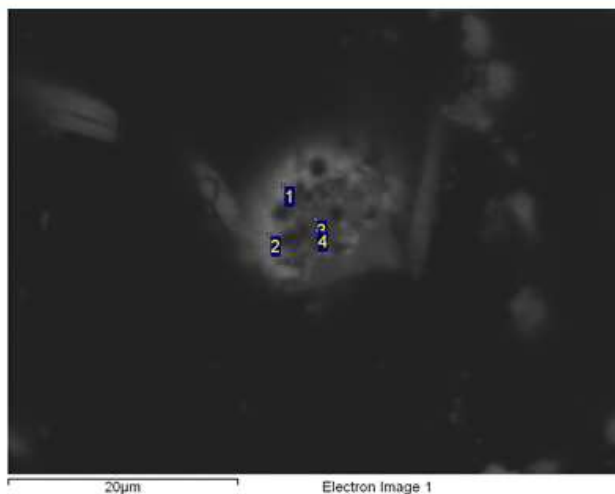
Project: Kaasupölynäyte Aalto nov2016
 Owner: semuser
 Site: Site of Interest 6

Feature Location:
 Sample: timanttipastalla kiillotus
 Area: timantilla
 Field: 37 - Feature: 4189 - (425.5, 563.5) pixels
 X: 23.0110mm, Y: 1.8890mm, Z: 11.0010mm

Processing option: All elements analysed (Normalised)

<u>Spectrum</u>	<u>In stats.</u>	<u>O</u>	<u>F</u>	<u>Al</u>	<u>Si</u>	<u>P</u>	<u>S</u>	<u>Cl</u>	<u>Ca</u>	<u>Ti</u>	<u>Cr</u>	<u>Mn</u>	<u>Fe</u>	<u>Ni</u>	<u>Cu</u>	<u>Zn</u>	<u>Total</u>
1	<u>Yes</u>	37.09	0.00	2.30	1.83	1.80	0.00	0.66	1.38	2.55	0.25	0.00	34.43	0.69	0.00	17.00	100.00
2	<u>Yes</u>	35.90	0.00	0.53	1.38	0.00	0.00	0.00	0.78	0.30	0.60	0.30	46.24	0.00	0.50	13.47	100.00
3	<u>Yes</u>	33.22	0.00	0.16	0.51	0.00	0.00	0.00	0.71	0.26	0.00	0.27	45.21	0.00	0.92	18.74	100.00
4	<u>Yes</u>	25.73	33.75	1.31	0.00	0.60	0.34	0.54	0.72	0.39	0.00	1.58	32.92	0.47	0.00	1.66	100.00
5	<u>Yes</u>	35.27	0.00	0.97	0.37	0.00	0.00	0.00	0.47	0.46	0.00	0.00	43.26	0.00	0.00	19.19	100.00
6	<u>Yes</u>	52.80	3.78	0.31	2.20	0.24	15.35	0.77	16.03	0.45	0.35	0.00	5.04	0.00	0.00	2.67	100.00

All results in weight%



Sample: timanttipastalla kiillotus
Type: C-coated
ID:

Project: Kaasupölynäyte Aalto nov2016
Owner: semuser
Site: Site of Interest 7

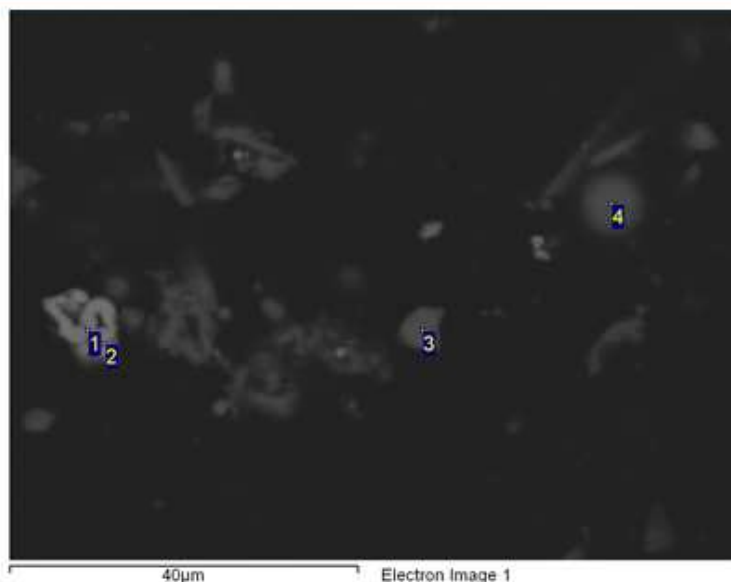
Feature Location:
Sample: timanttipastalla kiillotus
Area: timantilla
Field: 44 - Feature: 4943 - (701, 535) pixels
X: 19.8760mm, Y: 2.5830mm, Z: 11.0010mm

Processing option: All elements analysed (Normalised)

Spectrum	In stats	O	Si	P	S	Cl	K	Ca	Ti	Cr	Fe	Cu	Zn	As	Ba	Pb	Total
1	Yes	34.86	9.93	0.73	4.75	0.98	0.35	1.41	0.00	21.32	7.09	0.54	2.25	1.22	10.30	4.27	100.00
2	Yes	40.57	5.12	1.37	5.27	0.84	0.49	2.02	0.71	15.50	7.63	0.00	4.27	1.25	10.52	4.45	100.00
3	Yes	47.02	32.01	0.00	0.35	0.55	0.14	0.52	0.00	13.20	0.45	5.29	0.00	0.00	0.48	0.00	100.00
4	Yes	46.32	33.78	0.00	0.35	0.21	0.00	0.39	0.00	12.59	0.29	6.06	0.00	0.00	0.00	0.00	100.00

All results in weight%

Comment: 3-4 Cr silikaattisessa faasisa 5-6 % Cu. Ulkokuoressa BaPbFeZn oksidia (Ba sulfaattia mukana?)



Sample: timanttipastalla kiillotus
 Type: C-coated
 ID:

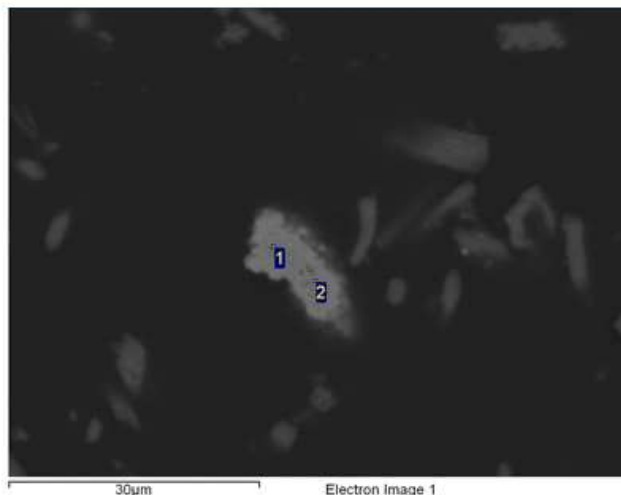
Project: Kaasupölynäyte Aalto nov2016
 Owner: semuser
 Site: Site of Interest 8

Feature Location:
 Sample: timanttipastalla kiillotus
 Area: timantilla
 Field: 37 - Feature: 4154 - (852, 83.5) pixels
 X: 22.6100mm, Y: 1.4390mm, Z: 11.0010mm

Processing option: All elements analysed (Normalised)

Spectrum	In stats	O	Na	Mg	Al	Si	K	Ca	Ti	Fe	Ni	Cu	Zn	Total	
1	Yes	37.20	0.00	0.38	0.28	0.87	0.14	0.48	0.00	53.72	5.51	0.39	1.03	100.00	Fe (Ni, Zn,Cu) ox
2	Yes	35.03	0.00	0.35	0.16	0.33	0.00	0.39	0.00	53.84	6.61	0.62	2.66	100.00	Fe (Ni, Zn,Cu) ox
3	Yes	52.52	0.00	6.72	0.76	20.73	0.00	13.01	0.00	6.27	0.00	0.00	0.00	100.00	diopsidi
4	Yes	52.81	5.00	0.78	6.40	22.57	4.92	0.63	0.28	4.22	0.00	0.00	2.39	100.00	silik

All results in weight%



Electron Image 1

Sample: timanttipastalla kiillotus
 Type: C-coated
 ID:

Project: Kaasupölynäyte Aalto nov2016
 Owner: semuser
 Site: Site of Interest 9

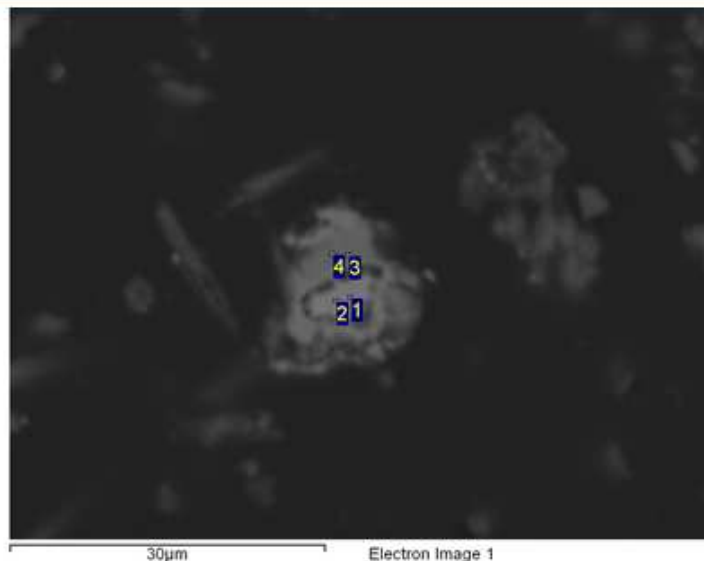
Feature Location:
 Sample: timanttipastalla kiillotus
 Area: timantilla
 Field: 10 - Feature: 1249 - (350.5, 679.5) pixels
 X: 25.9570mm, Y: -0.1580mm, Z: 11.0010mm

Processing option: All elements analysed (Normalised)

<u>Spectrum</u>	<u>In stats</u>	<u>O</u>	<u>Al</u>	<u>Si</u>	<u>Ca</u>	<u>Cr</u>	<u>Mn</u>	<u>Fe</u>	<u>Ni</u>	<u>Zn</u>	<u>Total</u>
1	<u>Yes</u>	34.42	0.55	0.75	0.63	9.96	0.65	45.86	2.91	4.26	100.00
2	<u>Yes</u>	33.78	0.32	0.33	0.39	15.80	1.14	35.63	4.44	8.15	100.00

All results in weight%

Comment: Fe (Cr,Ni,Zn) ox



Sample: timanttipastalla kiillotus
 Type: C-coated
 ID:

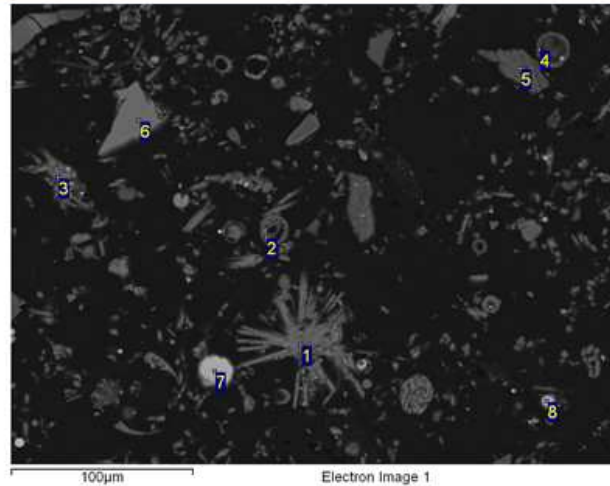
Project: Kaasupölynäyte Aalto nov2016
 Owner: semuser
 Site: Site of Interest 10

Feature Location:
 Sample: timanttipastalla kiillotus
 Area: timantilla
 Field: 33 - Feature: 3574 - (747.5, 173.5) pixels
 X: 18.8720mm, Y: 1.5230mm, Z: 11.0010mm

Processing option: All elements analysed (Normalised)

<u>Spectrum</u>	<u>In stats.</u>	<u>O</u>	<u>Na</u>	<u>Al</u>	<u>Si</u>	<u>Ca</u>	<u>Cr</u>	<u>Fe</u>	<u>Zn</u>	<u>Ba</u>	<u>Total</u>
1	<u>Yes</u>	0.00	0.00	0.00	0.00	0.44	99.56	0.00	0.00	0.00	100.00
2	<u>Yes</u>	0.00	0.00	0.00	0.00	0.37	99.63	0.00	0.00	0.00	100.00
3	<u>Yes</u>	39.63	1.01	0.61	4.12	1.54	48.48	1.58	1.47	1.54	100.00
4	<u>Yes</u>	41.51	0.82	0.69	4.16	1.54	46.97	1.69	1.26	1.35	100.00
<u>Mean</u>		20.29	0.46	0.33	2.07	0.97	73.66	0.82	0.68	0.72	100.00
<u>Std. deviation</u>		23.44	0.53	0.38	2.39	0.66	29.95	0.94	0.79	0.84	
<u>Max.</u>		41.51	1.01	0.69	4.16	1.54	99.63	1.69	1.47	1.54	
<u>Min.</u>		0.00	0.00	0.00	0.00	0.37	46.97	0.00	0.00	0.00	

All results in weight%



Sample: timanttipastalla kiillotus
 Type: C-coated
 ID:

Project: Kaasupölynäyte Aalto nov2016
 Owner: semuser
 Site: Site of Interest 11

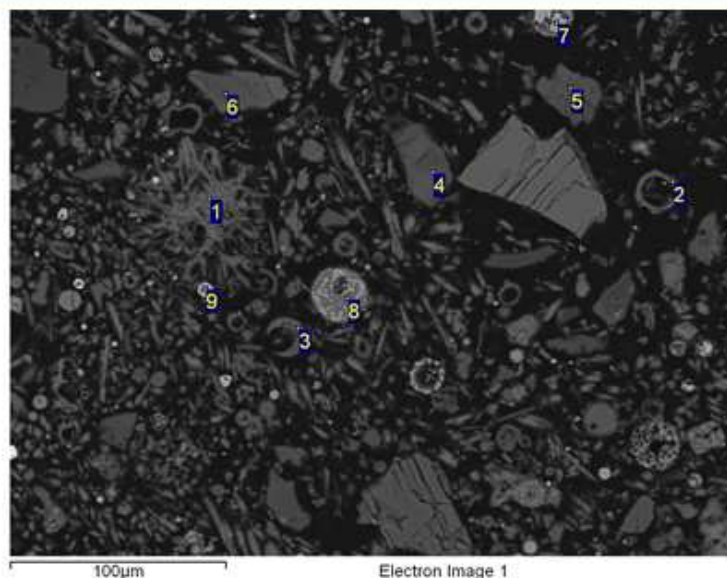
Feature Location:

Processing option: All elements analysed (Normalised)

Spectrum	In stats	O	F	Na	Mg	Si	S	Cl	K	Ca	Fe	Zn	I	Pb	Total	
1	Yes	47.83	0.00	0.00	0.00	0.70	24.37	0.27	0.00	22.90	1.96	1.97	0.00	0.00	100.00	
2	Yes	18.33	47.64	0.00	0.00	0.67	3.90	1.34	0.00	28.12	0.00	0.00	0.00	0.00	100.00	
3	Yes	59.10	0.00	0.00	0.00	0.00	21.29	0.23	0.00	18.93	0.00	0.00	0.46	0.00	100.00	
4	Yes	52.83	16.42	0.00	0.40	1.17	1.18	3.27	0.34	23.76	0.64	0.00	0.00	0.00	100.00	
5	Yes	13.23	0.00	4.80	0.00	1.45	1.14	24.17	2.57	1.06	0.00	3.17	34.01	14.39	100.00	
6	Yes	49.89	0.00	0.00	5.00	20.65	0.00	0.00	0.00	13.43	11.03	0.00	0.00	0.00	100.00	Pb I Cl ox
7	Yes	36.03	0.00	0.00	0.00	0.49	0.16	0.00	0.10	0.30	62.93	0.00	0.00	0.00	100.00	Fe ox
8	Yes	33.28	0.00	1.32	0.00	0.20	0.00	0.00	0.00	0.28	49.96	14.96	0.00	0.00	100.00	FeZn ox

All results in weight%

Comment: Fluoriittia (2,4) ja kipsia (1,3)



Sample: timanttipastalla kiillotus
 Type: C-coated
 ID:

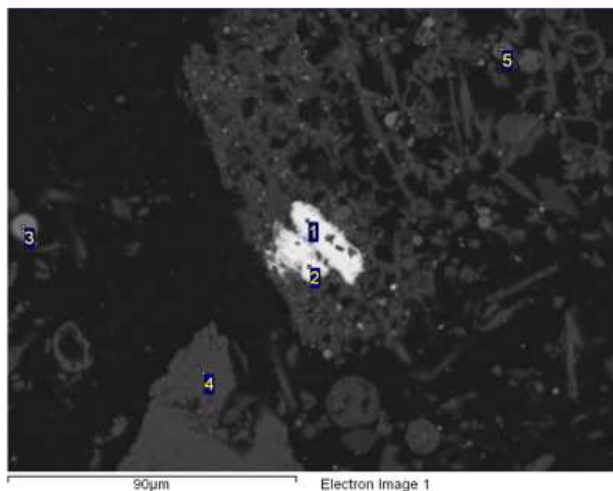
Project: Kaasupölynäyte Aalto nov2016
 Owner: semuser
 Site: Site of Interest 12

Feature Location:

Processing option: All elements analysed (Normalised)

Spectrum	In stats.	O	F	Na	Mg	Al	Si	S	Cl	Ca	Ti	Fe	Zn	I	Pb	Total	
1	<u>Yes</u>	46.66	0.00	0.00	0.18	0.78	0.37	22.38	0.25	19.71	0.00	7.91	1.75	0.00	0.00	100.00	Kipsi
2	<u>Yes</u>	21.62	47.84	0.48	0.25	1.01	0.43	0.81	2.34	24.92	0.00	0.30	0.00	0.00	0.00	100.00	Fluoriitti
3	<u>Yes</u>	19.93	45.13	0.89	0.00	0.94	0.31	0.76	2.34	29.19	0.00	0.52	0.00	0.00	0.00	100.00	Fluoriitti
4	<u>Yes</u>	22.57	0.00	3.59	0.00	1.23	0.63	0.00	20.67	0.93	0.00	1.02	2.99	30.21	16.16	100.00	Pb I Cl <u>ox</u>
5	<u>Yes</u>	22.37	0.00	0.00	0.00	1.12	2.74	1.62	27.26	6.89	0.94	4.10	3.30	15.24	14.41	100.00	Pb I Cl <u>ox</u>
6	<u>Yes</u>	19.37	0.00	2.03	0.00	2.24	0.59	2.37	16.57	0.00	0.00	0.00	0.00	46.71	10.12	100.00	Pb I Cl <u>ox</u>
7	<u>Yes</u>	40.05	0.00	0.00	2.12	6.15	0.00	0.00	0.00	0.23	2.70	48.75	0.00	0.00	0.00	100.00	Fe _{ox}
8	<u>Yes</u>	51.47	0.00	6.01	4.61	0.38	22.61	0.00	0.00	0.99	0.00	12.22	1.71	0.00	0.00	100.00	silik
9	<u>Yes</u>	31.21	0.00	0.00	0.00	0.00	0.00	0.29	0.00	0.42	0.00	64.06	4.02	0.00	0.00	100.00	FeZn <u>ox</u>

All results in weight%



Sample: kuivakiillotus
 Type: C-coated
 ID:

Project: Kaasupölynäyte Aalto nov2016
 Owner: semuser
 Site: Site of Interest 1

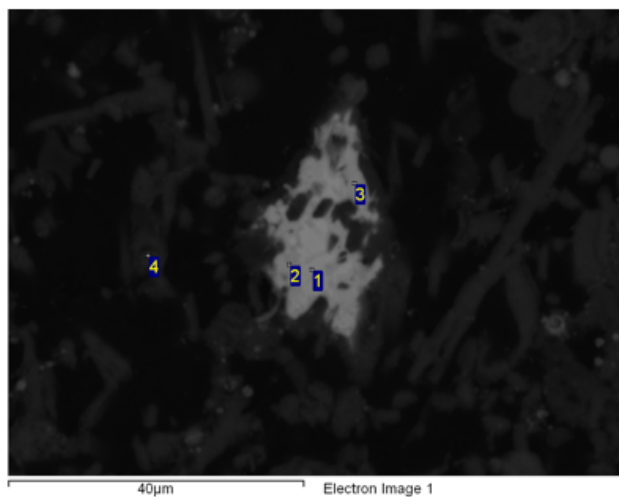
Feature Location:
 Sample: kuivakiillotus
 Area: kuiva
 Field: 24 - Feature: 4548 - (143.5, 131) pixels
 X: -8.2480mm, Y: -5.9430mm, Z: 11.0010mm

Processing option: All elements analysed (Normalised)

Spectrum	In stats.	O	Mg	Al	Si	Cl	K	Ca	Fe	Zn	Pb	Total
1	<u>Yes</u>	0.00	0.00	0.26	0.00	28.10	0.00	0.00	0.00	0.00	71.64	100.00
2	<u>Yes</u>	0.00	0.00	0.22	0.00	28.53	0.00	0.00	0.00	0.00	71.25	100.00
3	<u>Yes</u>	32.17	0.00	0.00	0.00	0.00	0.00	0.14	50.99	16.70	0.00	100.00
4	<u>Yes</u>	52.25	8.15	0.00	21.72	0.00	0.00	14.42	3.46	0.00	0.00	100.00
5	<u>Yes</u>	49.79	0.34	0.93	23.45	0.00	4.62	0.46	4.48	13.28	2.65	100.00

All results in weight%

Comment: Pb kloridia ja Fe-Zn rikkaita oksidifaaseja



Sample: kuivakiillotus
 Type: C-coated
 ID:

Project: Kaasupölynäyte Aalto nov2016
 Owner: semuser
 Site: Site of Interest 2

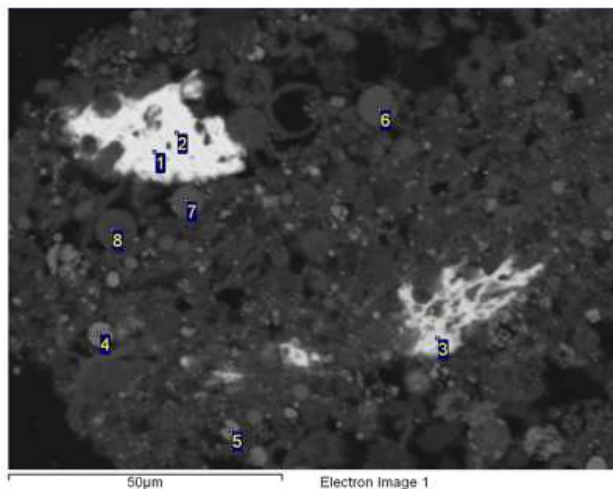
Feature Location:
 Sample: kuivakiillotus
 Area: kuiva
 Field: 24 - Feature: 4548 - (143.5, 131) pixels
 X: -8.2480mm, Y: -5.9430mm, Z: 11.0010mm

Processing option: All elements analysed (Normalised)

Spectrum	In stats	O	F	Mg	Al	Si	P	S	Cl	K	Ca	Ti	Fe	Zn	Pb	Total
1	<u>Yes</u>	0.00	0.00	0.00	0.00	0.00	0.00	0.00	26.96	0.00	0.00	0.00	0.57	0.84	71.63	100.00
2	<u>Yes</u>	0.00	0.00	0.00	0.24	0.43	0.00	0.00	31.67	5.67	0.40	0.00	0.63	0.00	60.97	100.00
3	<u>Yes</u>	4.26	0.00	0.00	0.26	0.29	0.00	0.00	29.61	5.22	0.90	0.00	0.00	0.00	59.46	100.00
4	<u>Yes</u>	20.45	38.11	0.72	0.96	1.37	0.55	4.24	3.91	0.51	24.90	0.48	1.88	1.93	0.00	100.00

All results in weight%

Comment: Pb Cl faasi ja ympärillä fluoriittia ja kipsiä



Electron Image 1

Sample: kuivakiillotus
 Type: C-coated
 ID:

Project: Kaasupölynäyte Aalto nov2016
 Owner: semuser
 Site: Site of Interest 3

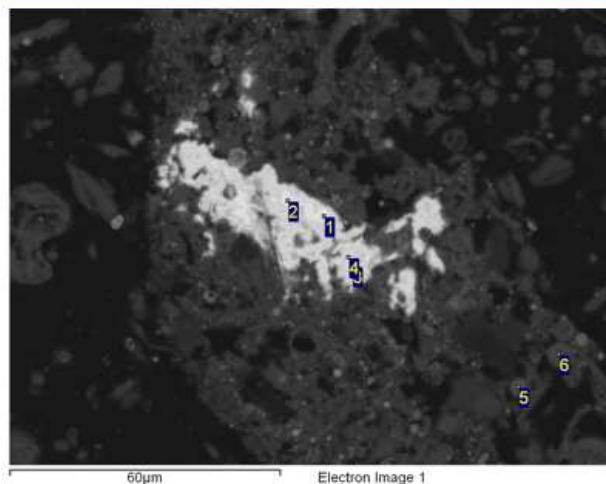
Feature Location:
 Sample: kuivakiillotus
 Area: kuiva
 Field: 10 - Feature: 1608 - (843.5, 116.5) pixels
 X: -13.6980mm, Y: -6.6710mm, Z: 11.0010mm

Processing option : All elements analysed (Normalised)

<u>Spectrum</u>	<u>In stats.</u>	<u>O</u>	<u>Na</u>	<u>Mg</u>	<u>Al</u>	<u>Si</u>	<u>P</u>	<u>Cl</u>	<u>K</u>	<u>Ca</u>	<u>Ti</u>	<u>Mn</u>	<u>Fe</u>	<u>Cu</u>	<u>Zn</u>	<u>Pb</u>	<u>Total</u>
1	<u>Yes</u>	0.00	0.00	0.00	0.28	0.00	0.00	30.04	0.00	0.00	0.00	0.00	0.00	0.00	0.00	69.68	100.00
2	<u>Yes</u>	0.00	0.00	0.00	0.38	0.00	0.00	29.44	0.00	0.28	0.00	0.00	0.00	0.00	0.00	69.90	100.00
3	<u>Yes</u>	9.58	0.00	0.00	0.25	1.29	0.00	25.06	4.91	1.42	0.85	0.00	2.36	0.00	2.87	51.41	100.00
4	<u>Yes</u>	32.64	1.54	0.00	0.00	0.21	0.16	0.00	0.00	0.39	0.00	0.00	49.76	0.71	14.58	0.00	100.00
5	<u>Yes</u>	36.13	1.48	0.00	0.30	0.68	0.00	0.15	0.00	0.45	0.48	0.73	44.18	1.04	14.38	0.00	100.00
6	<u>Yes</u>	49.85	5.59	1.78	0.78	17.40	0.58	0.19	1.08	5.14	2.30	0.41	11.31	0.00	3.03	0.57	100.00
7	<u>Yes</u>	48.06	4.52	1.37	4.24	13.42	0.30	0.00	1.31	0.82	0.68	0.00	15.85	0.00	9.44	0.00	100.00
8	<u>Yes</u>	56.99	2.64	0.00	7.51	24.65	0.00	0.21	6.07	0.24	0.00	0.00	1.69	0.00	0.00	0.00	100.00

All results in weight%

Comment: PbCl faasi kirkkainpana BSE kuvassa. Pyöreät rakeet Fe-Zn oksidia. Tummimmat pyöreät ovat silikaattisia.



Sample: kuivakiillotus
 Type: C-coated
 ID:

Project: Kaasupölynäyte Aalto nov2016
 Owner: semuser
 Site: Site of Interest 4

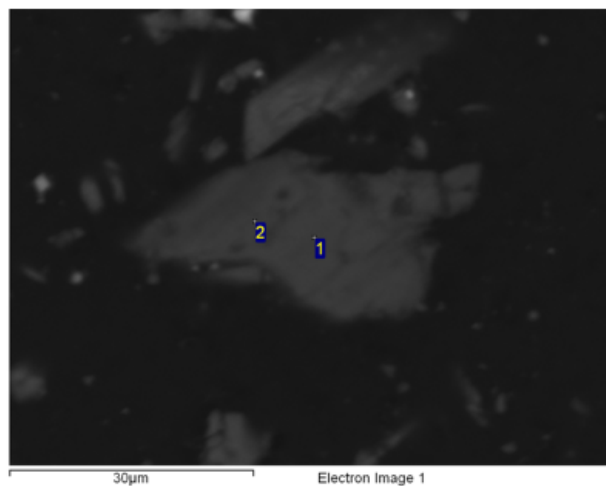
Feature Location:
 Sample: kuivakiillotus
 Area: kuiva
 Field: 10 - Feature: 1722 - (818, 611.5) pixels
 X: -13.6720mm, Y: -6.1980mm, Z: 11.0010mm

Processing option: All elements analysed (Normalised)

Spectrum	In stats.	O	Na	Mg	Al	Si	Cl	K	Ca	Ti	Fe	Zn	Pb	Total	
1	<u>Yes</u>	0.00	0.00	0.00	0.30	0.00	29.01	0.53	0.00	0.00	0.00	0.00	70.15	100.00	raskain
2	<u>Yes</u>	0.00	0.00	0.00	0.33	0.00	28.43	0.38	0.33	0.00	0.65	0.00	69.89	100.00	raskain
3	<u>Yes</u>	0.00	0.00	0.00	0.00	0.00	32.40	5.63	0.39	0.00	0.70	0.00	60.88	100.00	kevyempi
4	<u>Yes</u>	0.00	0.00	0.00	0.00	0.00	30.68	5.01	0.00	0.00	0.80	1.26	62.26	100.00	kevyempi
5	<u>Yes</u>	48.66	4.75	0.35	4.88	22.24	0.00	5.32	0.39	0.00	4.18	7.21	2.03	100.00	
6	<u>Yes</u>	52.51	5.98	0.47	9.00	18.16	0.17	3.52	1.15	0.85	7.31	0.88	0.00	100.00	

All results in weight%

Comment: Pb Cl faaseja. 5-6 silikaattista tavaraa (maasälpää jossa Fe, Zn mukana)



Sample: kuivakiillotus
 Type: Default
 ID:

Project: Kaasupölynäyte Aalto nov2016
 Owner: semuser
 Site: Site of Interest 5

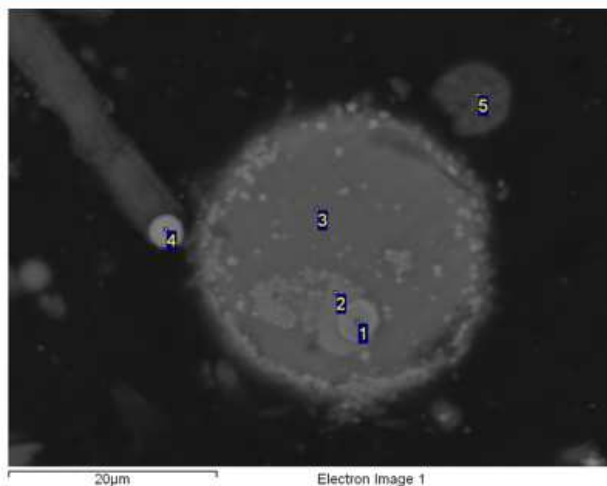
Feature Location:
 Sample: kuivakiillotus
 Area: kuiva
 Field: 8 - Feature: 1460 - (906.5, 89.5) pixels
 X: -7.0440mm, Y: -7.4130mm, Z: 11.0010mm

Processing option: All elements analysed (Normalised)

<u>Spectrum</u>	<u>In stats.</u>	<u>C</u>	<u>Na</u>	<u>Al</u>	<u>S</u>	<u>Cl</u>	<u>K</u>	<u>I</u>	<u>Total</u>
1	<u>Yes</u>	84.65	0.26	0.32	0.47	1.44	0.17	12.70	100.00
2	<u>Yes</u>	84.89	0.34	0.37	0.38	1.97	0.21	11.83	100.00

All results in weight%

Comment: Jodi ja kloori pitoinen orgaaninen aine.



Sample: kuivakiillotus
 Type: C-coated
 ID:

Project: Kaasupölynäyte Aalto nov2016
 Owner: semuser
 Site: Site of Interest 6

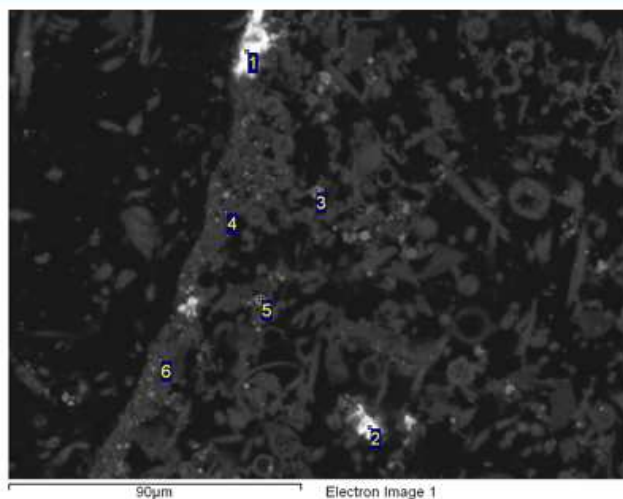
Feature Location:
 Sample: kuivakiillotus
 Area: kuiva
 Field: 11 - Feature: 1914 - (76, 396.5) pixels
 X: -12.0200mm, Y: -6.4050mm, Z: 11.0010mm

Processing option: All elements analysed (Normalised)

Spectrum	In stats	O	F	Al	Si	P	S	K	Ca	Ti	Cr	Mn	Fe	Ni	Zn	Total	
1	<u>Yes</u>	36.02	0.00	0.45	0.61	0.00	0.00	0.30	0.46	4.15	50.29	0.00	1.55	0.00	6.17	100.00	<u>CrZn ox</u>
2	<u>Yes</u>	43.77	0.00	4.09	8.71	0.55	0.00	1.89	1.63	1.16	6.92	0.88	12.05	0.00	18.33	100.00	<u>ZnFeCr ox</u>
3	<u>Yes</u>	51.48	0.00	3.97	15.60	1.03	0.00	2.71	3.85	1.21	0.00	1.29	4.04	0.00	14.82	100.00	<u>ZnFe silic faasi</u>
4	<u>Yes</u>	36.58	0.00	0.00	0.00	0.00	0.51	0.00	0.52	0.00	0.00	0.00	43.08	1.34	17.96	100.00	<u>ZnFe ox</u>
5	<u>Yes</u>	11.60	54.15	0.63	1.64	0.24	0.34	0.00	30.98	0.00	0.00	0.00	0.41	0.00	0.00	100.00	<u>fluoriittia</u>

All results in weight%

Comment:



Sample: kuivakiillotus
 Type: C-coated
 ID:

Project: Kaasupölynäyte Aalto nov2016
 Owner: semuser
 Site: Site of Interest 7

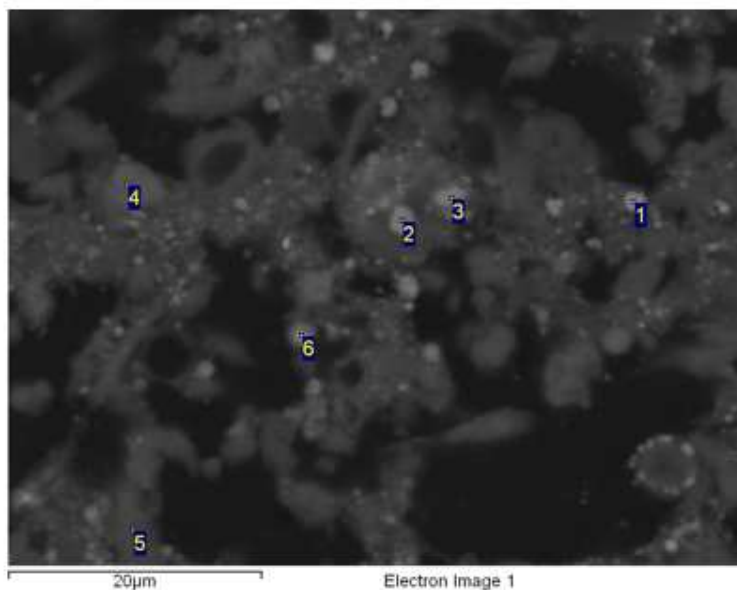
Feature Location:
 Sample: kuivakiillotus
 Area: kuiva
 Field: 11 - Feature: 1903 - (922, 389) pixels
 X: -12.8180mm, Y: -6.4170mm, Z: 11.0010mm

Processing option : All elements analysed (Normalised)

Spectrum	In stats.	O	F	Mg	Al	Si	P	S	Cl	K	Ca	Ti	Fe	Ni	Zn	Pb	Total	
1	<u>Yes</u>	3.30	0.00	0.00	0.00	0.37	0.00	0.00	26.35	0.00	0.31	0.00	1.13	0.00	0.00	68.54	100.00	<u>PbCl</u>
2	<u>Yes</u>	0.00	0.00	0.00	0.36	0.00	0.00	0.00	28.51	0.38	0.39	0.00	0.00	0.00	0.00	70.36	100.00	<u>PbCl</u>
3	<u>Yes</u>	40.64	0.00	1.16	0.86	3.30	0.47	0.87	0.30	0.43	1.40	14.10	12.36	0.00	22.45	1.66	100.00	<u>ZnFeTi ox</u>
4	<u>Yes</u>	43.13	8.40	0.75	1.44	12.21	0.93	3.87	1.72	0.79	9.17	1.21	9.81	0.00	6.57	0.00	100.00	<u>mixed</u>
5	<u>Yes</u>	39.66	0.00	0.36	1.84	5.49	0.33	1.24	0.18	1.03	2.31	0.85	26.42	0.60	18.77	0.92	100.00	<u>FeZn ox</u>
6	<u>Yes</u>	38.05	14.66	0.68	1.41	8.43	0.86	1.52	1.89	0.74	11.51	1.07	11.40	0.00	6.05	1.73	100.00	

All results in weight%

Comment: Nro. 4 ja 6 (harmaa "matriksi") on ilmeisesti sekoitus fluoriitista (+/- kipsi) ja FeZn oksidifaasista.



Sample: kuivakiillotus
 Type: C-coated
 ID:

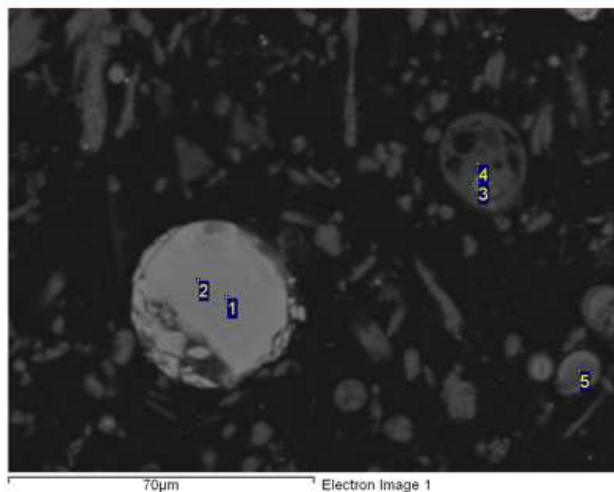
Project: Kaasupölynäyte Aalto nov2016
 Owner: semuser
 Site: Site of Interest 8

Feature Location:
 Sample: kuivakiillotus
 Area: kuiva
 Field: 1 - Feature: 173 - (508.5, 386.5) pixels
 X: -13.3870mm, Y: -7.1130mm, Z: 11.0010mm

Processing option: All elements analysed (Normalised)

<u>Spectrum</u>	<u>In stats.</u>	<u>O</u>	<u>F</u>	<u>Na</u>	<u>Mg</u>	<u>Al</u>	<u>Si</u>	<u>S</u>	<u>Cl</u>	<u>Ca</u>	<u>Ti</u>	<u>Cr</u>	<u>Fe</u>	<u>Zn</u>	<u>Pb</u>	<u>Total</u>	
1	<u>Yes</u>	39.32	0.00	1.91	0.96	0.68	2.76	0.61	0.61	1.81	0.24	0.61	35.97	14.51	0.00	100.00	<u>FeZn ox</u>
2	<u>Yes</u>	44.07	0.00	2.20	0.40	1.03	2.29	1.46	1.20	2.07	12.46	0.34	30.42	2.05	0.00	100.00	<u>FeTi ox</u>
3	<u>Yes</u>	38.78	0.00	4.84	2.54	4.03	1.38	0.00	1.82	1.02	8.06	0.23	15.19	22.11	0.00	100.00	<u>ZnFeTi ox</u>
4	<u>Yes</u>	12.02	51.51	0.53	0.29	1.06	1.65	1.09	1.12	28.24	0.37	0.00	1.34	0.77	0.00	100.00	<u>Fluorite</u>
5	<u>Yes</u>	58.18	3.30	0.00	0.00	0.00	1.04	17.66	0.65	16.94	0.00	0.00	1.37	0.86	0.00	100.00	<u>Gypsum</u>
6	<u>Yes</u>	49.11	0.00	1.61	0.52	0.79	2.08	2.03	0.56	2.04	17.67	0.00	8.97	13.17	1.44	100.00	<u>TiZnFe ox</u>

All results in weight%



Sample: kuivakiillotus
 Type: C-coated
 ID:

Project: Kaasupölynäyte Aalto nov2016
 Owner: semuser
 Site: Site of Interest 9

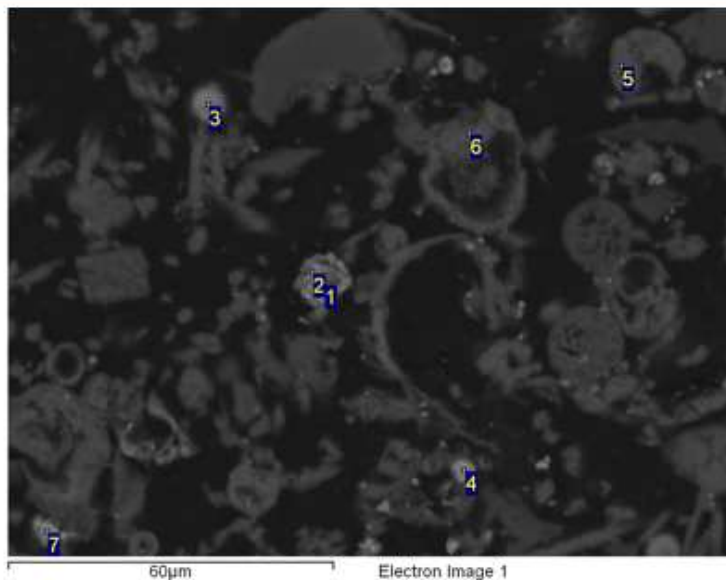
Feature Location:
 Sample: kuivakiillotus
 Area: kuiya
 Field: 1 - Feature: 173 - (508.5, 386.5) pixels
 X: -13.3870mm, Y: -7.1130mm, Z: 11.0010mm

Processing option: All elements analysed (Normalised)

<u>Spectrum</u>	<u>In stats.</u>	<u>O</u>	<u>F</u>	<u>Na</u>	<u>Mg</u>	<u>Al</u>	<u>Si</u>	<u>S</u>	<u>Ca</u>	<u>Ti</u>	<u>Fe</u>	<u>Zn</u>	<u>Sb</u>	<u>Pb</u>	<u>Total</u>
1	<u>Yes</u>	46.70	0.00	1.75	2.34	2.51	11.18	0.00	6.52	10.65	5.39	2.19	1.52	9.25	100.00
2	<u>Yes</u>	46.35	0.00	1.42	2.25	2.50	11.12	0.00	6.95	10.49	5.94	2.12	2.10	8.77	100.00
3	<u>Yes</u>	13.38	35.31	0.00	0.33	0.21	0.40	0.64	18.06	0.32	2.68	2.74	25.95	0.00	100.00
4	<u>Yes</u>	17.97	46.81	0.49	0.00	0.55	0.00	2.23	30.16	0.00	0.00	0.00	1.80	0.00	100.00
5	<u>Yes</u>	55.62	0.00	4.32	0.20	0.76	31.03	0.00	0.63	1.00	1.91	2.63	1.34	0.56	100.00

All results in weight%

Comment: Pitkänomaiset rakeet ovat yleensä kipsiä tai amfiboli-pyrokseeni silikaattien koostumuksellisia rakeita.



Sample: kuivakiillotus
 Type: C-coated
 ID:

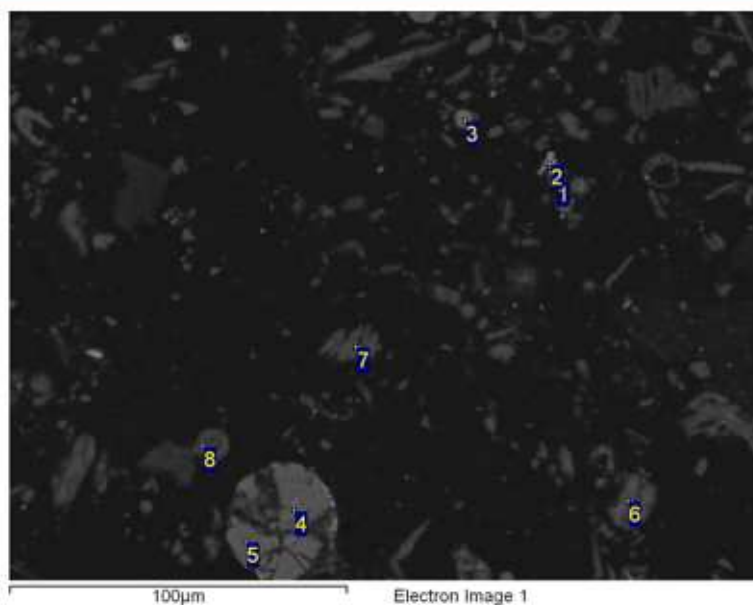
Project: Kaasupölynäyte Aalto nov2016
 Owner: semuser
 Site: Site of Interest 10

Feature Location:
 Sample: kuivakiillotus
 Area: kuiva
 Field: 30 - Feature: 5774 - (651, 18.5) pixels
 X: -11.5990mm, Y: -5.3210mm, Z: 11.0010mm

Processing option: All elements analysed (Normalised)

<u>Spectrum</u>	<u>In stats.</u>	<u>O</u>	<u>F</u>	<u>Na</u>	<u>Al</u>	<u>Si</u>	<u>S</u>	<u>Cl</u>	<u>Ca</u>	<u>Ti</u>	<u>Cr</u>	<u>Fe</u>	<u>Ni</u>	<u>Zn</u>	<u>Ba</u>	<u>Pb</u>	<u>Total</u>	
1	<u>Yes</u>	33.62	0.00	1.11	1.60	10.22	0.49	8.16	1.22	2.05	16.03	3.07	21.49	0.94	0.00	0.00	100.00	<u>NiCr ox</u>
2	<u>Yes</u>	35.19	0.00	1.26	1.23	6.30	0.29	0.91	0.94	1.75	23.98	5.03	18.55	4.57	0.00	0.00	100.00	<u>NiCrZn ox</u>
3	<u>Yes</u>	34.58	10.47	0.00	0.96	5.42	8.78	1.95	5.83	0.00	0.00	4.78	0.00	0.00	19.00	8.23	100.00	
4	<u>Yes</u>	43.04	0.00	0.78	0.72	1.56	0.00	0.00	1.39	25.08	0.00	14.19	1.39	2.66	9.20	0.00	100.00	
5	<u>Yes</u>	10.92	40.65	5.60	1.80	0.30	0.43	12.18	26.70	0.00	0.00	0.32	0.00	0.00	0.00	1.11	100.00	<u>Fluorite</u>
6	<u>Yes</u>	15.04	51.53	0.63	1.96	1.40	1.13	3.66	23.18	0.34	0.00	1.13	0.00	0.00	0.00	0.00	100.00	<u>Fluorite</u>
7	<u>Yes</u>	39.65	0.00	1.11	2.96	0.22	0.00	0.00	0.47	0.60	0.93	49.50	0.68	3.89	0.00	0.00	100.00	<u>Fe ox</u>

All results in weight%



Sample: kuivakiillotus
 Type: C-coated
 ID:

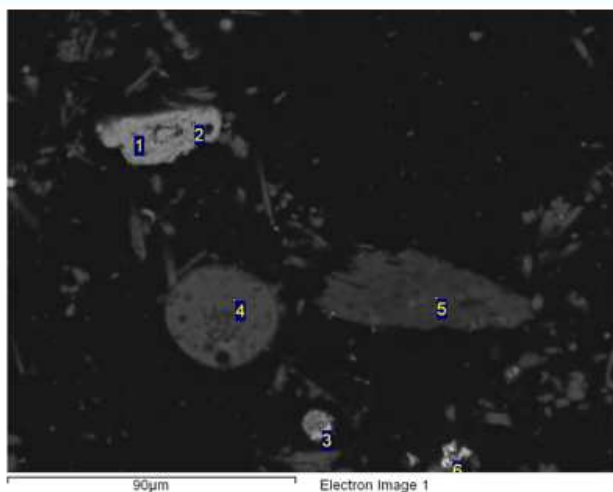
Project: Kaasupölynäyte Aalto nov2016
 Owner: semuser
 Site: Site of Interest 11

Feature Location:
 Sample: kuivakiillotus
 Area: kuiva
 Field: 12 - Feature: 2317 - (965.5, 681) pixels
 X: -11.8930mm, Y: -6.1380mm, Z: 11.0010mm

Processing option: All elements analysed (Normalised)

Spectrum	In stats	O	F	Na	Al	Si	S	Cl	K	Ca	Cr	Fe	Ni	Zn	I	Pb	Total	
1	<u>Yes</u>	32.09	0.00	1.51	0.27	0.48	0.31	0.16	0.00	0.58	18.62	25.90	12.44	7.64	0.00	0.00	100.00	<u>FeNiZn oxide</u>
2	<u>Yes</u>	33.81	0.00	1.96	0.24	0.45	0.00	0.00	0.00	0.53	10.07	31.56	6.46	14.91	0.00	0.00	100.00	<u>FeZnNi oxide</u>
3	<u>Yes</u>	39.83	0.00	5.17	3.21	8.25	0.00	0.00	1.15	2.01	0.00	23.46	0.00	16.02	0.00	0.89	100.00	<u>FeZn ox</u>
4	<u>Yes</u>	47.08	0.00	4.06	1.56	18.11	0.00	0.00	2.01	2.86	0.00	20.44	0.00	3.00	0.00	0.89	100.00	<u>Fe silic</u>
5	<u>Yes</u>	49.83	0.00	5.34	1.36	19.54	0.00	0.00	2.07	3.59	0.00	14.35	0.00	3.12	0.00	0.80	100.00	<u>Fe silic</u>
6	<u>Yes</u>	9.68	0.00	3.39	1.32	0.63	0.00	18.54	1.96	0.73	0.00	0.00	0.00	0.00	42.81	20.94	100.00	<u>Pb I Cl phase</u>
7	<u>Yes</u>	59.05	0.00	0.00	0.21	0.61	20.80	0.27	0.00	17.75	0.00	0.81	0.00	0.52	0.00	0.00	100.00	
8	<u>Yes</u>	12.51	50.72	0.89	1.09	0.71	0.69	1.92	0.35	30.37	0.00	0.75	0.00	0.00	0.00	0.00	100.00	

All results in weight%



Sample: kuivakiillotus
 Type: C-coated
 ID:

Project: Kaasupölynäyte Aalto nov2016
 Owner: semuser
 Site: Site of Interest 12

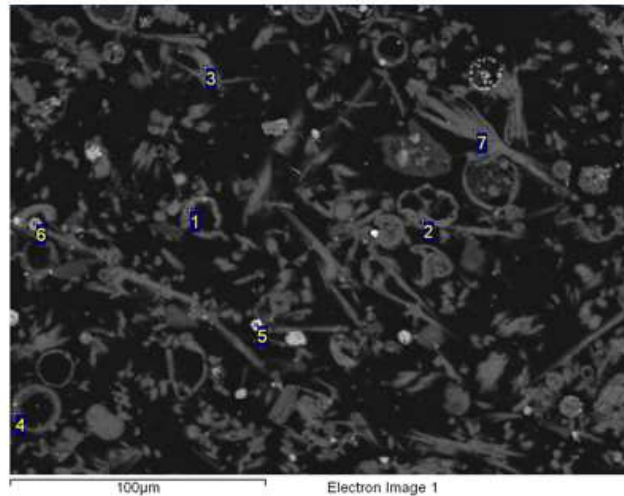
Feature Location:
 Sample: kuivakiillotus
 Area: kuiiva
 Field: 27 - Feature: 5139 - (426.5, 76) pixels
 X: -5.6380mm, Y: -5.9900mm, Z: 11.0010mm

Processing option: All elements analysed (Normalised)

Spectrum	In stats	O	F	Na	Mg	Al	Si	S	Cl	K	Ca	Ti	Fe	Zn	I	Pb	Total
1	<u>Yes</u>	33.50	0.00	0.00	0.00	0.00	0.00	0.00	0.00	0.00	0.33	0.00	66.17	0.00	0.00	0.00	100.00
2	<u>Yes</u>	37.04	0.00	0.00	0.00	0.00	0.00	0.00	0.00	0.00	0.22	0.00	62.74	0.00	0.00	0.00	100.00
3	<u>Yes</u>	29.53	0.00	0.00	0.66	0.43	0.66	0.00	6.33	2.06	0.73	1.50	45.39	5.15	0.00	7.55	100.00
4	<u>Yes</u>	57.20	0.00	4.32	0.00	9.78	23.69	0.00	0.00	3.75	1.27	0.00	0.00	0.00	0.00	0.00	100.00
5	<u>Yes</u>	28.37	0.00	0.00	0.91	0.97	0.64	1.32	35.16	0.00	12.06	0.00	1.63	2.68	5.86	10.42	100.00
6	<u>Yes</u>	22.11	3.17	0.00	0.00	0.41	1.45	3.05	21.25	4.07	4.64	0.00	1.65	1.25	0.00	36.93	100.00

All results in weight%

Comment: Rautarikkaita faaseja (Fe-oksidi) ja PbCl (+/- I).



100µm

Electron Image 1

Sample: kuivakiillotus
 Type: C-coated
 ID:

Project: Kaasupölynäyte Aalto nov2016
 Owner: semuser
 Site: Site of Interest 13

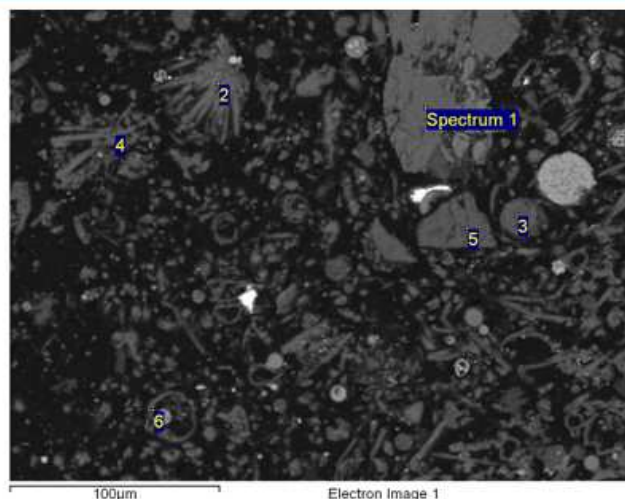
Feature Location:

Processing option: All elements analysed (Normalised)

<u>Spectrum</u>	<u>In stats</u>	<u>O</u>	<u>F</u>	<u>Na</u>	<u>Mg</u>	<u>Al</u>	<u>Si</u>	<u>S</u>	<u>Cl</u>	<u>Ca</u>	<u>Ti</u>	<u>Fe</u>	<u>Zn</u>	<u>Pb</u>	<u>Total</u>
1	<u>Yes</u>	17.72	49.62	1.98	0.00	0.99	0.59	0.69	5.56	21.91	0.00	0.31	0.61	0.00	100.00
2	<u>Yes</u>	12.62	48.39	1.16	0.41	1.62	0.72	0.86	2.53	24.21	0.38	3.79	2.42	0.89	100.00
3	<u>Yes</u>	55.21	1.30	0.00	0.00	0.17	0.38	20.82	0.26	19.79	0.00	0.26	0.38	1.43	100.00
4	<u>Yes</u>	23.72	45.33	0.00	0.00	0.76	0.72	1.11	2.34	25.37	0.00	0.66	0.00	0.00	100.00
5	<u>Yes</u>	37.02	0.00	0.85	0.55	2.99	9.38	0.00	0.26	2.16	2.01	8.29	3.35	33.14	100.00
6	<u>Yes</u>	39.32	0.00	2.25	0.47	1.73	4.01	0.00	0.00	0.77	1.90	39.60	9.95	0.00	100.00
7	<u>Yes</u>	57.10	0.00	0.00	0.00	0.11	0.14	22.54	0.20	19.90	0.00	0.00	0.00	0.00	100.00

All results in weight%

Comment: Yleiskuva kuivakiillotetusta näytteestä. Kipsi ja fluoriitti tavallisia, raskaat ovat Pb ja Fe-Zn rikkaita oksideja.



Sample: kuivakiillotus
 Type: C-coated
 ID:

Project: Kaasupölynäyte Aalto nov2016
 Owner: semuser
 Site: Site of Interest 14

Feature Location:

Processing option: All elements analysed (Normalised)

<u>Spectrum</u>	<u>In stats.</u>	<u>O</u>	<u>F</u>	<u>Na</u>	<u>Mg</u>	<u>Al</u>	<u>Si</u>	<u>S</u>	<u>Cl</u>	<u>K</u>	<u>Ca</u>	<u>Ti</u>	<u>Fe</u>	<u>Zn</u>	<u>Pb</u>	<u>Total</u>	
<u>Spectrum 1</u>	<u>Yes</u>	52.96	0.00	0.00	7.85	0.50	21.50	0.00	0.00	0.00	6.97	0.00	10.22	0.00	0.00	100.00	
<u>Spectrum 2</u>	<u>Yes</u>	54.14	0.00	0.00	0.00	0.00	0.43	23.51	0.41	0.00	21.00	0.00	0.51	0.00	0.00	100.00	kipsi
<u>Spectrum 3</u>	<u>Yes</u>	57.89	0.00	4.85	0.13	8.89	23.14	0.00	0.00	2.83	0.62	0.00	1.63	0.00	0.00	100.00	Na K maasälpä
<u>Spectrum 4</u>	<u>Yes</u>	55.13	0.00	0.00	0.00	0.15	0.41	22.96	0.20	0.00	20.76	0.00	0.00	0.39	0.00	100.00	kipsi
<u>Spectrum 5</u>	<u>Yes</u>	56.01	0.00	0.00	0.00	7.99	25.52	0.00	0.00	10.48	0.00	0.00	0.00	0.00	0.00	100.00	k-maasälpä
<u>Spectrum 6</u>	<u>Yes</u>	47.31	8.30	1.41	0.73	1.63	4.30	1.24	8.54	0.78	16.12	3.03	1.89	2.17	2.54	100.00	fluoriittia

All results in weight%

Comment: Toinen yleiskuva kuivakiillotetusta näytteestä.